AUS DEM LEHRSTUHL FÜR
HUMANGENETIK
PROF. DR. RER.NAT. BERNHARD WEBER
DER FAKULTÄT FÜR MEDIZIN
DER UNIVERSITÄT REGENSBURG

FUNCTIONAL ANALYSIS OF SELECTED ABCA4 AND CNGB3 VARIANTS IDENTIFIED IN RETINAL DEGENERATION PATIENTS

Inaugural – Dissertation
zur Erlangung des Doktorgrades
DER MEDIZIN

der
Fakultät für Medizin
der Universität Regensburg

vorgelegt von

JENNIFER LOEWEN-HORSCH

2019

AUS DEM INSTITUT
FÜR HUMANGENETIK
PROF. DR. RER.NAT. BERNHARD WEBER
DER FAKULTÄT FÜR MEDIZIN
DER UNIVERSITÄT REGENSBURG

FUNCTIONAL ANALYSIS OF SELECTED ABCA4 AND CNGB3 VARIANTS IDENTIFIED IN RETINAL DEGENERATION PATIENTS

Inaugural – Dissertation
zur Erlangung des Doktorgrades
DER MEDIZIN

der
Fakultät für Medizin
der Universität Regensburg

vorgelegt von
JENNIFER LOEWEN-HORSCH

2019

Dekan: Prof. Dr. Dr. Torsten E. Reichert

1. Berichterstatter: *Prof. Dr. rer.nat. Bernhard Weber*

2. Berichterstatter*:* *Prof. Dr. Horst Helbig*

Tag der mündlichen Prüfung: *02.Oktober 2019*

TABLE OF CONTENTS

1 INTRODUCTION

Retinal dystrophies comprise a class of eye diseases displaying broad clinical and genetic heterogeneity. Common to all is the degeneration of photoreceptors and/or retinal pigment epithelium in the posterior pole of the eye, eventually resulting in significant loss of vision and in some patients even blindness.[1] Retinal degenerative diseases range in severity, with a subform of retinitis pigmentosa (Leber's congenital amaurosis) being the most severe, and the juvenile form of hereditary macular dystrophy (Stargardt disease) on the milder side of the spectrum.[2] Due to technological advances in therapeutic options, the diagnostic importance and clinical implications brought about by genetic testing for retinal degenerative diseases have become increasingly significant. As a result, at least five retinal dystrophy phenotypes have been linked to mutations in the *ABCA4* gene: Stargardt disease (STGD), fundus flavimaculatus (FF), cone-rod dystrophy (CRD), retinitis pigmentosa (RP), and age-related macular dystrophy (AMD).[3]

1.1 STARGARDT DISEASE (STGD)

This dissertation was part of a larger study focused on Stargardt patients with variants in the *ABCA4* and *CNGB3* genes. Stargardt disease was first characterized by German ophthalmologist Karl B. Stargardt in 1909 and is one of the most common forms of autosomal recessive macular dystrophy, with a prevalence of 1: 10,000 to 1:15.000.[9] In addition to an early onset typically in the first two decades, further hallmarks include progressive loss of central vision, bilateral atrophy of the foveal retinal pigment epithelium and neuroepithelium, delayed dark adaptation, as well as the appearance of yellowish flecks surrounding the macula and retinal periphery (Stargardt, 1909 in Lewis et al.[11]). Additional clinical symptoms observed are the presence of a dark or silent choroid, as well as a hypofluoresent peripapillary ring.[3] To date, three molecular distinct origins have been described for Stargardt disease. Autosomal recessive STGD1 is caused by homozygous or compound heterozygous mutations in *ABCA4*, located on chromosome 1p22; [4] autosomal dominant STGD3 is linked to a mutation in the *ELOVL4* gene (chr. 6q14), [5] whereas autosomal dominant STGD4 has been linked to mutations in the *PROM1* gene (chr. 4p15.32).[6]

The *ABCA4* gene, first identified in 1997, is located on human chromosome 1p22 and contains 50 exons.[10] The protein product of *ABCA4* belongs to a class of ATP-binding cassette (ABC) transporters, which are ubiquitously expressed integral membrane proteins and constitute the largest family of eukaryotic transmembrane proteins.[12] The ABC transporters

employ energy generated from ATP hydrolysis in order to transport various substrates such as metabolic products, lipids and sterols, as well as drugs, unidirectionally across cellular membranes.[13, 14] Seven subfamilies of mammalian ABC transporters are currently known, with *ABCA4* constituting member 4 of the ABCA subfamily.[12] *ABCA4* is a single-chain protein consisting of 2,273 residues organized in two tandem halves (**Fig. 1**).[19] Each half includes an exocytoplasmic domain, a six helical transmembrane domain, and a cytoplasmic domain upon which the nucleotide binding site resides.[19] The exocytoplasmic domains are joined by a disulfide bridge, display multiple glycosylation sites, and the cytoplasmic domain is phosphorylated.[19,20]

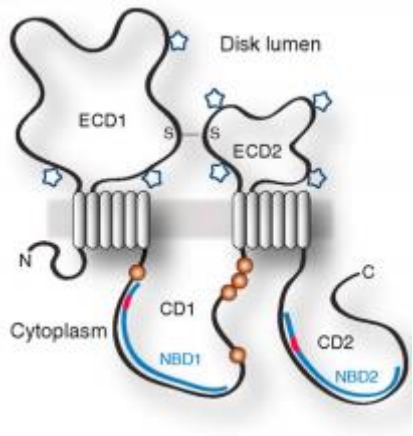

Figure 1: ABCA4 structure
Two tandem halves each with an exocytoplasmic domain (ECD1; ECD2), a cytoplasmic domain (CD1; CD2), and a nucleotide binding domain (NBD1; NBD2); Stars: glycosylation sites; Spheres: phosphorylation sites
Figure borrowed from Tsybovsky et al., 2013 (Fig.2a) [19]

ABCA4 is expressed exclusively in the retina photoreceptors, [15] primarily on the rims and incisures of rod outer segments discs, [16] but has also been found in foveal and peripheral cone cells.[17] The discovery of the *ABCA4* gene, and with it the growing understanding of the role of the *ABCA4* protein in the visual cycle, served to shift the understanding of Stargardt disease from being a disease of the retinal pigment epithelium (RPE) to one of rod photoreceptors.[18] Biochemical experiments, phenotype analysis of mice deficient for *ABCA4 (Abca4 $^{-/-}$)*, as well as clinical studies of macular degeneration patients, have aided in conceptualizing the role *ABCA4* plays in the visual cycle.[22] Quasi and Molday were able to show that *ABCA4* transports N-retinylidene-phosphatidylethanolamine (NRPE) from the exocytoplasmic to the cytoplasmic side (**Fig. 2**), and it is the only mammalian ABC transporter known to be an importer.[23]

Faulty transporting due to a mutated protein, as appears to be the case in Stargardt disease, results in the accumulation of N-retinylidene-phosphatidylethanolamine and all-trans-retinal in the interdiscal space, increasing the likelihood of a second molecule of all-*trans*-retinal binding to NRPE and thereby forming A2E, an oxidative component of lipofuscin (**Fig. 2**).[24] A build up of lipofuscin deposits, as is seen in retinal degenerative patients, is suspected to have toxic effects on the retinal pigment epithelium (RPE), including disrupting membrane permeability, lysosomal dysfunction, and apoptotic signaling leading to photoreceptor death.[3]

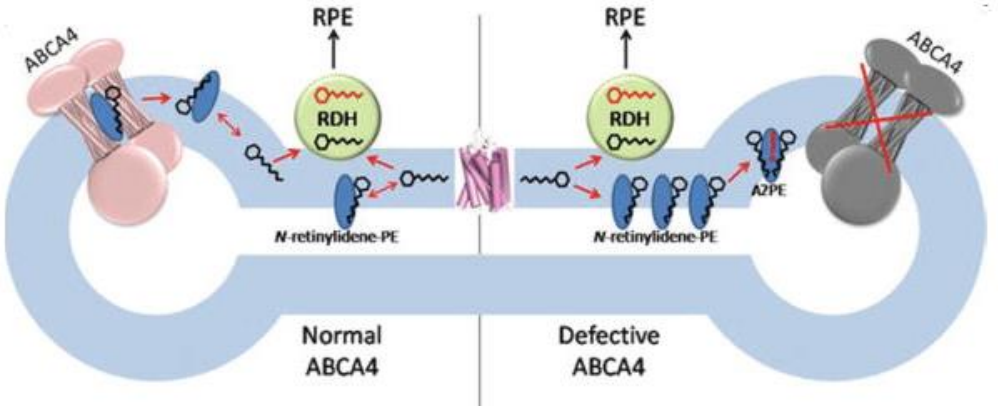

Figure 2: Proposed biological role of *ABCA4*
Left: rod outer segment disc with a functional *ABCA4*; Right: inactive *ABCA4*; Circles with carbon backbone: all-*trans*-retinal (*black*) and all-*trans*-retinol (*red*); RDH: all-*trans*-retinol dehydrogenase 8. RPE: retinal pigment epithelium.
Figure borrowed from Tsybovsky et al., 2010 (Fig.7)[22]

ABC transporter genes typically encode structural proteins and genetic mutations may lead to a significant reduction or even complete loss of protein function. The resulting disorders are inherited in an autosomal recessive or X-linked recessive fashion.[14] Experimental data have shown that disease severity is often inversely proportionate to the activity level of the *ABCA4* protein (**Fig. 3**).[25] In other words, depending on whether an *ABCA4* allele produces a normally functioning protein, a damaged protein, or complete lack of protein, the resulting phenotype can remain unaffected, or vary from mild to severe. On the severe end, mutations causing misfolded or truncated proteins are characterized by an early disease onset, primary photoreceptor loss, and secondary RPE damage.[25] In contrast, milder mutations may initially leave photoreceptors intact, yet the diminished *ABCA4* functioning results in gradual accumulation of toxic by-products in the RPE consequently leading to photoreceptor death.[25]

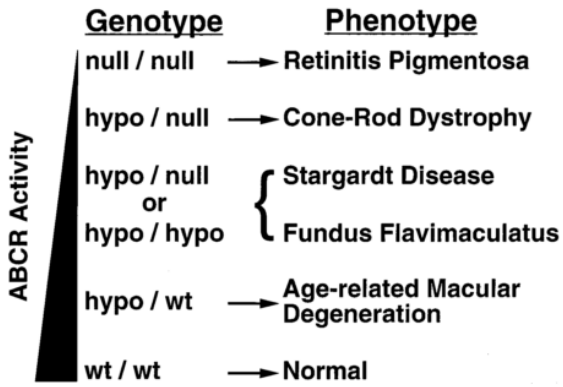

Figure 3: Progressive phenotypes resulting from ABCA4 mutations

Left: triangle representing ABCA4 activity; Genotype: (both alleles): null: no functional protein, hypo: reduced functioning alleles, WT: wild-type/normal alleles; Arrows: association between phenotypes and genotypes; Brackets: both STGD and FF can be caused by either genotype.

Figure borrowed from Shroyer et al., 1999 (Fig.3)[25]

The residual *ABCA4* function model, as described above (**Fig. 3**), has been criticized in for being "oversimplified".[22] Studies in tadpoles, for instance, have shown that protein mislocalization may be a contributing factor in disease severity.[26] Moreover, Cideciyan et al. were able to demonstrate that several patients with missense and splicing mutations showed greater phenotype severity than those with truncating mutations, and thus proposed a two-pathway model of understanding *ABCA4* disease pathogenesis. [1] Initially, conventional loss-of-function occurs. As a result, stress is placed on the cellular degradation system, subsequently inducing a toxic gain-of-function response, and eventually apoptotic signaling.[1] As further evidence of the complexity surrounding the genotype-phenotype correlation, other groups have shown that non-*ABCA4* modifying factors are also instrumental in determining the level of visual functioning in patients with confirmed *ABCA4* eye disease.[27]

1.2 BACKGROUND

As outlined below (**Table 1**), the variants (N=21) for this study were selected from a pool of possibly pathogenic variants found in a cohort of 335 patients clinically diagnosed with Stargardt disease who had undergone diagnostic testing at the Institute of Human Genetics, University of Regensburg between 2008 and 2015. The sequencing analysis included the coding regions and canonical site junctions of *ABCA4* and *CNGB3*. Although the majority of variants stemmed from Stargardt patients, three additional variants identified in cone-rod dystrophy patients were also included.

Gene	Unique Variants	Unique variants with MAF* in controls <1%	Novel unique variants with MAF* in controls <1%
ABCA4	136	116	32
CNGB3	16	10	8

Table 1: Sequence variants identified in 197 Stargardt disease patients tested between the years 2009 and 2012 at the Institute of Human Genetics, University of Regensburg (2009-2012) * minor allele frequency

The unique variants with a minor allele frequency (MAF) <1% in controls were further analyzed *in silico* to assess for possible spliceogenic effects. Based on positive predictive results from several bioinformatics tools, seventeen *ABCA4* variants, one *CNGB3*, as well as the three *ABCA4* variants found in cone-rod dystrophy patients (not included in the above table) were selected for subsequent *in vitro* functional investigations.

1.3 CNGB3

The *CNGB3* gene is located at 8q21.3, contains 18 exons[31] and encodes for a cyclic nucleotide-gated (CNG) cation channel.[28] CNGs belong to the superfamily of Voltage-gated Ion Channels (VIC) and play a crucial role in visual and olfactory transduction.[28] Specifically, they are responsible for the generation of light-evoked electrical responses in the red, green, and blue sensitive cones.[7] In the absence of light, channels are held open by cGMP, maintaining an inward current; light causes cGMP to be hydrolyzed, upon which the CNG channels close, hyperpolarizing the cell and transduction commences.[29] CNG channels found in the outer segments of cone cells in the human retina consist of two subunits: α (ion-conducting) and β (modulatory), and are encoded for by *CNGA3* and *CNGB3* respectively.[29, 30] Even though its function is considered to be only modulatory and the mechanism is not yet fully understood, the β subunit appears to vital to cone functioning and survival.[29] *CNGB3* mutations are most commonly linked to achromatopsia and juvenile macular degeneration.[7, 8] Some evidence exists that mutations in the β subunit may result in gain-of-function leading to Ca^{2+} overload, in turn causing cytotoxicity and increased susceptibility to cell death.[32]

1.4 CONE-ROD DYSTROPHY

Cone-rod dystrophy (CRD) is a rare form of pigmentary retinopathy with a prevalence of 1:40,000.[33] It is characterized by pigment deposits in the macula, decreased visual acuity, photophobia, dyschromatopsia, progressive loss of peripheral vision, and night blindness in later disease stages.[33] Cone-rod dystrophy can be differentiated from rod-cone dystrophy (retinitis pigmentosa, RP) in that the latter typically presents in initial stages with night blindness, whereas the clinical course of cone-rod dystrophy is more severe with an earlier onset of blindness.[33] Although a number of genes have been linked to cone-rod dystrophy, including *ABCA4, CNGB3, CRX, KCNV2*, and *RPGR*, a recent study published that 65% of the CRD patients in their sample were found to have *ABCA4* mutations and suffered the fastest progression to legal blindness.[34]

1.5 SPLICING REGULATION AND DISEASE

Research in the previous two decades has demonstrated that correct splicing, a process by which the non-coding introns are removed and the exons joined together to form the mature mRNA (messenger RNA), relies on the correct recognition of exons. [35, 36, 37, 38] Involved in this process are so-called "cis" elements including the highly conserved consensus sequences at the intron 5' donor splice site (GU), the 3′ acceptor site (AG), the polypyrimidine tract, and the branch point sequence slightly upstream from the 3′ end. [92] "Trans" elements refer to the spliceosome snRNP (small nuclear ribonucleoproteins) and the enhancer or silencer elements that either activate or repress splicing. [92] The 5′ splice site (**Fig. 4**) beginning with GU is comprised of nine partially conserved nucleotides from nucleotide position -3 to +6 found at the exon-intron border (**Fig. 4**).[39] Nucleotide changes in the highly-conserved, i.e. the canonical -1, +1, and +2 sites, are very likely to affect splicing, [40] whereas less conserved sites, such as the -3, can tolerate more variance. [41]

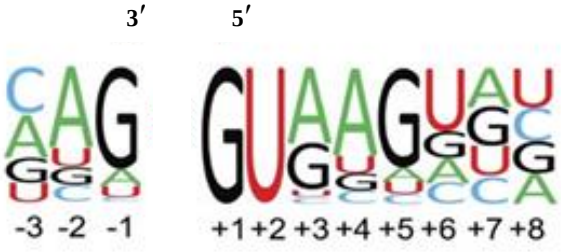

Figure 4: Splice site consensus site motif* showing intron 3′ acceptor (AG) and 5′ donor (GU) sites, based on an updated collection of 201,541 human 5′ splice sites. The varying height of each nucleotide represents the degree of conservation at that position.
Figure borrowed from Roca et al., 2013 *modified (Fig. 1b) [39]

The 3′ terminus **(Fig. 5)** consists of an AG dinucleotide acceptor site, a 14-26 nucleotide polypyrimidine tract, and the branch point located 18-40 nucleotides upstream from the 3′ junction. [92, 94]

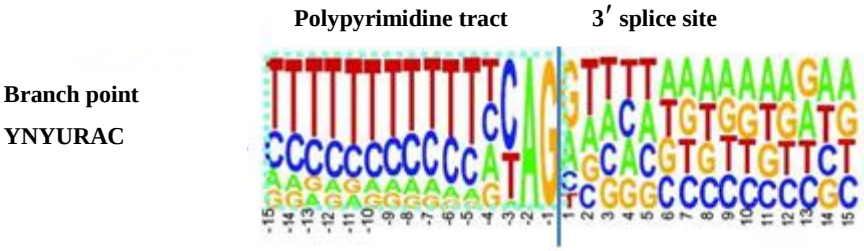

Figure 5: 3′ terminus with (AG) acceptor site, the CT (CU) rich polypyrimidine tract and branch point [92]
Figure borrowed from Zhang et al. 2007 *modified (Fig. 1C) [93]

The major human spliceosome is made up of five types of small nuclear ribonucleoproteins (snRNP) and numerous core proteins.[96] Upon recognition, the spliceosome machinery hybridizes at the 5′ and 3′ splice sites and in a series of catalyzed steps, two transesterification reactions carry out intron excision and subsequent exon ligation (**Fig. 6**).[97]

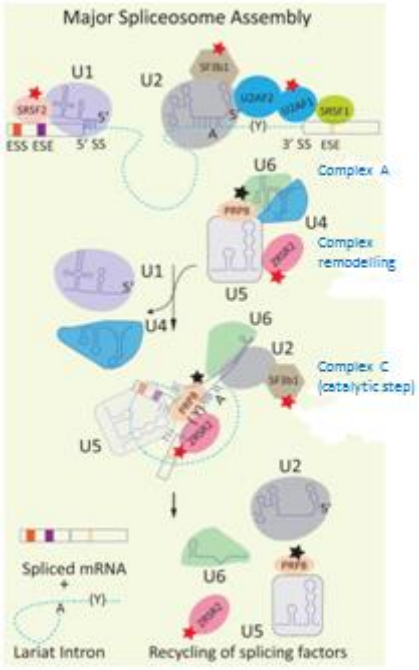

Figure 6: Model for the major human spliceosome assembly and function

U1 and U2 snRNPs bind to the 5′ splice site and branch point respectively. The U2-auxiliary factor heterodimer interacts with the polypyrimidine tract (Y) and 3′ splice site to form complex A. The catalytic complex C is formed when the U4/U5 snRNPs bind, leading to a remodeling and removal of the U1 and U4 snRNPs. Two transesterification reactions ligate the exons and release an intron lariat, which is then degraded. The spliceosome is disassembled and recycled for use on another intron.
rectangles: exons; dashed line: intron; A: branch point; Y: polypyrimidine tract; ESE: exonic splicing enhancers; ESS: exonic splicing silencers
red, black, & orange stars: show mutated component associated with neoplasias, retinitis pigmentosa and MOPD1 respectively (not relevant here)
Figure borrowed from Singh & Cooper, 2012 (Fig.1)[44]

Research has shown that exon recognition and splicing efficiency are equally dependent on both the 5′ and 3′ splice sites, yet high 5′ splice site complementarity to the U1 complex and a lengthy polypyrimidine tract seem to be especially important for spliceosome affinity.[95] In addition to the highly conserved consensus sequences at intron-exon borders, other splicing

regulatory elements found within exons and introns can act as either splicing enhancers or silencers.[42]

Correct gene expression requires extraordinary precise choreography among all splicing elements in order to facilitate correct exon recognition and intron removal, and variations in nucleotides may disrupt the splicing machinery. In general, the higher the degree of conservation at the site where the variant/mutation occurs, the more severe the consequence. Hence, the nature of the outcome depends on the extent to which correct splicing can still occur, as well as on what molecular changes are brought forth by the change. Most frequently, exon skipping is seen (**Fig. 7**), but cryptic splice site activation is also very common (**Fig. 8**).[39] Whereas total intron retention is rare, partial intron sequence may be included in the mRNA as a result of cryptic splice site activation or mutations within the intron, creating a pseudoexon and possibly leading to a frameshift (**Fig. 8 & 9**).[39, 44]

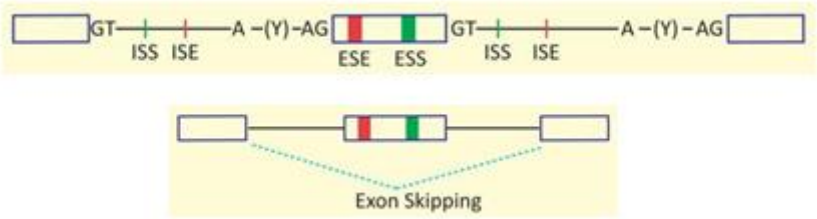

Figure 7: Mutations that reduce the strength of 5′ or 3′ splice sites decrease exon identification and are therefore likely to result in exon skipping. *GT*: 5′ splice site; *AG*: 3′ splice site; *Y*: polypyrimidine tract; *A*: branch point; *ESE, ISE*: exonic & intronic enhancers; *ESS, ISS*: exonic & intronic silencers (here not relevant)
Figure borrowed from Singh & Cooper, 2012 (Fig.2a) [44]

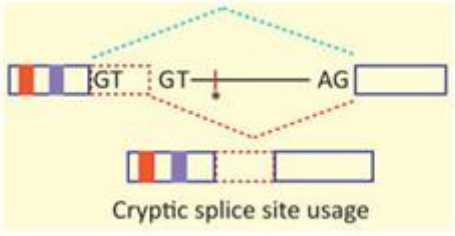

Figure 8: Mutations that activate cryptic splice sites, i.e. sequence identical to the consensus site that is not used for splicing, but which increases in strength due to a mutation. This may result in the inclusion of extra sequence in the spliced mRNA, thus disrupting the reading frame (frameshift). *GT*: 5′ splice site; *AG*: 3′ splice site; *asterisk*: enhancer element; *blue line*: normal splicing pattern; *red line*: splicing pattern due to mutation; *dashed red rectangle*: inclusion of intronic sequence.
Figure borrowed from Singh & Cooper, 2012 (Fig.2c) [44]

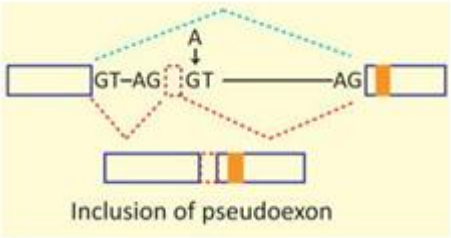

Figure 9: Mutations in intron (indicated by arrow) may also lead to inclusion of intronic sequence creating a pseudoexon. Extra sequence may result in a frame shift. *GT*: 5′ splice site; *AG*: 3′ splice site; *blue line*: normal splicing pattern; *red line*: splicing pattern due to mutation; *dashed red rectangle*: inclusion of intronic sequence; Figure borrowed from Singh & Cooper, 2012 (Fig.2c) [44]

Possible pathological consequences on the molecular level include premature stop codons resulting in a truncated protein, as well as insertions or deletions of amino acids leading to frame shifts.[45] The outcome depends largely on which scenario is brought about by the nucleotide change (**Fig. 7-9**). To date, most recorded data on splicing mutations remains at the genomic sequence level, [91] posing a problem for both researchers and clinicians in interpreting and predicting the functional implication of the mutation. These challenges are particularly multifaceted for the *ABCA4* gene given its wide allelic diversity, [46] which not only displays variance in the resulting phenotype,[47] but also in the pathogenic severity.[48] *ABCA4* disease alleles are found at a frequency of approximately 1 in 50 in the general population, [47] and many sequence variants are intronic, making them difficult to interpret.[46] The complexity is compounded by tissue inaccessibility preventing direct RNA analysis of possible pathological isoforms in the retina of living patients.

1.6 ABCA4 VARIANTS AND EFFECT ON SPLICING

Research from previous decades demonstrated that up to 15% of point mutations leading to human genetic disease are located within the highly conserved splice site regions, [49] and current research supports these findings.[98] A growing number of studies are expanding the scope to focus on how nucleotide changes both within the coding region, as well as those at splicing regulatory element sites, may affect splicing and what role they play in disease pathogenesis.[43,50,51] In line with broader data available on splicing mutations, the Human Genome Mutation Database shows that ≈15% of first-report mutations in the *ABCA4* gene are classified as splicing mutations (**Table 2**), yet descriptive data regarding the nature of spliceogenic variants remains scarce due to lack of *in vitro* analyses, as will be discussed further on.

Mutation Type	**Number of Mutations**
Missense/ nonsense	536
Splicing	117
Deletions	107
Insertions	23
Indels	7
Com. rear.	1
Total	791

Table 2: ABCA4 mutation types and number

http://www.hgmd.cf.ac.uk/ac/gene.php?gene=ABCA4; Public Version 13.01.2019

1.7 IN SILICO PROGRAMMES TO PREDICT VARIANT EFFECT ON SPLICING

Numerous web-based prediction tools are available for performing bioinformatic analyses of the potential effect a variant may have on splicing. This study incorporated five such programmes for the *in silico* variant analysis (**Table 3**).

Software	Application	Provider
Gene Splice Finder	Splice site predictor (scale 0-15)	Accessed through Alamut platform (Interactive Biosoftware, Rouen, France)
Human Splicing Finder	Splice site predictor (scale 0-100)	Accessed through Alamut platform (Interactive Biosoftware, Rouen, France)
Neural Network	Splice site predictor (scale 0-1)	Accessed through Alamut platform (Interactive Biosoftware, Rouen, France)
MaxEntScan	Splice site predictor (scale 0-12)	Accessed through Alamut platform (Interactive Biosoftware, Rouen, France)
Splice Site Finder	Splice site predictor (scale 0-100)	Accessed through Alamut platform (Interactive Biosoftware, Rouen, France)

Table 3: Software used for in silico predictions in this study

In silico analyses have demonstrated effectiveness in their ability to predict the disruption of canonical donor and acceptor sites due to single nucleotide changes, with some studies showing up to 100% specificity and sensitivity for certain programmes.[73] However, not all studies have been able to obtain such high accuracy rates, and wide discrepancy has been reported in some cases.[52,54] Moreover, interpreting the effect of nucleotide changes on the enhancement or *de novo* creation of cryptic splice sites has proven difficult. Deciphering how sequence variations in enhancer or silencer splicing regions may affect splicing poses an even greater challenge.[40]

Researchers caution against relying on a single *in silico* prediction programme,[54] others stress *in vitro* analysis' indispensability in characterizing the effect of variants deemed spliceogenic by such programmes,[40, 73] yet both approaches present several challenges. Interpreting the results of numerous programmes can be complex, as each tool relies on different baseline algorithms and scoring systems and may vary in the amount of input sequence required or analytical procedures utilized.[40] Similarly, functional analyses, while providing an *in vivo* picture of possible effects on splicing, can be time and resource consuming, particularly when tissue is limited or inaccessible, as is the case with *ABCA4*. An effective means of optimizing the process could be implementing *in silico* tools for initial selection and

prioritization of variants, which are subsequently analyzed *in vitro* in hopes of characterizing their potential putative *in vivo* effect.[52, 53, 54]

1.8 PURPOSE OF STUDY

This study carried out *in vitro* analyses of a selection of *ABCA4* variants found in patients with retinal dystrophy (STGD and CRD) which had been predicted *in silico* to affect splicing. Because *ABCA4* and *CNGB3* are transcribed exclusively in the retina, it is not feasible to investigate splicing via direct RNA analysis from native tissue. To circumvent this problem, an *in vitro* exon trapping method was employed based on work done by Cepko et al. [55] This approach capitalizes on the highly conserved sequences flanking splice sites and implements transmissible expression vectors to generate and recover genomic inserts.[56, 57] Following replication and selection in E.*coli*, the pSPL3b vector containing the construct was transfected in transient cells, the RNA isolated, reverse transcribed, and RT-PCR amplified. Visualizing the products via gel electrophoresis allowed for initial comparison of splicing activity between the normal allele and mutant variants.

2 MATERIAL

2.1 ANALYZED VARIANTS, SOURCES, AND CHARACTERISTICS OF CONSTRUCT

Patient ID (Medistar No.)	Working ID	Variant	Geno-type	Exon	Product size (bp)	Included 5′ intron seq. (bp)	Included 3′ intron seq. (bp)	Phenotype
18962	A	c.67-1G>C	Homo	2	263	103	54	STGD
16843	G	c.67-2A>G	Het	2	263	103	54	CRD
17412	U	c.160+2T>C	Het	2	263	103	54	STGD
21066	B	c.4773+3A>G	Het	33_34	506	138	50 (131 between)	STGD
15977	C	c.4919G>A	Het	35	404	141	81	STGD
17002	D	c.5018+2T>C	Het	35	404	141	81	STGD
17002	E	c.6386+2C>G	Het	46_47	475	100	93 (73 between)	STGD
15485	F*	CNGB3 c.991-3T>G	Het	9	327	176	74	STGD
17716	H	c.179C>T	Het	3	358	67	149	STGD
15282	I	c.1239+1G>C	Het	9	431	112	180	STGD
20364	J	c.1937+1G>A	Het	13	411	85	149	STGD
21529	K	c.1819G>A	Het	13	411	85	149	STGD
15023	L	c.2894A>G	Het	19	415	54	186	STGD
16178	M	c.3808G>T	Het	25	478	151	121	STGD
15286	N	c.4352+1G>A	Het	29	407	192	116	STGD
14686	O	c.4354G>T	Het	30	424	96	141	STGD
16827	P	c.4457C>T	Het	30	424	96	141	STGD
16272	Q	c.5196+1G>A	Het	36	358	95	85	CRD
17575	R	c.5189G>A	Het	36	358	95	85	STGD
20882	S	c.5312+1G>A	Het	37	390	184	90	CRD
16518	T	c.6732G>A	Het	49	301	114	100	STGD

Table 4: Analyzed variants, sources, and characteristics of construct

*** All variants in ABCA4: NM reference NM_000350.2, except *F: CNGB3 NM reference NM_019098.4**

STGD = Stargardt disease; CRD = cone-rod dystrophy

2.2 PATIENTS

Between the years of 2008 and 2015, DNA samples of 335 Stargardt patients (191 female, 144 male) were analyzed for *ABCA4* mutations in the 50 coding exons and adjacent intronic sequences as part of routine diagnostic screening at the Institute of Human Genetics, University of Regensburg. Informed written consent was obtained from each patient in accordance with established guidelines of the German Medical Association, the German Society of Human Genetics, and the German Genetic Diagnosis Act of 2010, agreeing to the use of their DNA for research purposes aimed at underlying genetic cause of their disease. Genomic DNA was isolated from peripheral blood lymphocytes.

2.3 OLIGONUCLEOTIDES/PRIMER

Gene/Exon /Restriction Site	Sequence
ABCA4-ex02-F-EcoRI	gaattcACTGCACACATGGGATCTGA
ABCA4-ex02-R-BAMHI	ggatccAGGCCCAGACCAAAGTCTCT
ABCA4-ex03-F-EcoRI	gaattcTCCTAGGTCTGCATCCTGCT
ABCA4-ex03-R-BAMHI	ggatccGGAAACCTGCTCTGCTCCTA
ABCA4-ex09-F-EcoRI	gaattcAATCCTCCAGCATGGAGTTG
ABCA4-ex09-R-BAMHI	ggatccCACTGAAGCAAAGCATTCCA
ABCA4-ex13-F-EcoRI	gaattcTGAGTTCCGAGTCACCCTGT
ABCA4-ex13-R-BAMHI	ggatccGTCAGAGCTCCATGCTCTCC
ABCA4-ex19-F-EcoRI	gaattcGGGCCATGTAATTAGGCATT
ABCA4-ex19-R-BAMHI	ggatccCCTCCCCATCAAGAGAATACA
ABCA4-ex25-F-EcoRI	gaattcTGGAGCATCAGTCCTCTGAA
ABCA4-ex25-R-BAMHI	ggatccCTATGCTTGGGTGGGGAAC
ABCA4-ex29-F-EcoRI	gaattcGTGACATGCCATCAGACCAC
ABCA4-ex29-R-BAMHI	ggatccAGTGACCAGCAGAGCAGGAT
ABCA4-ex30-F-EcoRI	gaattcAGAGGAGGAGGAAAGGGTTG
ABCA4-ex30-R-BAMHI	ggatccGGTGCAGGGAGTTTGGTTTA
ABCA4-ex33_34-F-EcoRI	gaattcTTTGTAAAGTGGAGCCATGTTG
ABCA4-ex33_34-R-BAMHI	ggatccGGTAAATTTTTAGCTCCAGAGCAG
ABCA4-ex35-F-EcoRI	gaattcATCCCTCCTCCTGCTGAAAT
ABCA4-ex35-R-BAMHI	ggatccGGTGGTGAGAATCCTCTCAGG
ABCA4-ex36-F-EcoRI	gaattcGTGTAAGGCCTTCCCAAAGC
ABCA4-ex36-R-BAMHI	ggatccCCCTCTTGGTCTGGTCCTTC
ABCA4-ex37-F-EcoRI	gaattcGGGTGGGGTAGGAGGACTA
ABCA4-ex37-R-BAMHI	ggatccACAGCCCAGGTTTTCTGTCA
ABCA4-ex46_47-F-EcoRI	gaattcCTGTCAGCTCATCCTCCACA
ABCA4-ex46_47-R-BAMHI	ggatccGAGCAGCAGGACTCTTCCAA
ABCA4-ex49-F-EcoRI	gaattcTACCAGCAGGGCTGTATGTG
ABCA4-ex49-R-BAMHI	ggatccGGCATATCTGAGCCTTGGAG
CNGB3-ex9-F-EcoRI	gaattcCCATGCTATAAAATGTACTGTCCAGAGGA
CNGB3-ex9-R-BAMHI	ggatccCCTGCCAAATTCCGTCTAAAATGTTGT
M13-F	CGCCAGGGTTTTCCCAGTCACGAC
M13-R	AGCGGATAACAATTTCACACAGGA
pSPL3bF	GAGAAATATCAGCACTTGTG
pSPL3bR	GTACACCGGCATGTGTGGCC

SD2	GTGAACTGCACTGTGACAAGC
SD6	TCTGAGTCACCTGGACAACC
SA2	ATCTCAGTGGTATTTGTGAGC
SA4	CACCTGAGGAGTGAATTGGTCG

Table 5: Primers*, including gene, exon, restriction site, and sequence

***cc 100 µM, dilution 1:10; company: Metabion. (see Appendix)**

2.4 ORGANISMS AND CELL TYPES

Strain/Cell line	Characteristics	Source
E.coli strain DH5α	nuclease deficient	Inst. of Human Genetics UR
HEK 293 EBNA	human embryonic kidney cells	Inst. of Human Genetics UR

Table 6: Bacteria strains and cell lines

2.5 PLASMIDS

Plasmid	Size (kb)	Resistance	Application	Source
pGEM-T	3	Ampicillin	WT/Mut selection	Promega
pSPL3b	6	Ampicillin	Transfection	Inst. of Human Genetics UR

Table 7: Plasmids

2.6 ENZYMES

Enzyme	Application	Company
Go-Taq polymerase (5U/µl)	PCR cDNA	Promega
Pfu polymerase *(Pyrococcus furiosus)*	PCR	Inst.Human Genetics UR
Restriction enzymes (*Eco*RI, *Bam*HI)	Plasmid digestion	Biolabs
Taq polymerase (*Thermos aquaticus)*	PCR	Inst.Human Genetics UR
T4-DNA Ligase	Ligation	Promega
Trypsin (0,5%) EDTA (0,2%) 1 x in PBS	Cell culture	PAA

Table 8: Enzymes

2.7 KITS

Kit	Application	Company
BigDye Terminator v1.1, v3.1 Cycle Seq. Kit	Sequencing	Applied Biosystems
RevertAid ™ H First Strand cDNA Synthesis Kit	Reverse transcription	Thermoscientific
NucleoSpin® Gel and PCR Clean Up	PCR purification	Macherey-Nagel
NucleoSpin® Plasmid Clean Up	Plasmid DNA purification	Macherey-Nagel
pGEM T- Vector System	Cloning	Promega
Rneasy Micro Kit	RNA isolation	Qiagen
TransIT®-LT1 Transfection reagents	Transfection	Mirus

Table 9: Kits

2.8 CHEMICALS/SUBSTANCES

Chemical/Substance	Application	Company
Agarose	Gel electrophoresis	Biozym
Ampicillin Sodium Salt	LB-med./plates	Carl Roth
β-Mercaptoethanol	RNA isolation	Sigma
Bacto agar	LB-ampicillin plates	Becton, Dickson & Co.
Bacto yeast extract	LB-ampicillin plates	Becton, Dickson & Co.
Boric acid	TBE	Merck
Bromphenol blue	Loading buffer	Sigma
Buffer 4	Ligation into pSPL3b	Biolabs
Chloroquin 25mM	Transfektion	Biomol
DMEM	Cell culture	Gibco
dNTPs	PCR	Genaxxon Bioscience
EDTA	TBE/cell culture	Merck
Ethanol ≥ 99,8 %; 70%	DNA percipitation	Carl Roth
Ethidium bromide	Gel electrophoresis	AppliChem
Fetal Calf Serum (FCS)	Cell culture	Gibco
Ethylenediaminetetraaceticacid (EDTA)	Cell culture	AppliChem
Generuler 1kb	Gel electrophoresis	Invitrogen
Glycerin 99,5%	Stock perservation	Inst.Human Genetics UR
HiDi Formamide	DNA percipitation	AppliBiosys
Instant Sticky-end Ligase	Ligation into pSPL3b	Biolabs
Isopropylthio-β-galactoside (IPTG)	Blue/white selection	AppliChem
Lysin (Poly-L)	Cell culture	Sigma
PBS 10x pH 7.4	Cell culture	Gibco
Penicillin/Streptomycin	Antibiotics	Gibco
Peptone from casein, tryptin digested	LB-med./plates	Carl Roth
Sodiumacetate 3M	DNA percipitation	Merck
Sodiumchloride	LB-med./plates	VWR
Tris	TBE	VWR
X-Gal	Blue/white selection	Sigma
Xylencyanol blue	Loading buffer	Sigma

Table 10: Chemicals/Substances

2.9 SOLUTIONS/BUFFERS/MEDIUM

Solutions/Buffer	Composition	Amount	Application
Agarose gel	TBE 1x Agarose	 1-2%	Gel electrophoresis
Buffer 4 pH 7.9	50 mM K-acetate 20 mM Tris-acetate 10 mM Mg-acetate 1mM DTT		Restriction digestion
dNTPs (cc 100 mM)	dATP dTTP dGTP dCTP	12,5 µl in 950 µl dH_2O 12,5 µl in 950 µl dH_2O 12,5 µl in 950 µl dH_2O 12,5 µl in 950 µl dH_2O	PCR
Instant Sticky-end Ligase	Gylcerol PEG-6000 Proprietary Information Tris-HCL	20% 13.6% 5% 1.5%	pSPL3 Ligation
Poly-L-Lysin	Dil 1:50 with 1x PBS		Cell culture
TBE 5x pH 8,0	Tris (0.44 M) Boric acid (0.44 M) EDTA (0.5 M) pH 8 dH_2O	216 g in 4 L 110 g in 4 L 80 ml in 4L 4 L	Gel electrophoresis
Xylencyanol blue	Xylencyanol Glyerin dH_2O	0,05 g 20 ml Ad 50 ml	Loading buffer gel electrophoresis

Table 11: Solutions/Buffers

Medium	Composition	Amount	Application
HEK 293 EBNA (DMEM+)	DMEM (glucose 4,5g/L) FCS Pen/Strep	500 ml 10% 1%	Cell culture
LB Medium	Pepton Yeast extract NaCl dH_2O Ampicillin (cc 100 µg/ml)	10g 5g 10g 1L 1 ml	Bacteria growth and selection
LB Plates	+ Agar	15g	Cloning
SOC	Pepton (2%) Yeast extract (o.5%) NaCl (10mM) KCl (2.5mM) dH_2O pH 7.0 autoclave	20g 5g 0.5g 0.186g 1L	E. *coli* DH5α recovery

Table 12: Medium

2.10 LABORATORY MATERIAL

Material	Application	Company
6-well plates	Transfection	Corning, Inc.
96-well plates	Sequencing	VWR
Cassette	Gel electrophoresis	Serva
Cell culture dishes	Cell culture	Sarstedt
Cell scraper	RNA isolation	Orange Scientific
Combs	Gel electrophoresis	Serva
Disposable Pasteur pipettes 3 ml	Gel electrophoresis	VWR
Eppendorf cups 0.5ml/1.5ml/2.0 ml	Miscellaneous	Sarstedt
Falcon® tubes 15 ml/50 ml	Miscellaneous	Sarstedt
Glass pipettes	Miscellaneous	Brand
Nitrile gloves (blue)	Miscellaneous	VWR
Nitrile gloves (green)	Miscellaneous	KIMTECH
Needles 0.6/30 mm	RNA isolation	Becton, Dickson & Co.
PCR cups	Miscellaneous	Biozym
Petri dishes – bacteria culture	Cloning	Sarstedt
Pipette tips 10 µl/100µl, 1000µl	Miscellaneous	VWR
Scalpel	Gel purification	Feather
Syringe Omnifix 10	RNA isolation	Braun

Table 13: Laboratory material

2.11 INSTRUMENTS AND APPLIANCES

Instrument/appliance	Company
Autoclave V-150	Systec GmbH
Bacteria hood	ThermoScientific
Cell culture hood	BDK GmbH
Centrifuge (mikro)	Qualitron
Centrifuge 5415R	Eppendorf
Centrifuge Multifuge 3L	ThermoScientific
Centrifuge Megafuge 1.0R	ThermoScientific
Centrifuge 5810	eppendorf
Dark hood DH 30/32	Biostep
Gel electrophoresis voltage boxes	Serva
Gel electrophoresis chambers Blue Marine 200	Serva
Scepter®Hand-held automatic cell counter	Millipore
Ice machine AF 100	Scotsman
Incubator 37°C	Memmert
Incubator shaker Certomat® R	B.Braun Biotech
Microwave	Daewood
Millipak® Water System	Millipore
Multichanel pipette	Abimed
Multipipette® Plus	eppendorf
ND1000 Spectrophotometer	NanoDrop®
Pump - cell culture hood	eppendorf
Pipettes10µl/100µl/1000µl	Applied Biosystems
3130x1 Genetic Sequenzer	Biometra
Thermocycler	Biometra
Thermocycler T3	eppendorf

Thermomixer compact	eppendorf
Vortex 2 Genie	ScientificIndustries
Water bath Aqualine	Lauda
Water distiller 2012	GFL

Table 14: Instruments and Appliances

2.12 SOFTWARE

Software	Application	Provider
Argus 3.0	Gel documentation	Biostep Jahnsdorf GmbH
ApE	Check for restriction sites	http://biologylabs.utah.edu/jorgensen/wayned/ape/
Chromas	Sequence analysis	www.technelysium.com.au
ExPASy Bioinformatics Resource Portal	Protein translation	http://web.expasy.org/translate/
Gene Splice Finder	Splice site predictor (scale 0-15)	Accessed through Alamut platform (Interactive Biosoftware, Rouen, France)
Human Splicing Finder	Splice site predictor (scale 0-100)	Accessed through Alamut platform (Interactive Biosoftware, Rouen, France)
Interactive Biosoftware	Protein translation	http://www.interactive-biosoftware.com/
Neural Network	Splice site predictor (scale 0-1)	Accessed through Alamut platform (Interactive Biosoftware, Rouen, France)
MaxEntScan	Splice site predictor (scale 0-12)	Accessed through Alamut platform (Interactive Biosoftware, Rouen, France)
Primer 3	Primer design	http://primer3.ut.ee/
Splice Site Finder	Splice site predictor (scale 0-100)	Accessed through Alamut platform (Interactive Biosoftware, Rouen, France)
USCS Genome Browser	Sequence mapping	http://genome.ucsc.edu/

Table 15: Software

3 METHODS

3.1 POLYMERASE CHAIN REACTION (PCR)

Patient DNA was extracted from peripheral blood and diluted to a concentration of 25 ng/µl and the regions of interest PCR amplified. Unless otherwise specified, the polymerase used was a 7:1 ratio of Taq:Pfu (*Thermus aquaticus:Pyrococcus furiosus).* The following tables show the protocol implemented for PCR reactions in this work.

Reagent	Volume
H_2O	16.0 µl
$MgCl_2$ (15 mM)	2.5 µl
dNTP	2.0 µl
Forward primer	1.0 µl
Reverse primer	1.0 µl
Taq-Pfu	0.5 µl
DNA template	2.0 µl

Table 16: PCR Protocol

Step	Temperature	Time
Initial denaturation	94 ° C	3 min
Denaturation	94 ° C	30 s*
Annealing	57 ° C	30 s*
Elongation	72 ° C	2 min*
Final elongation	72 C	5 min

Table 17: PCR Thermocycler programme

***33 cycles**

3.2 AGAROSE GEL ELECTROPHORESIS AND DOCUMENTATION

This method of separation relies on an electrical current to move negatively charged DNA molecules towards the positively-charged anode. Smaller molecules can pass more readily through the gel matrix than larger ones and enables separation according to molecular size.[42] The PCR amplified DNA was separated on a 1% agarose gel at 200 V, unless otherwise stated. Agarose was dissolved in 1x TBE buffer by heating the mixture to near-boiling point in a microwave. After cooling, 1-2 drops of ethidium bromide were added to enable fluorescence of the DNA fragments under UV light. The mixture was poured into a cast fitted with individual

combs to form the wells. Once hardened, the gel cast was placed into an electrophoresis tank containing 1x TBE running buffer. 4 µl loading buffer and 10 µl PCR product were pipetted into each well. A DNA ladder (GeneRuler) allowed for estimation of the molecular size (kb) of the DNA fragments. Once the fragments were separated adequately, they were visualized using UV light and documented with the Argus 3.0 software.

3.3 GEL PURIFICATION

DNA extraction from the agarose gel was done using the NucleoSpin® Gel and PCR Clean Up kit, which also removed contaminants such as excess nucleotides, primers, enzymes, salts and dyes (Macherey-Nagel manual 2012). The following modifications were made to the protocol:

Step 4: centrifuge for 2 min leave open to dry for 3 min

Step 5: eluted with 25µl Millipore water

3.4 SPECTROPHOTOMETRY

The NanoDrop ND1000 Spectrophotometer measures nucleic acid samples (V=1 µl) on a spectrum of 220nm-750 nm up to concentrations of 3700 ng/µl (Nanodrop1000). The sample concentration given in ng/µl is based on an absorbance of 260 nm. Sample intensities along with blank intensities (deionized water) are used to calculate the sample absorbance.

3.5 CLONING

3.5.1 Ligation

The Taq polymerase creates an adenine overhang on the 3′ end of the amplified PCR fragment, which can then be ligated into the linearized pGEM® T vector due to the complementary thymidine overhang on both 3′ ends of the insertion site (Promega manual, 2010). The protocol used for ligation is shown in the table below:

Reagent	Volume
pGEM®T Vector	0.5 µl
T4 DNA Ligase	1.0 µl
2X Rapid Ligation Buffer	5.0 µl
Insert	3.5 µl

Table 18: Ligation protocol (incubation at 4° C overnight)

3.5.2 Transformation

After approximately 18 h, the ligation product was transformed in competent E. *coli* DM5α cells. The bacteria (stored at – 80°C) were thawed slightly in an ice bath before adding 5 µl of the ligation preparation. A reaction time of 30 min on ice was followed by a heat shock phase of 40 s at 42°C and a 120s recovery time on ice. 900 µl of SOC medium was added and the cells were placed in the incubator shaker Certomat R for 3 h at 37°C and 165 rpm. Prior to plating out 200 µl of the transformed cell mixture, 50 µl X-gal (40 mg/ µl) and 10 µl 100 mM IPTG were added to the LB + ampicillin plates for the purpose of blue-white screening of positive clones. The pGEM® T vector contains promoters on either side of a multiple cloning region within the α-peptide coding region of the β-galactosidase. Proper insertion of the DNA fragment into the vector disrupts the reading of α-peptide, thus preventing functional β-galactosidase from being formed and resulting in white (+) colonies (Promega manual, 2010). The plates were incubated for 18 h at 37° C.

3.5.3 Screening positive clones

Positive colonies were further screened for correct insertion and size via colony PCR. Positive colonies were picked and incubated for 60 min at 37° C in 20 µl LB+ampicillin broth. The colony PCR was performed using M-13 forward and reverse primers (**Table 5**). Gel electrophoresis on a 1% agarose gel and UV documentation were used to separate the DNA fragments and assess the size. From those colonies showing correct insertion and appropriate fragment size, four to six were selected for inoculation. 5 µl of the 20 µl inoculated LB+ampicillin medium was added to 5 ml of LB+ampicillin broth and incubated in the Certomat R for 18 h at 37° C and 165 rpm.

3.6 PLASMID DNA PURIFICATION

The cultured medium was centrifuged at 4000 rpm for 5 min in order to pellet the bacteria cells. Purification was performed using the NucleoSpin® Plasmid kit (Macherey-Nagel manual, 2010). The cell pellet was re-suspended in a buffer before liberating the plasmid DNA

from the host cells via SDS/alkaline lysis. The lysate was then neutralized in order to allow it to bind to the silica membrane of the column. Unwanted debris can be pelleted via centrifugation before loading the supernatant onto the column. The Macherey-Nagel protocol for plasmid DNA preparation (2010) was adhered to, apart from the following modifications:

Step 1: centrifugation 5 min at 4000 rpm
Step 4: discard overflow and dry an additional 60 s at 11 000 g
Step 5: omitted Buffer AW
Step 6: centrifuge 3 min, leave open to dry 3 min
Step 7: elute with 30 µl purified water

The concentration of the plasmid DNA was measured using the NanoDrop ND1000 spectrophotometer.

3.7 SEQUENCING

The plasmid DNA was diluted to 25 ng/µl and 2 µl was used as a template for the sequencing reaction. For the PCR, the BigDye Terminator v1.1.v3.1 Cycle Sequencing Kit from Applied Biosystems was used, according to following protocol:

Reagent	Volume
Big Dye Reaction mix	0.3 µl
5x Buffer	2.0 µl
Primer	1.0 µl
H_2O	4.7 µl
DNA	2.0 µl

Table 19: Sequencing protocol

Step	Temperature °C	Time	Cycle
Initial denaturation	94	2 min	
Denaturation	94	30s	
Annealing	57	30s	30
Elongation	72	3 min	
Final elongation	72	5 min	

Table 20: Amplification conditions

3.7.1 Sequencing PCR products directly

When sequencing PCR product directly, an initial step to remove excess 5′ phosphates and dNTPs was carried out using Antarctic Alkaline Phosphatase and Exonuclease I respectively.

Reagent	Volume
Exo	0.10 µl
AAP	0.25 µl
H_2O	3.65 µl
PCR Product	1.00 µl

Table 21: Exo/AAP digestion

After incubating for 15 min at 37°C and a further 15 min at 80°C, the following was added:

Reagent	Volume
Big Dye Reaction mix	0.30 µl
5x Buffer	1.85 µl
Primer	1.00 µl
H_2O	1.85 µl

Table 22: Sequencing protocol following Exo/AAP digestion

Amplification conditions (Table 20).

The reaction products for sequencing were purified by adding 2 µl NaAc and 50 µl 100% ethanol and vortexing briefly before centrifuging for 30 min at 4°C and 4000 rpm. The supernatant was immediately discarded and the pellet centrifuged again for 2 min at 800 rpm. Next, 70 µl 70% ethanol was added and centrifuged for another 30 min at 4°C and 4000 rpm. After discarding the supernatant and centrifuging for 2 min at 800 rpm, the pellet was dried at RT for 15 min, re-suspended in 15 µl HiDi Formamide and pipetted into the 96 well plate for sequencing (Abi3130x1 Genetic Analyzer). Sequences were analyzed with Chromas 2.

3.8 EXON TRAPPING

This study utilized the pSPL3b expression vector to examine splicing behavior (**Fig. 10**). The vector consists of two exons flanking an intron containing a multiple cloning site, into which the fragment of interest can be inserted. The vector was linealized with restriction enzymes identical to those used to digest the construct. The SV40 promoter region, located

upsteam from the cloning sites, is used to drive transcription in eukaryotic cells, with the *ori* (replication origin) and *amp* (ampicillin resistance) sites being necessary for replication and selection in E. *coli*.[58] As shown in **Fig. 10**, the specific vector primers SD6 and SA4 (**Table 5**) were used for sequencing. Each insert consisted of one, in some cases two, exons with flanking intronic sequence of varying size (**Table 4**).

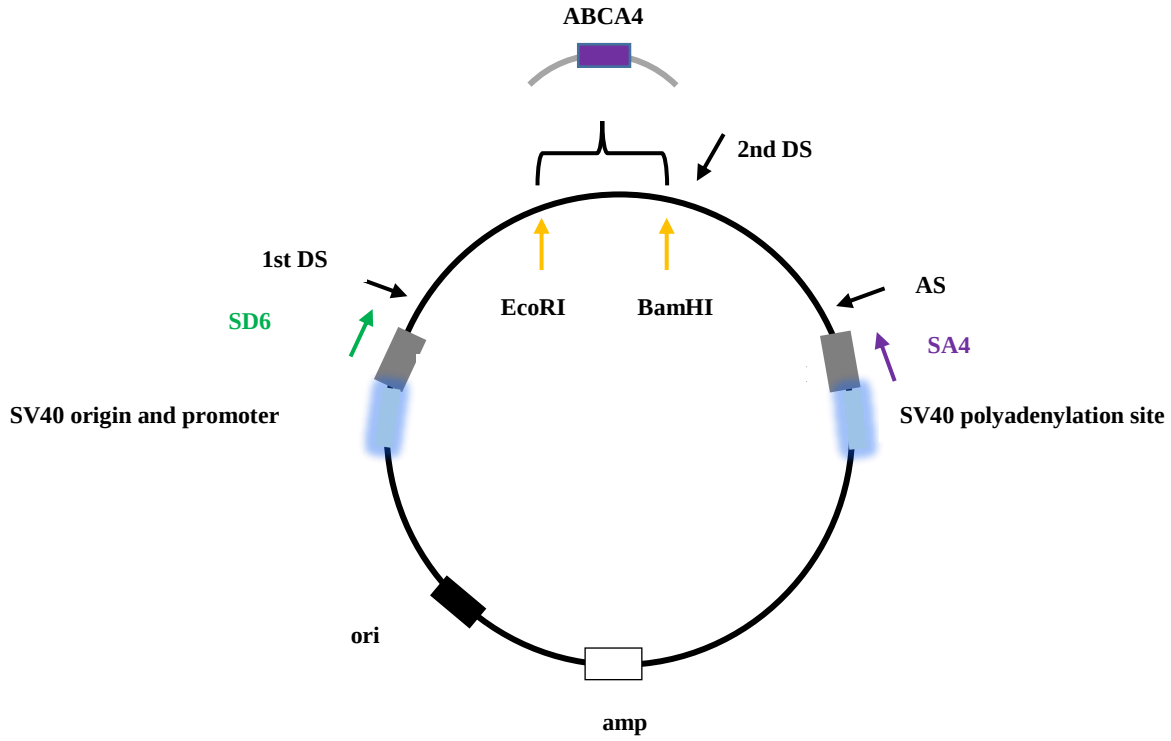

Figure 10: pSPL3b vector

BamHI	G/GATCC
	CCTAG/G
EcoR1	G/AATTC
	CTTAA/G

Figure 11 Restriction enzymes BamH1 and Eco R1

3.8.1 **Preparation of pSPL3b vector**

Reagent	Amount
pSPL3b vector plasmid DNA stock	2.0 µl
EcoR1	0.5 µl
BamH1	0.5 µl
Buffer 4	3.0 µl
H_2O	24.0 µl
Temperature	37°C
Time	Overnight

Table 23: Vector preparation protocol – linearization

The reaction was set up in fourfold. Digested plasmid was loaded on a 1% agarose gel, the band containing the linearized vector was cut out, purified using the NucleoSpin® Gel and PCR Clean Up kit (Macherey-Nagel manual, 2012) according to protocol, and eluded with 50 µl Millipore H_2O. All four were pooled together (V_{Total} = 200 µl), and 5 µl from the pooled vector samples was loaded onto a gel to estimate the concentration. To ensure proper linearization, transformation of competent E. *coli* DM5α was performed according to the following protocol:

Reagent	Amount
pSPL3b vector	1 µl
Sticky end master mix	5 µl
H_2O	24 µl

Table 24: Vector preparation protocol – control transformation

No colonies appeared on the LB + ampicillin plates indicating the vector had been completely linearized.

3.8.2 **Digestion of Plasmid DNA**

A double restriction enzyme digestion with *Eco*RI and *Bam*HI was carried out to first excise the constructs from the pGEM vector for subsequent cloning in pSPL3b. For plasmids of a concentration of 250-500 ng/ µl the following protocol was used:

Reagent	Volume
Plasmid	10.0 µl
EcoRI	0.5 µl
BamHI	0.5 µl
Buffer 4	3.0 µl
H_2O	16.0 µl
Temperature	37°C
Time	Overnight

Table 25: Restriction enzyme digestion protocol

Up to 23 µl of digested plasmid was used for plasmids with very low concentrations. The digested products were fragmented on a 1% agarose gel and purified using the NucleoSpin® Gel and PCR Clean Up kit (Macherey-Nagel manual, 2012)

3.8.3 Ligating into pSPSL3b

4 µl of the purified construct was ligated into 1 µl pSPL3b splicing vector in 5 µl of Instant Sticky-end Ligase Master Mix, transformed in *E. coli* DH5α competent cells (see 3.5.2), and 200 µl plated out. Overnight culture in 5 ml LB+Amp was made from 3 colonies per plate and the plasmid purified. In order to confirm proper insertion, the digestion (**Table 25**) was repeated with a shorter incubation time (2h), and the product fragmented on a 2% agarose gel. All clones selected for transfection were sequenced before use to verify correct clone integrity. A colony stock of pSPL3b + construct was preserved in a glycerin solution (130 µl stock in 870 µl 99.5 % glycerin) and stored at -80°C.

3.9 TRANSFECTION OF HEK 293 EBNA CELLS

DMEM+ medium refers to Dulbecco`s Modified Eagle Medium supplemented with FCS and pen/strep (**Tables 10 & 12**). **DMEM-** refers to medium without additives. In order to enable cell adherence, thus increasing transfection efficiency, the culture dishes were coated with poly-L-lysine. For this purpose, 6-well plates were incubated at 37°C overnight with 2 ml of poly-L-lysine solution (1:1 PBS1x: poly-L-lysin+pen-strep).

Substance	Amount
Poly-L-Lysin	1000 µl
Pen-Strep	500 µl
from above solution	50 µl
in PBS 1x	50 µl

Table 26: Poly-L-Lysine solution

The solution was removed, and the wells rinsed with 1xPBS before sowing.

3.9.1 Splitting and sowing HEK 293 EBNA cells

Prior to beginning, a thorough disinfection of the working space with 70% ethanol, including all instruments under the cell culture hood, was carried out. The DMEM+ medium and trypsin were warmed in a 37°C water bath for 30 minutes. Cell growth and confluency were assessed under the microscope before splitting, which was generally done at a ratio of 1:5.

The old medium was removed with a glass Pasteur pipette, then 5 ml of 1x PBS carefully pipetted against the petri dish wall, redrawn, and 5 ml 0,5M EDTA+1xPBS added (incubation: 7 min at 37°C). The 5 ml 0,5M EDTA+1xPBS was removed and 3 ml of 2x trypsin added (incubation: 3 min at 37°C). 7 ml DMEM+ was added to the trypsin to re-suspend the cells. To do so, the medium was repeatedly pipetted up and down while turning the dish, until all cells were in suspension. This cell solution was then transferred to a 15 ml Falcon® tube and centrifuged for 3 min at 1500 rpm. The supernatant was removed, the pellet re-dissolved in 10 ml of fresh DMEM+ medium, of which 2 ml was sowed in 8 ml of fresh DMEM+ medium (splitting 1:5).

3.9.2 Transfection reaction

For transfection, confluency should ideally be 50-70%. 18 h prior to transfection, the HEK 293 EBNA cells were split and sown at 1 000 000 cells/ well in 6 well plates. The transfection was performed with TransIT®-LT1 Transfection Reagent (Mirus). For a 6 well plate, 16 µl of chloroquine was added to 16 ml DMEM+ medium. The old DMEM+ medium was removed from the wells and 2.5 ml of the chloroquine-enriched DMEM+ added (incubation: max. 90 min at 37°C). After 60 min, two Eppendorf cups per plasmid were prepared:

Cup 1: 250 µl DMEM- + 3 µg plasmid
Cup 2: 250 µl DMEM - + 6 µl TransIT®-LT1 transfection reagent
(1 µg plasmid: 2 µl TransIT®-LT1 Transfection reagent).

Both cups were vortexed and incubated for five min at room temperature before adding the contents of **cup 1 to cup 2** and incubating for a further 25 min at room temperature.

After a 90 min total incubation time, the chloroquine-enriched DMEM+ was replaced with 2 ml fresh DMEM+ before adding 500 µl of the Mirus/construct. To avoid a rapid change

in pH, the transfection mix must be added very carefully while gently shaking the plate back and forth.

3.9.3 Harvesting of HEK 293 EBNA cells

The cells were incubated post-transfection for 72 h and harvested as follows: the DMEM+ medium was discarded and each well washed with 2 ml 1x PBS. A solution of 5 ml RLT Buffer (RNeasy Mini Kit, Qiagen) and 50 µl β-Mercaptoethanol was prepared. After taking up the 2 ml 1x PBS, 350 µl of the RLT Buffer/β-Mercaptoethanol was added to each well. Using a sterile cell scraper, the wells were scraped to loosen the cells, and the cell-containing liquid was transferred to a 2ml tube. This step was done twice to increase the yield (V_{Total} = ca. 700 µl).

3.10 RNA ISOLATION

Total cytoplasmic RNA extraction from the HEK 293 EBNA cells was done using RNeasy Mini Kit (Qiagen). In order to shear the DNA, the 700 µl cell suspension was aspirated and flushed out of a syringe seven times. Subsequently, 700 µl 70% ethanol was added, homogenized and pipetted up and down several times. The cell suspension was loaded onto the column (V_{max} 700 µl), centrifuged for 15 s at 10 000 rpm, the supernatant discarded, and this step repeated with the remaining 700 µl.

The column was washed with 350 µl RW-1 buffer and centrifuged for 15 s at 10 000 rpm before adding a solution of 10 µlDNase + 70 µlRDD buffer, incubated for 15 min at room temperature and washed as follows:

Wash step	Buffer	Volume	Centrifuge time (10 000 rpm)
1	RW-1	350 µl	15 s
2	RPE	500 µl	15s
3	RPE	500 µl	2 min

Table 27: RNA isolation: washing steps

After the final washing step, the column was placed in a clean 2 ml collection tube and centrifuged for 2 min at maximum speed. The RNA was eluted in 30 µl RNase free water by centrifuging 60 s at 9000 rpm, the concentration measured using the ND1000 Spectrophotometer, and the samples stored at -80°C.

3.11 cDNA Synthesis via Reverse Transcriptase PCR

Using the RevertAid ™ H First Strand cDNA Synthesis Kit and Random Hexamer primer, the RNA isolated from the HEK 293 EBNA cells was reverse transcribed into complementary DNA (cDNA) for further analyses as follows:

Step	Reagent	Volume/Amount
1	Random Hexamer Primer	1.0 µl
	RNA	5.0 µg
	H_2O, nuclease-free	12.5 µl
2	Incubate	5 min 70°C
3	Place on ice	
4	5 x Buffer	4.0 µl
	NTPs	2.0 µl
	Reverse Transcriptase	0.5 µl

Table 28: cDNA synthesis protocol

Temperature	Time
25 ° C	10 min
42 ° C	60 min
70 ° C	10 min

Table 29: cDNA synthesis Thermocycler programme

Storage of cDNA -20°C

3.12 cDNA PCR

To characterize and carry out further analysis of the splicing behavior in the transfected HEK 293 EBNA cells, a PCR using the synthesized cDNA was performed (**Table 30**) according to the method outlined in 3.1. Separating the cDNA fragments on a 2 % agarose gel via electrophoresis (3.2) enabled an initial visual analysis to compare product sizes to the calculated estimations, based on an assumption of correct splicing activity in the normal allele.

Reagent	Volume
H_2O	14.9 µl
GoTaq buffer	5.0 µl
dNTP	2.0 µl
SD 6	1.0 µl
SA 4	1.0 µl
Go-Taq (cc 5U/ µl)	0.1 µl
Master Mix	24.0 µl
DNA Template	1.0 µl

Table 30: cDNA PCR Protocol

Amplification conditions: (see 3.1)

If correct splicing occurred, we expected to observe the phenomenon depicted by Product B (**Fig. 12**). However, should a splice site be diminished in strength due to a mutation, the region of interest may become spliced out entirely, as is shown in Product A. Alternatively, a cryptic site may be used, resulting in a product size deviating from the transcript of the normal allele, as seen in Product C.

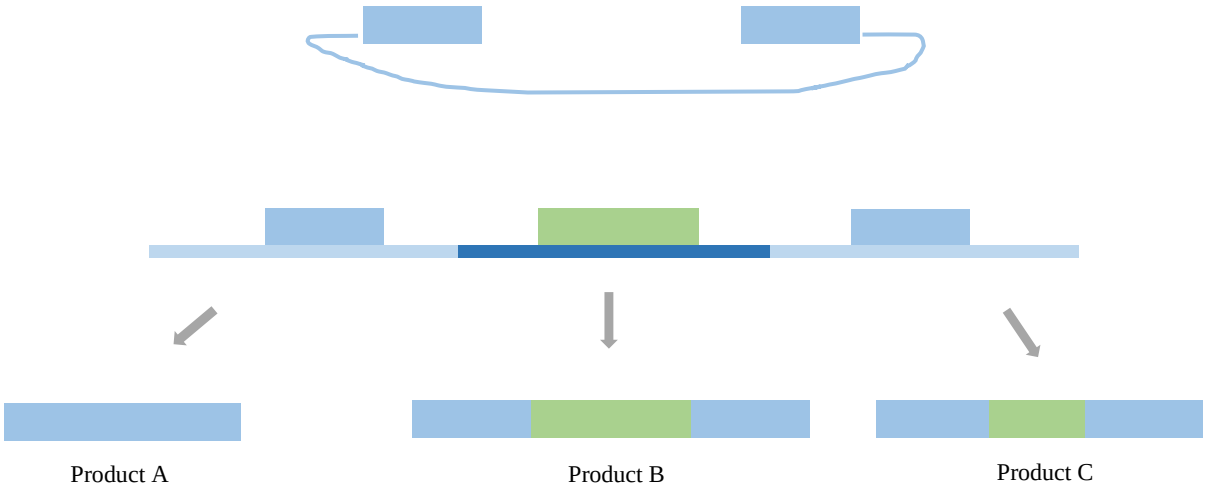

Figure 12: Possible splicing scenarios, depending on variant effect on splicing

In order to verify the nature of each band, products were cloned and/or sequenced according to the methods described in 3.5 through 3.7.

4 RESULTS

Prior to beginning this dissertation, the coding region including the immediate flanking intronic sequences of *ABCA4*, *CNGB3* and *ELOVL4* in patients clinically diagnosed with Stargardt disease or cone-rod dystrophy had been analyzed at the Institute for Human Genetics at the University of Regensburg, Germany. Of the total 152 unique variants found (**Table 1**), those with a minor allele frequency of <1% were subjected to further *in silico* testing using five bioinformatics prediction programmes (**Table 15**) to assess the spliceogenic potential. The purpose of the dissertation was to perform functional analyses of splicing behaviour in variants (N=21) that that had been predicted *in silico* to affect splicing.

4.1 RESULTS OF BIOINFORMATIC PREDICTIONS OF VARIANTS' EFFECT ON SPLICING

Pat. ID (Medistar)	Ex ID	Variant	Nearest canonical splice site	Predict-ion for	SSF [≥70]	MaxEnt [≥0]	NNSplice [≥0.4]	Genesplicer [≥0]	HSF [≥60]
18962	A	c.67-1G>C	Exon 2 - c.67 (A)	c.67 (A)	95.2⇒ lost	10.87 ⇒ lost	0.99 ⇒ lost	12.03 ⇒ lost	92.11 ⇒ lost
16843	G	c.67-2A>G	Exon 2 - c.67 (A)	c.67 (A)	95.2⇒ lost	10.87 ⇒ lost	0.99 ⇒ lost	12.03 ⇒ lost	92.11 ⇒ lost
17412	U	c.160+2T>C	Exon 2- c.160 (D)	c.160 (D)	81.30 ⇒ 78.5 (-3.4%)	6.12 ⇒ lost	0.94 ⇒ lost	No prediction	86.00 ⇒ lost
17716	H	c.179C>T	Intron2 - c.161-1	c.177 (D)	gained⇒ 77.92	gained ⇒ 5.22	gained ⇒ 0.59	gained⇒ 4.39	No predict-ion
15485	F*	CNGB3 c.991-3T>G	Intron 8 - c.991 (A)	c.991-2 (A)	gained ⇒ 85.58	gained ⇒ 9.77	gained ⇒ 0.99	gained ⇒ 1.79	gained ⇒ 81.99
15485		CNGB3 c.991-3T>G	Exon 9 - c.991 (A)	c.991 (A)	81.65 ⇒ 77.00	7.60 ⇒ lost	0.94 ⇒ lost	no prediction	82.86 ⇒ 80.25
15282	I	c.1239+1G>C	Exon 9 - c.1239 (D)	c.1239 (D)	81.75 ⇒ lost	5.55 ⇒ lost	0.61 ⇒ lost	6.20 ⇒ lost	85.84 ⇒ lost
20364	J	c.1937+1G>A	Exon 13 - c.1937 (D)	c.1937 (D)	no prediction	7.90 ⇒ lost	0.83 ⇒ lost	4.22 ⇒ lost	81.10 ⇒ lost

21529	K	c.1819G>A	Exon 13 c.1761(A)	c.1837 (A)	No change	7.70 ⇒ 6.36 (-17.4%)	0.69 ⇒ 0.65 (-5.8%)	2.68 ⇒ 2.09 (-21.8%)	no predict-ion
15023	L	c.2894A>G	Exon 19 c.2744 (A) c.2918 (D)	c.2895 (A)	gained ⇒ 75.24	gained ⇒ 4.35	no prediction	no prediction	no predict-ion
16178	M	c.3808G>T	Exon 25 - c.3813 (D)	Exon 25 - c.3813 (D)	gained ⇒ 73.14	gained ⇒ 4.35	-	-	-
15286	N	c.4352+1G> A	Intron 28 - c.4352 (D)	Exon 29 - c.4352 (D)	73.65 ⇒ lost	10.27 ⇒ lost	0.98 ⇒ lost	4.67⇒ lost	no predict-ion
14686	O	c.4354G>T	Exon 30 - c.4353 (A)	c.4353-1 (D)	no prediction	gained ⇒ 4.45	gained ⇒ 0.56	no prediction	gained ⇒ 75.25
16827	P	c.4457C>T	Exon 30 - c.4353 (A)	c.4467 (A)	84.51 ⇒ 87.79	9.24 ⇒ 9.79	0.91 ⇒ 0.93	6.51 ⇒ 7.23	89.64 ⇒ 90.35
21066	B	c.4773+3A> G	Exon 33 - c.4773 (D)	c.4773 (D)	77.81 ⇒ 73.45 (-5.6%)	7.48 ⇒ 3.14 (-58.1%)	0.96 ⇒ lost	1.99 ⇒ lost	86.04 ⇒ 74.99
15977	C	c.4919G>A	Exon 35 - c.4849 (A)	c.4921 (A)	gained ⇒ 81.21	gained ⇒ 5.78	no prediction	gained ⇒ 1.97	gained ⇒ 88.40
17002	D	c.5018+2>C	Exon 35 - c.5018 (D)	c.5018 (D)	72.34 ⇒ lost	5.32 ⇒ lost	0.87 ⇒ lost	1.11 ⇒ lost	81.15 ⇒ lost
16272	Q	c.5196+1G> A	Intron 36 c.5196+4 (D)	Exon 36 - c.5196 (A)	77.87 ⇒ lost	10.44 ⇒ lost	0.98 ⇒ lost	6.49 ⇒ lost	83.28 ⇒ lost
17575	R	c.5189G>A	Intron 36 c.5196 (D)	Exon 36 - c.5191 (A)	gained ⇒ 78. 81	gained ⇒ 6.6 6	no prediction	gained ⇒ 3.49	gained ⇒ 82.96
20882	S	c.5312+1G> A	Exon 37 - c.5312 (D)	c.5312 (D)	81.13 ⇒ lost	8.84 ⇒ lost	0.99 ⇒ lost	2.22 ⇒ lost	90.99 ⇒ lost
17002	E	c.6386+2C> G	Exon 46 - c.6386 (D)	c.6386 (D)	91.79 ⇒ lost	-	-	-	-
16518	T	c.6732G>A	Exon 48 - c.6730 (A)	c.6730-1 (D)	gained ⇒ 73 .31	gained ⇒ 5.39	gained ⇒ 0.71	no prediction	75.74 ⇒ 76.90 (+1.5%)

Table 31: Alamut predictions for ABCA4 (N=20) and CNGB3* (N=1) variants investigated in this study, grouped according to exon in ascending order

Variants completed during this doctoral dissertation are highlighted in bold grey (far left column: Patient ID); the remaining were completed in a subsequent study (Baier, 2014)[89].

***A*: acceptor site; *D*: donor site; *SSF*: Splice Site Finder; *MaxEnt*: Maximum Entropy Scan*; NNsplice:* Neural Network Splice; *GeneSplicer:* Gene splicer; *HSF*: Human Splicing finder (Table 3)**

In vitro investigations in this study relied on the exon trapping method using the pSPL3b vector. Following replication and selection in E. *coli*, one construct containing the normal allele and another containing the mutation were inserted into the vector. The plasmids were transfected in transient cells, the RNA isolated, reverse transcribed, and RT-PCR amplified using the vector primers (**Table 5**). The cDNA products were separated via electrophoresis and their sizes compared to the calculated estimations based on an assumption of correct splicing activity in the normal allele. The products were subsequently cloned and/or sequenced to verify the nature of each band. Several were also investigated via fragment analysis in a later project carried out by Maria Baier, [89] and are cited as such.

4.2 CANONICAL SITE VARIANTS

4.2.1 In vitro splicing effect of the ABCA4 c.5312+1G>A variant

All five bioinformatics tools foresaw a total loss of regular donor site for this guanine to adenine change in the highly conserved first base of the splicing donor site.

Figure 13: Schematic representation of exon 37, position of ABCA4 variant c.5312+1G>A, and predicted effect of loss of donor site

As can be seen in the gel electrophoresis documentation (**Fig.14**), amplification of the cDNA transcribed from the normal allele sequence using primers specific to the artificial exons in the pSPL3 vector produced a correctly spliced product (310 bp). The sequence containing the variant resulted in a product where the construct had been completely spliced out (194 bp; c.5197_5312del; p.Asn1734Glyfs*14), indicating that the splice sequences of internal exons had been used. The use of cryptic sites within the pSPL3b vector is a common problem seen in the exon-trapping method, [58, 59] which is why it is important to include the normal allele as a

negative control. Because this nucleotide change is at a canonical splice site, it is not surprising that the *in vitro* results concurred with the *in silico* predictions for total loss of donor site.

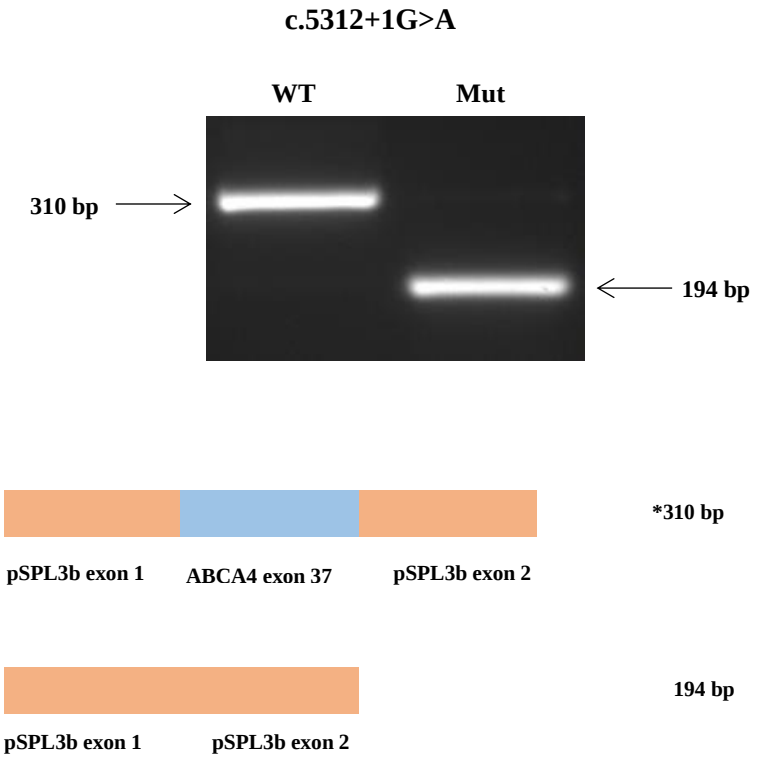

Figure 14: *Above*: cDNA gel electrophoresis of ABCA4 variant c.5312+1G>A transcribed from wild-type and mutant sequence *indicates correctly spliced reference sequence *Below*: schematic representation of gel electrophoresis

4.2.2 In vitro splicing effect of the ABCA4 c.5018+2T>C variant

This thymine to cytosine change at the second base of the splicing donor site was predicted by all five *in silico* tools to lead to a complete loss of regular donor site.

Figure 15: Schematic representation of exon 35, position of ABCA4 variant c.5018+2T>C, and predicted effect of loss of donor site

In vitro results of the amplification of the cDNA containing the normal allele sequence showed a correctly spliced product (364 bp) in this clone (**Fig.16**). In addition, a smaller band is present

with vector-only sequence (194 bp; p.Val1617Alafs*113), indicating that even in normal allele sequence some constructs will excise this exon. Amplification of the cDNA transcribed from the variant sequence resulted in several products. The largest product (538 bp) arose due to the loss of the donor site of exon 35 of *ABCA4*, and consequently included intron 35 and pSPL3b sequence up to the next donor site in the vector. The strongest band visible on the gel (194 bp) contained vector-only sequence.

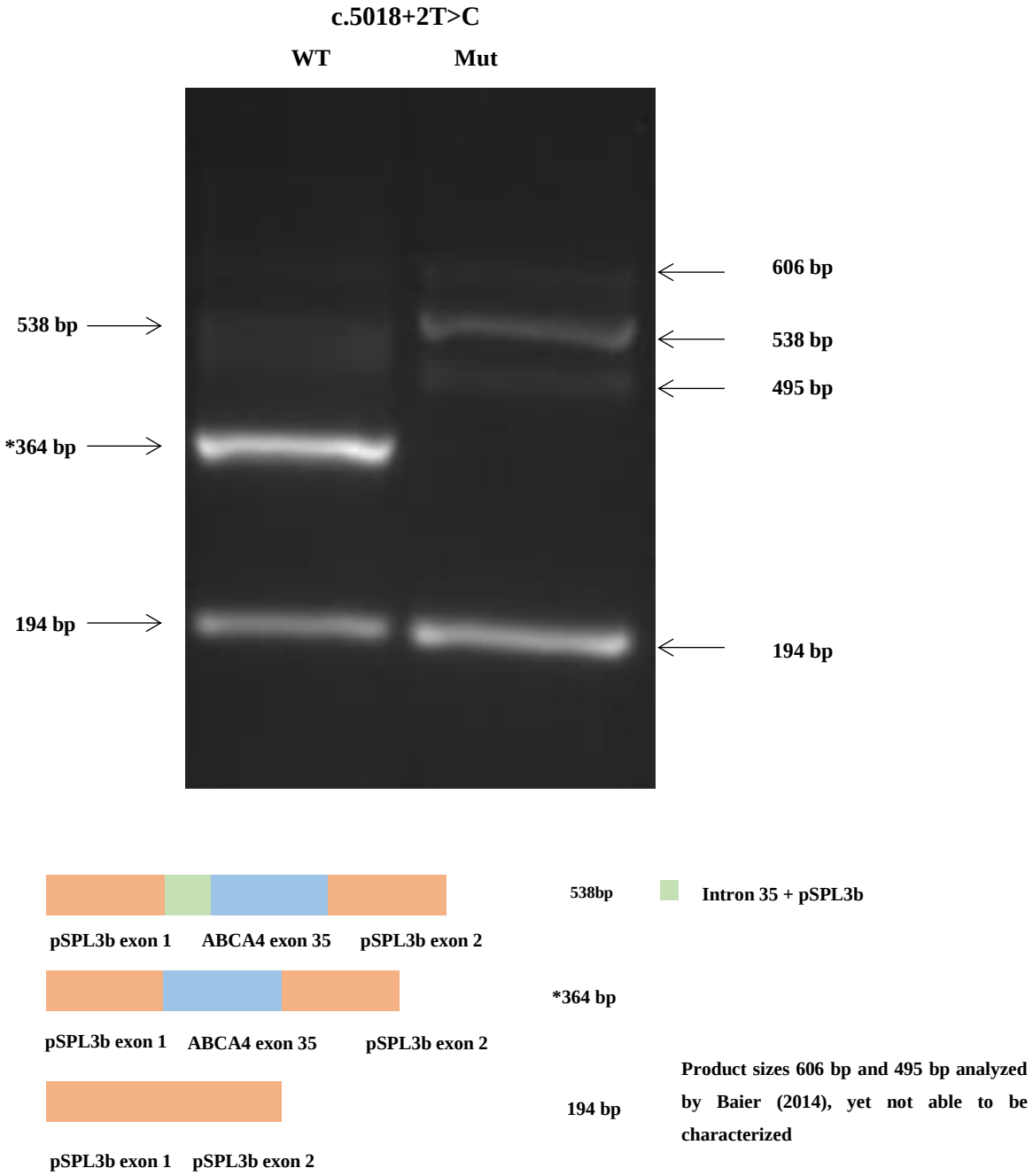

Figure 16 : *Above*: cDNA gel electrophoresis of ABCA4 variant c.5018+2T>C transcribed from normal allele and mutant sequence *indicates correctly spliced reference sequence *Below:* schematic representation of gel electrophoresis results

The absence of an RT-PCR product containing correctly spliced exon 35 in the mutant transcript is indicative of total loss of splice donor potential at the canonical site due to the variant. The *in vitro* results coincide with *in silico* predictions that the donor site would be completely abolished, even though some donor sites tolerate and use a cytosine at the +2 position.

4.2.3 In vitro splicing effect of the ABCA4 c.1239+1G>C variant

As in the previous two examples involving a single nucleotide change at a canonical site, all five programmes predicted a complete loss of the regular donor site for this guanine to cytosine change in the first base of the splicing donor.

Figure 17 : Schematic representation of exon 9, position of ABCA4 variant c.1239+1G>C, and predicted effect of loss of donor site

The gel electrophoresis (**Fig. 18**) revealed a correctly spliced product (334 bp) from amplifying cDNA transcribed from the normal allele sequence. The band of 454 bp was generated from use of a cryptic acceptor site in *ABCA4* intron 9 (c.1239+152/153). The extra exon that was included contained sequence from intron 9, as well as pSPL3b vector sequence up to the alternative donor site located in the vector. cDNA amplification of the variant sequence cDNA failed to produce any correctly spliced product. The strongest visible band (194 bp; c.1100_1239del; p.Thr367Serfs*6) contained vector-only sequence. Also detectable was a large product (607 bp) generated by correct splicing at the first donor site, but rather than splicing at the end of exon 9, the guanine-thymidine donor 2 of the vector was used and included pSPL3b intronic sequence. Similarly, some transcripts appear to have arisen from using an acceptor at c.1100-45/44 (377 bp).[89] The smaller product (308 bp; c.1100_1125del; p.Thr367Lysfs*28) is probably the result of using a cryptic acceptor at c.1124/25.[89] These latter two products could not be sequenced, therefore their nature is merely hypothesized based on *in silico* predictions and congruency with observed sizes. [89]

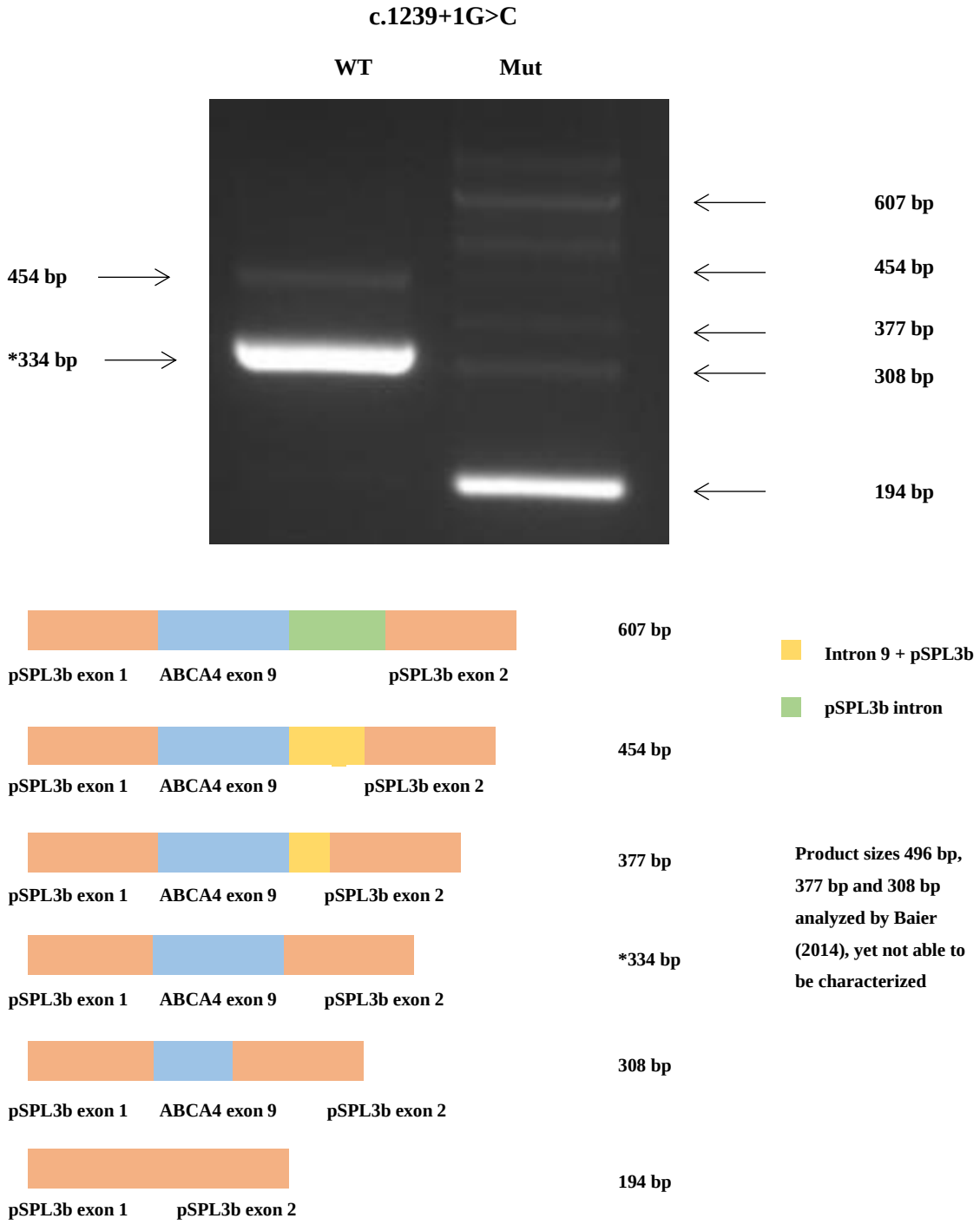

Figure 18 : *Above*: cDNA gel electrophoresis of *ABCA4* variant c.1239+1G>C transcribed from normal allele and mutant sequence *indicates correctly spliced reference sequence Below*: schematic representation of gel electrophoresis results

These *in vitro* results support *in silico* predictions that the nucleotide change at the +1 position causes the regular donor site to become too weak for correct splicing to occur.

4.3 INTRONIC VARIANTS

4.3.1 In vitro splicing effect of the ABCA4 c.4773+3A>G variant

This adenine to guanine change at the +3 position of the intron is a site at which some nucleotide variance is tolerated (**Fig. 4**). Two of the five programmes predicted a loss of the donor site, whereas three merely foresaw a reduction in strength.

Figure 19 : Schematic representation of exon 33, position of ABCA4 variant c.4773+3A>G, and predicted effect of loss/reduction of donor site

Due to the small intron size between exons 33 and 34, both exons were included in the construct to provide a more natural sequence environment. The top band (375 bp) present in both the normal allele and mutant cDNA corresponds to the correctly spliced product and includes both exon 33 and 34. The bottom band (300 bp; c.4774_4848del; p.Gly1592_Lys1616del) contains exon 33 only. As in the previous cases, there is also a band at 194 bp containing vector-only sequence (c.4668_4848del; p.Tyr1557Cysfs*45). The smaller 291 bp product probably arose from the use of a cryptic donor site from exon 33 and is missing the last nine bases of exon 33 (c.4765_4773del; p.Val1589_Gly1591del).[89] This may have only a minor effect on protein function, as only three amino acids are lost. The product of 269 bp contains only exon 34.

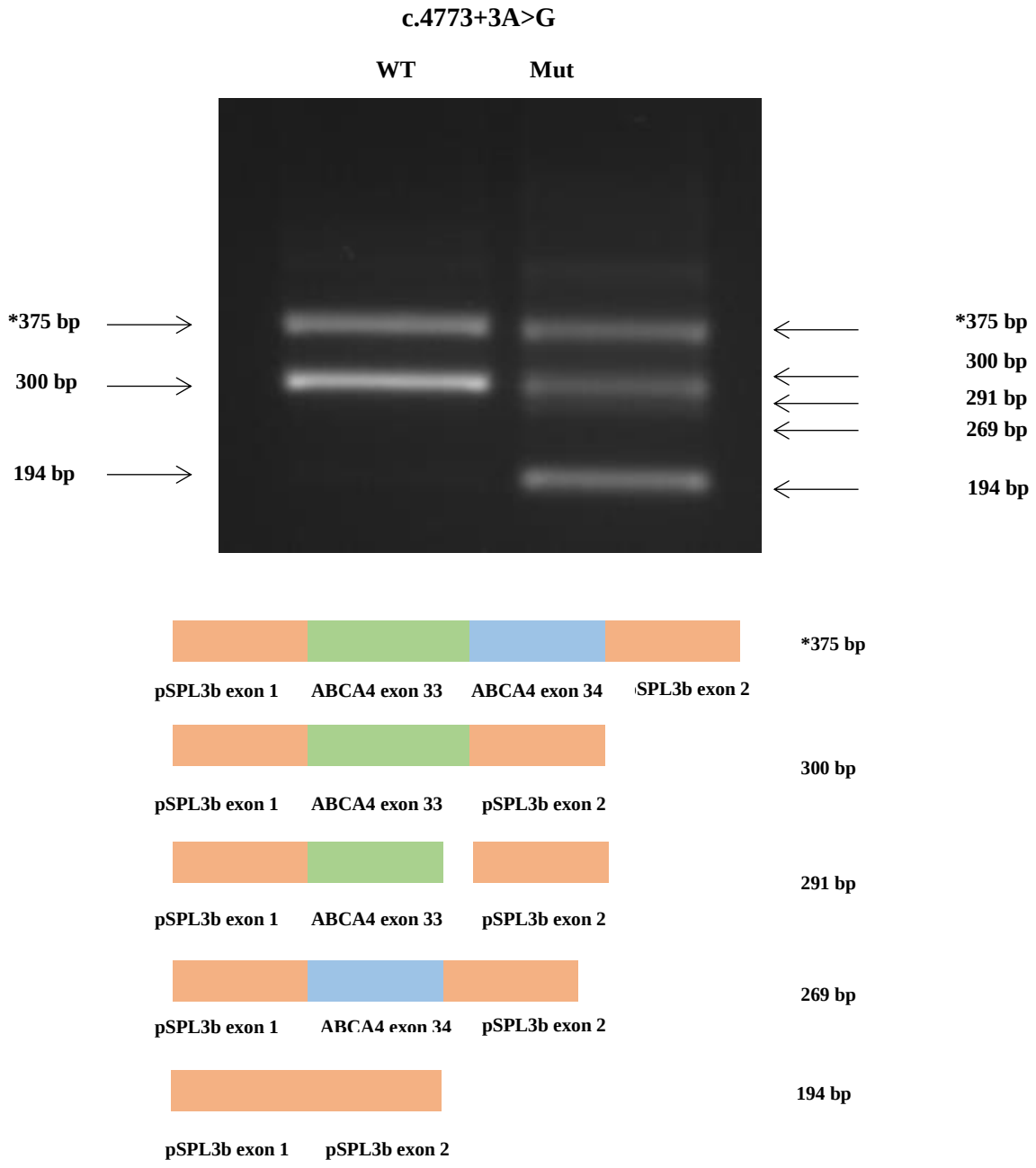

Figure 20 : *Above*: cDNA gel electrophoresis of *ABCA4* variant c.4773+3A>G transcribed from normal allele and mutant sequence *indicates correctly spliced reference sequence *Below*: schematic representation of gel electrophoresis results

In the case of c.4773+3A>G, the effect on the protein level as a result of exon skipping is difficult to foresee. The nucleotide change is found in exon 33, and whether exon 34 would also be skipped *in vivo* remains speculative. This appears to be a relatively frequent phenomenon, as RNA sequencing by other groups has demonstrated similar results to those for normal allele and mutant transcripts observed here. For example, exon 34 may be spliced out in some isoforms even in healthy subjects, or both *ABCA4* exon 33 and 34 may be skipped.[87, 88] Others

report skipping of *ABCA4* exon 28 and 29 in normal retinal cells.[62] These results, coupled with those of this study, seem to indicate that particular regions of *ABCA4* can be polyisoformic, thus making it difficult to evaluate what impact *ABCA4* c.4773+3A>G would truly have *in vivo*. Nevertheless, despite some variance being tolerated at the +3 position, these *in vitro* results support the *in silico* predictions that this variant would adversely affect mRNA splicing and, at the very least, likely reduce the amount of normal protein.

4.3.2 In vitro splicing effect of the CNBG3 variant c.991-3T>G

This thymine to guanidine change at the intronic -3 position was the only *CNGB3* variant included in the study. It was predicted to be spliceogenic and lead to the loss of the canonical acceptor site, resulting in an alternative acceptor site and the inclusion of two extra bases at the 5′ end of exon 9.

Figure 21: Schematic representation of exon 9, position of CNGB3 c.991-3T>G variant, and predicted effect of loss of canonical acceptor site and creation of alternative acceptor site

Due to the limited size difference of the transcript generated from the mutant sequence, the effect cannot be observed in the gel electrophoresis documentation (**Fig.22**). However, sequencing of the normal allele and mutant RT-PCR products confirmed the *in silico* prediction of a novel acceptor site being used, resulting in a 2 bp insertion (p.Tyr331Serfs*12) and complete absence of normal transcript. Because this leads to a frame-shift with a stop codon being generated 12 amino acids downstream, the variant has a clear pathogenic effect. The stop codon is only 31 bp from the next exon junction, making it unlikely to be degraded by the nonsense mediated decay mechanism, [83] thus increasing the pathogenic nature of this variant.

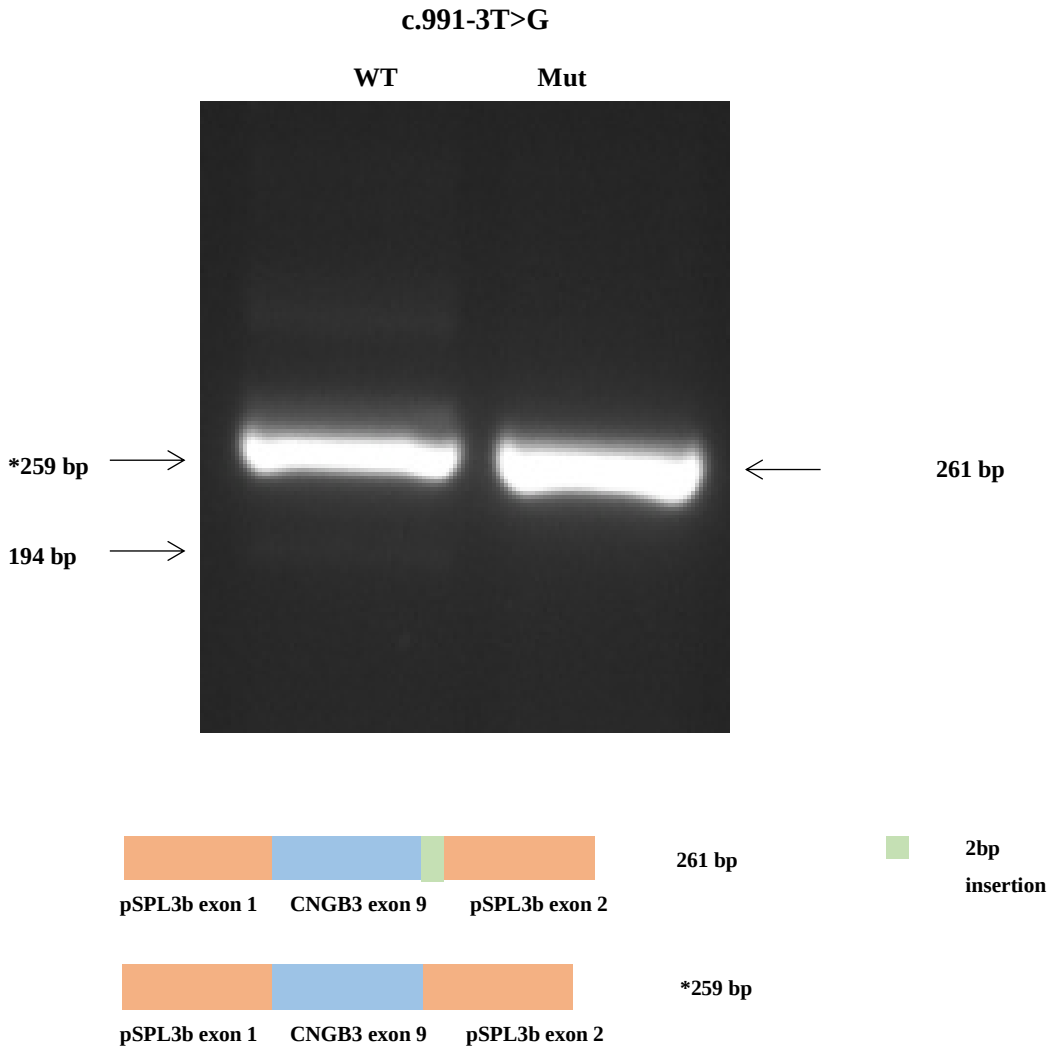

Figure 22: ***Above*****: cDNA gel electrophoresis of CNGB3 c.991-3T>G variant transcribed from wild-type and mutant sequence * indicates correctly spliced reference sequence Below: schematic representation of gel electrophoresis results**

4.4 EXONIC VARIANTS

Nine of the 21 variants included in this study were exonic. An increasing number of studies are focusing on exonic variants' effect on splicing and their potential disruption of the enhancing and silencing motifs necessary for correct exon recognition.[50,60,80]

4.4.1 In vitro splicing effect of the ABCA4 variant c.4919G>A

This guanine to adenine change mid exon is located 70 bases from the next acceptor site. The use of novel cryptic splice sites is a common phenomenon due to exonic variants,[51] and in this case, four of the five *in silico* tools predicted the abolishment of an existing cryptic acceptor site and the creation of another in its vicinity.

Figure 23: Schematic representation of exon 35, position of ABCA4 variant c.4919G>A, and predicted effect of loss of canonical acceptor site and creation of alternative acceptor site

The gel electrophoresis documentation shows a correctly spliced product obtained from the normal allele cDNA (**Fig. 24**: 364 bp). Additionally, transcripts with vector-only sequence in which the region of interest was spliced out are evident (194 bp; c.4849_5018del; p.Val1617Alafs*113). The large product of 538 bp arose from the inclusion of intronic sequence.[89] cDNA amplification of the transcribed variant sequence showed the correctly spliced 364 bp product, transcripts void of reference sequence (194 bp), and those with intronic inclusion (538 bp). Sequencing confirmed that the 294 bp product arose from a new acceptor site being used at c.4919/20 and is missing 72 bp at the 5′ end of exon 35 (c.4850_4921del; p.Val1617_Arg1640del). The 464 bp product is hypothesized to have arisen from using an acceptor site upstream from the canonical one (c.4849-102/101) and includes intron 34 sequence.[89]

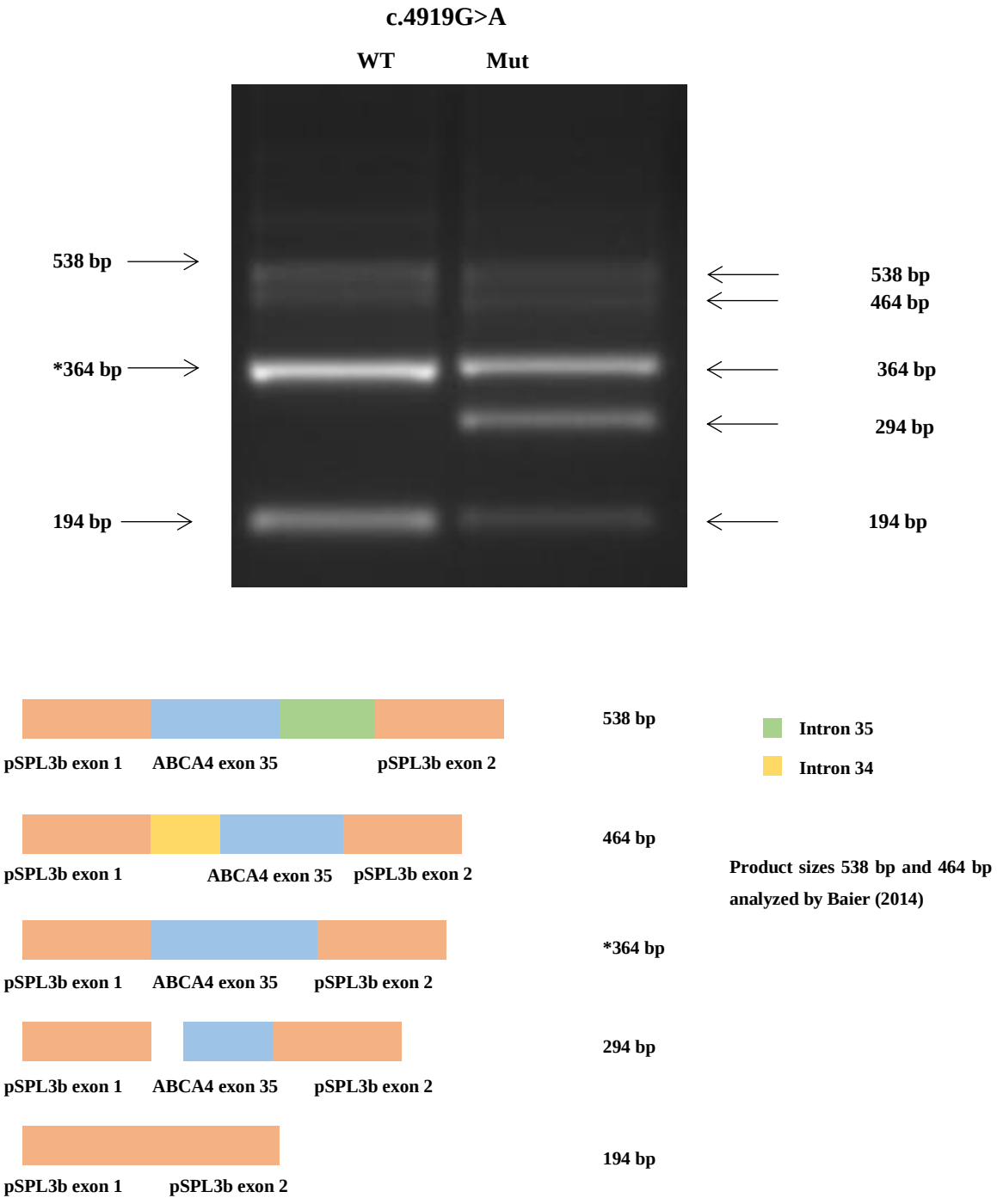

Figure 24: ***Above:*** **cDNA gel electrophoresis of ABCA4 variant c.4919G>A transcribed from wild-type and mutant sequence *indicates correctly spliced reference sequence** ***Below*****: schematic representation of gel electrophoresis results**

These *in vitro* results coincide with the *in silico* predictions that this exonic variant will lead to the use of a cryptic splice site and consequently disrupt splicing.

4.4.2 In vitro splicing effect of the ABCA4 variant c.4354G>T

This guanine to thymine change is near an acceptor site and *in silico* predictions indicated a new donor site being generated at the -1 position directly adjacent to the acceptor site.

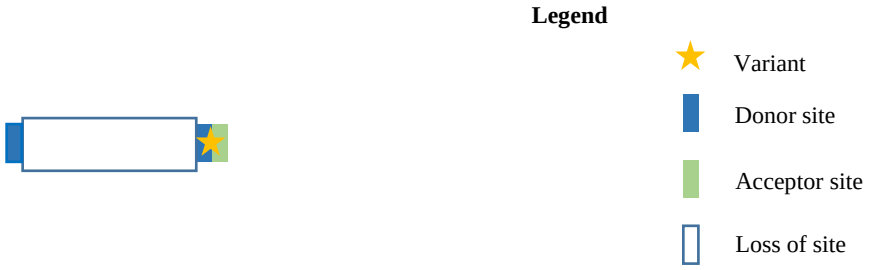

Figure 25: Schematic representation of exon 30, position of *ABCA4* variant c.4354G>T, and predicted effect of the creation of a novel donor site at the -1 position

As was the case with the *CNGB3* c.991-3T>G variant, the high percentage gel electrophoresis results (**Fig.26**) failed to show any visible size differences between the normal allele sequence and the variant transcript. Subsequent investigation via sequencing and fragment analysis of the cDNA transcribed from the normal allele demonstrated correctly spliced product (381 bp), as well as a 308 bp product missing the last 73 bp of exon 30 due to use of a cryptic splice donor site (c.4467/68; p.C1490Efs*12). The product of 411 bp is hypothesized to have arisen from the use of a donor site downstream from the canonical one (c.4539+31/32), and likely includes 30 bp of intron 30 (p.Q1513_R1514insVPDLQTTGPQ).[89] The large product at 615 bp resulted from the inclusion of intronic sequence.[89] Fragment analyses revealed that all transcripts containing the variant also additionally exist with a four base pair deletion at the 5′ end of the exon (304, 377, 407, and 611 bp).[89] These findings support *in silico* predictions that the appearance of a new donor site disrupts correct splicing, even though no evidence of the novel donor site being used was seen in the *in vitro* investigation. This may be because the construct only contains a small region of the natural intron. A cryptic acceptor may be present in the intervening sequence 29 and including the entire sequence in the construct may have made the effect of the mutation giving rise to a novel donor site evident.

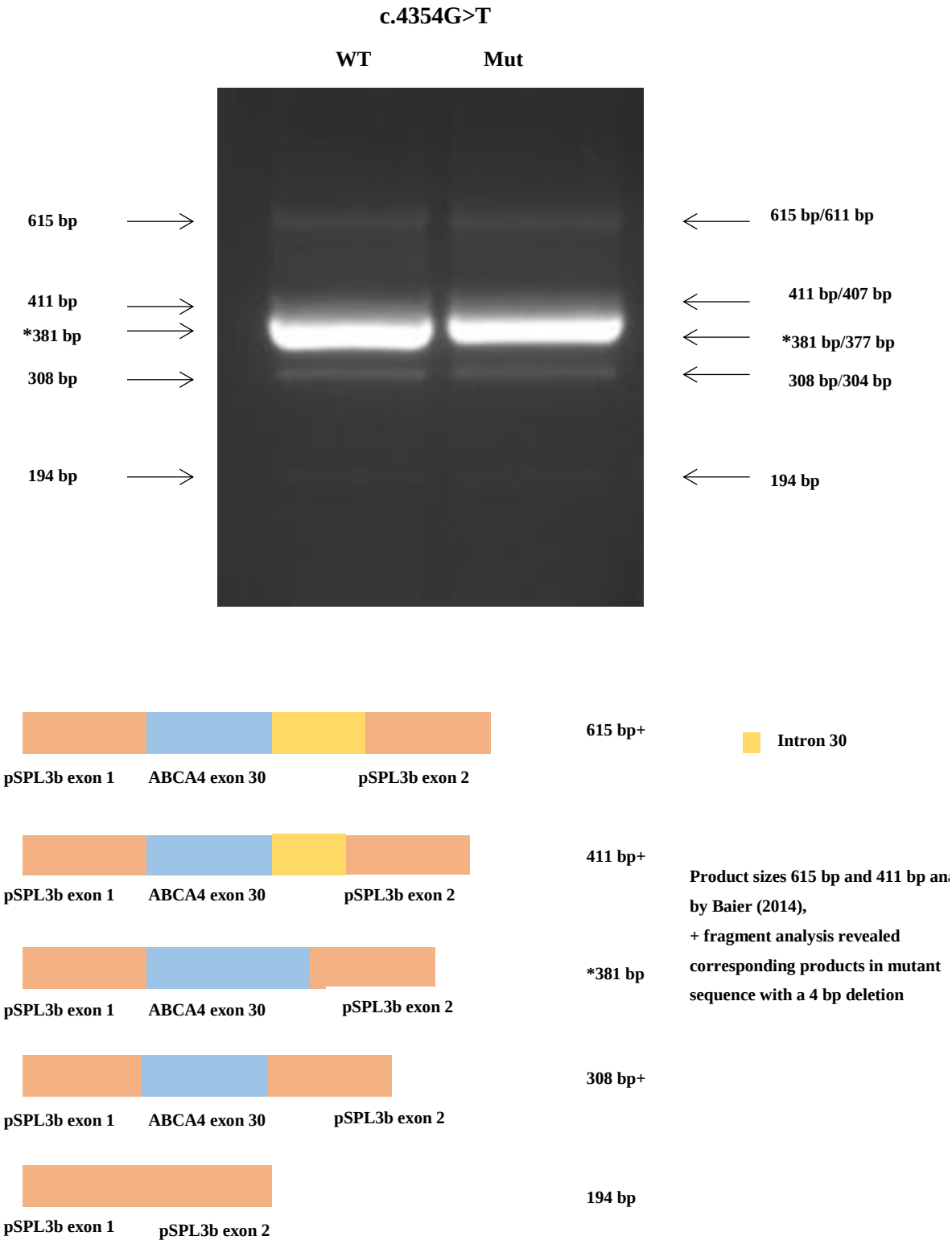

Figure 26: ***Above:*** **cDNA gel electrophoresis of** ***ABCA4*** **variant c.4354G>T transcribed from normal allele and mutant sequence *indicates correctly spliced reference sequence** ***Below:*** **schematic representation of gel electrophoresis results**

4.4.3 In vitro splicing effect of the ABCA4 variant c.4457C>T

This variant is characterized by a cytosine to thymine change four bases from the natural acceptor site. A cryptic acceptor site exists mid-exon and all programmes predicted it to gain in strength as a result of the variant.

Figure 27: Schematic representation of exon 30, position of *ABCA4* variant c.4457C>T, and predicted effect of increased exonic cryptic acceptor site strength due to the variant, as indicated by the yellow highlighting

Analogous to variant *ABCA4* c.4354G>T, no visible size difference between the normal and mutant cDNA could be detected in the high percentage gel electrophoresis and sequencing also failed to reveal evidence of alternative splicing behaviour in the mutant product. The reference sequence of 381 bp is evident in both, the large product of 615 bp due to intronic inclusion, [89] the product of 308 bp with the 73 bp deletion resulting from the use of a cryptic donor site, and the transcript of 194 bp containing vector-only sequence. The product of 411 bp is thought to have arisen from using a donor site downstream from the canonical one, and likely contains 30 bp of intron 30.[89]

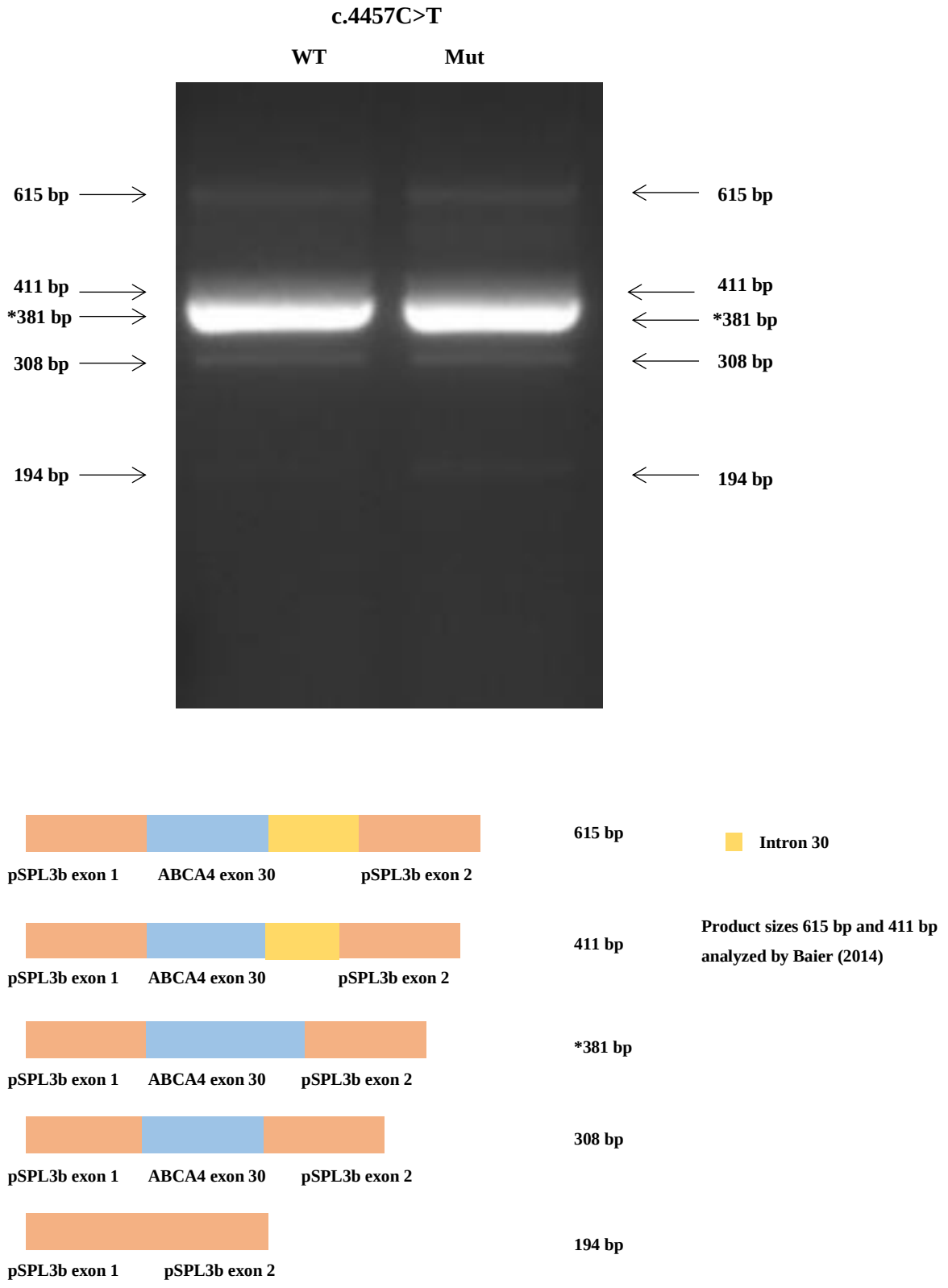

Figure 28: ***Above:*** **cDNA gel electrophoresis of** ***ABCA4*** **variant c.4457C>T transcribed from normal allele and mutant sequence * indicates correctly spliced reference sequence** ***Below:*** **schematic representation of gel electrophoresis results**

4.4.4 In vitro splicing effect of the ABCA4 variant c.6732G>A

This guanidine to adenine change is two bases away from the canonical acceptor site and four of the five programmes predicted the appearance of a novel donor site at the -1 position adjacent to the acceptor site. For this reason, this variant was a particularly interesting case to include in the study.

Figure 29: Schematic representation of exon 49, position of *ABCA4* variant c.6732G>A, and predicted effect of the appearance of a novel donor site

Gel electrophoresis and sequencing of the cDNA products revealed that both the normal allele and mutant had been correctly spliced, as well as produced transcripts in which intronic sequence from the pSPL3b vector had been included.

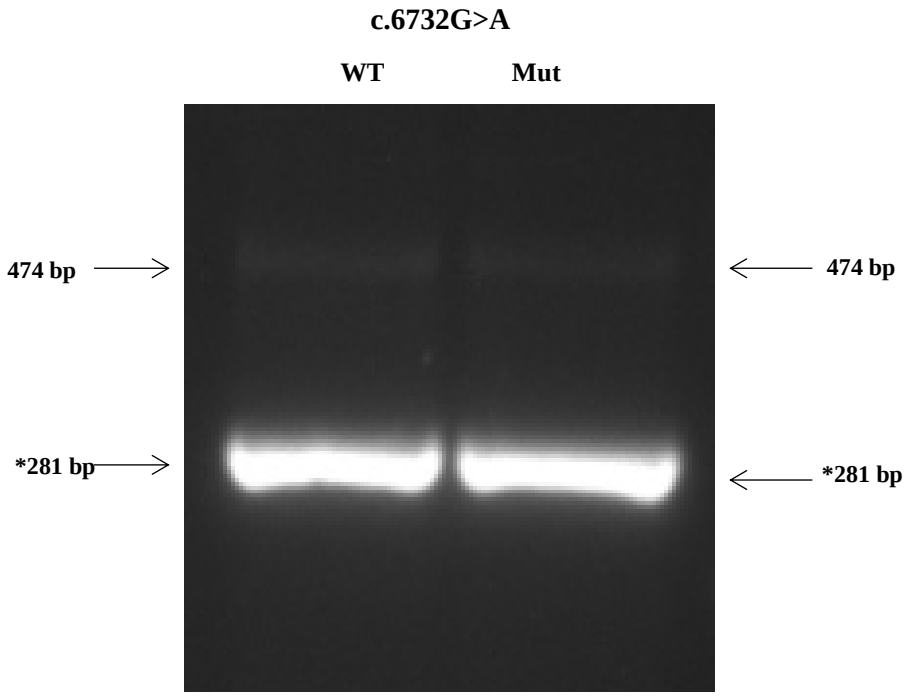

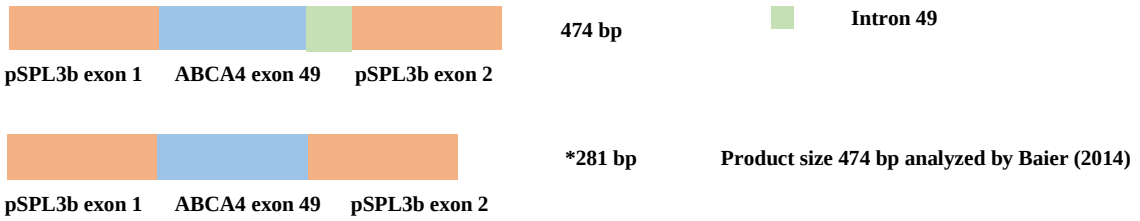

Figure 30: *Above*: cDNA gel electrophoresis of *ABCA4* variant c.6732G>A transcribed from normal allele and mutant sequence * indicates correctly spliced reference sequence *Below*: schematic representation of gel electrophoresis results

4.5 SUMMARY OF RESULTS

Functional analyses of all canonical (N=3) and intronic variants (N=2) completed in this study demonstrated aberrant splicing in accordance with *in silico* calculations. Of the four exonic variants completed, *in silico* predictions of abnormal splicing could be verified *in vitro* for two (**Table 32**). For the remaining two, including additional sequence to better replicate natural splicing conditions may have increased the sensitivity of the exon-trapping system and thus produced more significant *in vitro* results.

Type of Variant	Variant	Product Size (bp)	Effect on splicing	Putative Effect on Protein
Canonical	*ABCA4* c.5312+1G>A	310		Reference sequence
		194	c.5197_5312del (exon spliced out)	p.Asn1734Glyfs*14
Canonical	*ABCA4* c.5018+2T>C	538	Intron retention - prediction not possible	
		364	Reference sequence	
		194	Exon spliced out	p.Val1617Alafs*113
Canonical	*ABCA4* c.1239+1G>C	607	Intron retention - prediction not possible	
		454	c.1239+152/153 acceptor	
		377*	c.1100-45/44 acceptor	
		334	Reference sequence	
		308*	c.1124/25 acceptor; c.1100_1125del	p.Thr367Lysfs*28
		194	c.1100_1239del (exon spliced out)	p.Thr367Serfs*6
Intronic	*ABCA4* c.4773+3A>G	375	Reference sequence	
		300	c.4774_4848del (exon 34 deleted)	p.Gly1592_Lys1616del
		291	c.4765/66 donor; c.4765_4773del	p.Val1589_Gly1591del
		269	c.4668_4773del (exon 33 deleted)	p.Tyr1557Alafs*18
		194	c.4668_4848del (exon spliced out)	p.Tyr1557Cysfs*45

Intronic	*CNGB3* c.991-3T>G	261		p.Tyr331Serfs*12
		259	Reference sequence	
Exonic	*ABCA4* c.4919G>A	538*	Intron retention - prediction not possible	
		464*	c.4849-102/101 acceptor	
		364	Reference sequence	
		294	c.4919/20 acceptor; c.4850_4921del	p.Val1617_Arg1640del
		194	c.4849_5018del (exon spliced out)	p.Val1617Alafs*113
Exonic	*ABCA4* c.4354G>T	615*	Intron retention - prediction not possible	
		611*	c.4355/56 acceptor Intron retention – prediction not possible	
		411*	c.4539+31/32 Donor	p.Q1513_R1514insVPDLQTTGPQ
		407*	c.4355/56 acceptor + c.4539+31/32 donor	p.E1452Tfs*86
		381	Reference sequence	
		377*	c.4355/56 acceptor	p.E1452Tfs*73
		308	c.4467/68 donor	p.C1490Efs*12
		304*	c.4355/56 acceptor + c.4467/68 donor	p.E1452Tfs*77
		194	c.4353_4539del (exon spliced out)	p.W1453Hfs*11
Exonic	*ABCA4* c.4457C>T	615*	Intron retention - prediction not possible	
		411*	c.4539+31/32 donor	p.Q1513_R1514insVPDLQTTGPQ
		381	Reference sequence	
		308	c.4467/68 donor	p.C1490Efs*12
		194	c.4353_4539del (exon spliced out)	p.W1453Hfs*11
Exonic	*ABCA4* c.6732G>A	474	Intron retention - prediction not possible	
		281	Reference sequence	

Table 32: Summary of in vitro analyses

Variants grouped according to type and in descending cDNA position, with the exception of ABCA4 c.4457C>T and ABCA4 c.6732G>A. Those marked * were analyzed via fragment analysis by Baier (2014).

5 DISCUSSION

Experiments for this medical dissertation focused on functional *in vitro* analyses of twenty *ABCA4* variants and one *CNGB3* found in retinal degeneration patients, all of which had been predicted *in silico* to affect splicing. Because *ABCA4* and *CNGB3* are transcribed exclusively in the retina, using native tissue for direct *in vitro* splicing analyses was not possible. Instead, an established method of exon-trapping using the pSPL3b vector was employed. Of the nine variant analyses fully completed during the time of this dissertation, seven demonstrated disrupted splicing behaviour *in vitro*.

All three canonical site variants (*ABCA4* c.5018+2T>C, *ABCA4* c.5312+1G>A, *ABCA4* c.1239+1G>C) produced *in vitro* results matching those foreseen by *in silico* tools. Subsequent analyses of the putative effect on protein translation suggested that all three would likely lead to a frameshift with varying consequences, including intron retention and exon skipping. Both intronic variants also demonstrated aberrant splicing behaviour with the putative effect ranging from reduced protein synthesis (*ABCA4* c.4773+3A>G), to a frameshift with a premature stop codon (*CNGB3* c.991-3T>G). Conversely, two of the four exonic variants predicted *in silico* to be spliceogenic failed to produce *in vitro* results that confirmed this (*ABCA4* c.4457C>T, *ABCA4* c.6732G>A).

These findings highlight the great complexity involved in predicting and correctly interpreting the effect a variant may have. Also, they underscore the importance of utilizing *in vitro* analysis as a follow-up to *in silico* predictions for genes linked to retinal degenerative disease, as is done for genes implicated in breast and ovarian cancer and autosomal dominant polycystic kidney disease. [73, 101] *In vitro* analyses of retinal tissue undoubtedly play a fundamental role in enhancing current knowledge on potential variant effects, yet also pose several challenges and limitations. In addition to obstacles in obtaining viable retinal tissue, the retina displays even more diverse alternative splicing and novel gene transcription activity than previously assumed, [88] and there also appears to be retina-specific splice factors.[106] Vector systems for *in vitro* investigation constitute fabricated, static environments and cannot possibly replicate the great intricacy and manifoldness of tissue specific splicing factors at work in the neural retina. Consequently, caution must be exercised when interpreting *in silico* results to avoid faulty assumptions regarding the *in vivo* situation.

5.1 IN SILICO - IN VITRO ANALYSES

The agreement between the *in silico-in vitro* results for single nucleotide substitutions at canonical sites is due to the high degree of conservation found at these sites. An abundance of data is available on the various nucleotide frequencies at intron-exon boundaries and can be drawn upon when developing algorithmic scoring systems for bioinformatics programmes. Consequently, *in silico* prediction accuracy for canonical sites is quite reliable and this study's findings are consistent with those of other groups.[53, 63, 64]

Even though it was not surprising that all three canonical variants led to splicing alterations as predicted *in silico*, it is important to note that single base exchanges at canonical sites cannot automatically be assumed to cause splicing aberrations. At least one variant at a canonical site (*BRCA2* c.8331+1G>T) is described in the literature as having been predicted by bioinformatics to cause splicing aberration, yet *in vitro* results failed to confirm this.[40]

There are several issues to consider regarding the discrepancy between *in silico* predictions and the *in vitro* findings of this and other studies. Incongruity may be partially due to current software's limitations in assessing variants outside the canonical sites. Although the nature of exonic splicing regulatory elements and their role in Mendelian disease remain poorly understood, there is evidence suggesting that up to 25% of exonic mutations affect splicing. [65, 66] Despite this high frequency, *in silico* tools still appear lacking in their ability to accurately analyse exonic variants. For example, Théry et al. [52] reported a 55 % false negative *in silico* prediction rate for internal exonic variants (*BRCA1/BRCA2*) which had subsequently been subjected to *in vitro* follow-up analyses - a shortcoming that could have serious clinical implications. Conversely, Claverie-Martin et al. investigated 32 exonic mutations predicted by bioinformatics to be spliceogenic, of which only three demonstrated splicing defects *in vitro*.[101] Computational tools can only increase in accuracy as more data is generated to fine-tune existing algorithms and improving *in silico* assessment of exonic variants' effects on splicing has become the focus of recent efforts. [102]

Despite persisting imperfections, bioinformatics play an integral role in the molecular diagnosis process. In addition to enabling the spliceogenic potential of variants to be studied in genes with expression restricted to specialized/non-accessible tissue, as is the case for *ABCA4* and *CNGB3*, computational prediction is key to establishing a priority hierarchy for further analyses. Variants deemed *in silico* most likely to be spliceogenic can be subjected *a priori* to functional splicing analysis. This has obvious clinical and economic advantages. Nonetheless, *a priori* testing does not circumvent the problem of high false negative rates. Relying solely on

in silico results poses the danger of leaving false negative patients "under-investigated" and therefore under-diagnosed. Despite on-going development on the frontiers of bioinformatic prediction tools,[103] to date we are still reliant on functional analyses for verification. [104] This process, albeit resource-consuming, minimizes the risk of missing mutations deemed non-spliceogenic *in silico* and is necessary for characterising and cataloguing the nature of aberrant transcripts.

Functional analyses serve as an instrumental source of empirical bio data for software tools and aid in the diagnostic process, yet as already discussed, pose several drawbacks. Exon trapping is an artificial system that includes only short segments of natural introns and presents the danger of disrupting or eliminating important splicing regulatory elements.[57] For this reason, it can be beneficial to include additional neighbouring sequence as a means of replicating a more natural splicing environment. Doing so for variants such as *ABCA4* c.6732G>A, c.4457C>T, and even c.4354G>T, may have led to more conclusive *in vitro* results, yet a larger construct size generally requires the tedious undertaking of increased cloning work. In the case of variant *ABCA4* c. 6732G>A, the prediction was for a donor site to appear at the beginning of exon 49. Ideally, approximately 50 bp of intron 47, and then exon 48, intron 48 and exon 49 containing the variant should have been included, leading to a construct with 1850-1900 extra base pairs. In this case, the chosen pSPL3b expression vector would not have been suitable, as other groups have found it unable to retain inserts > 1kb.[100] The *in vitro* method of exon-trapping is likely not sensitive enough to detect subtle splicing defects, and utilizing a vector system with endogenous splice sites for certain variants may have proven to be more effective.[99] In fact, five years after the experiments for this dissertation were completed, Sangermano et al. addressed precisely this issue by designing a robust multi-exon midigene construct which allowed for the reliable assessment of functional consequences of putative splice defects.[105]

Despite their numerous shortcomings, *in silico* and *in vitro* analyses are complementary procedures allowing researchers and clinicians to first prioritize variants of unknown significance before commencing with expensive, time-consuming functional assessments.

5.2 ABCA4 TOPOLOGY AND DOMAINS AFFECTED BY ABERRANT SPLICING

Following *in vitro* analyses, the putative effect that the aberrant transcripts may have on the protein level was examined.[89] **Fig. 31** provides a schematic representation of human *ABCA4* topology, [22] including the location of the protein changes that may arise as a result of the variants analyzed in this study.

Six of the seven variants which displayed aberrant splicing *in vitro* lie within domains found in the extracellular loops (**Fig. 1 & Fig 31**: ECD1, ECD2) on the rims of the rod outer segment discs (**Fig. 2 & Fig.31**). The biological significance of these domains has yet to be fully clarified,[19] yet research suggests that the binding of all-*trans*-retinal causes the otherwise highly stable secondary structure of ECD2 to undergo important conformational changes necessary for proper substrate transport.[85] Similarly, it has also been demonstrated for *ABCA1,* another A class ABC transporter, that the two large extracellular domains play an instrumental role in transport processes by mobilizing cellular phospholipids to apolipoprotein A-I.[86] These findings imply that structural alterations in the ECD2 caused by disease-associated mutations may impede the clearance process,[85] resulting in all-*trans*-retinal accumulation in the interdiscal space and ultimately the formation of retina-toxic lipofuscin.

The pathogenic significance of the frameshift mutations located within the ECD domains is obvious, as they will likely lead to a truncated protein. The effect of the other two (ECD2: c.4773+3A>G; c.4919G>A) however, is less apparent because they show deletions of various sizes. In such cases, it is conceivable that the ensuing protein could, in fact, retain enough of its function to only minimally alter the phenotype, perhaps even leaving it unaffected. Such scenarios may partially account for the considerable phenotypic variance found in Stargardt disease. [99]

The putative effect of variant *ABCA4* c.5312+1G>A is a truncated protein, potentially resulting in the loss of the intracellular C-terminal in one of the transmembrane domains (**Fig. 31**: p.Asn1734Glyfs*14). Each transmembrane domain consists of six membrane-spanning helices and the flipping of NRPE from the luminal to the cytoplasmic side of the disc membrane is brought about by conformational changes caused by ATP binding to the intracellular nucleotide binding domains (**Fig.2**).[19] Although a truncating mutation in the C-terminal could theoretically still result in a protein being incorporated into the membrane and allow for a certain degree of functionality,[99] it is likely to disrupt the clearance process and lead to an accumulation of retinal toxic by-products.

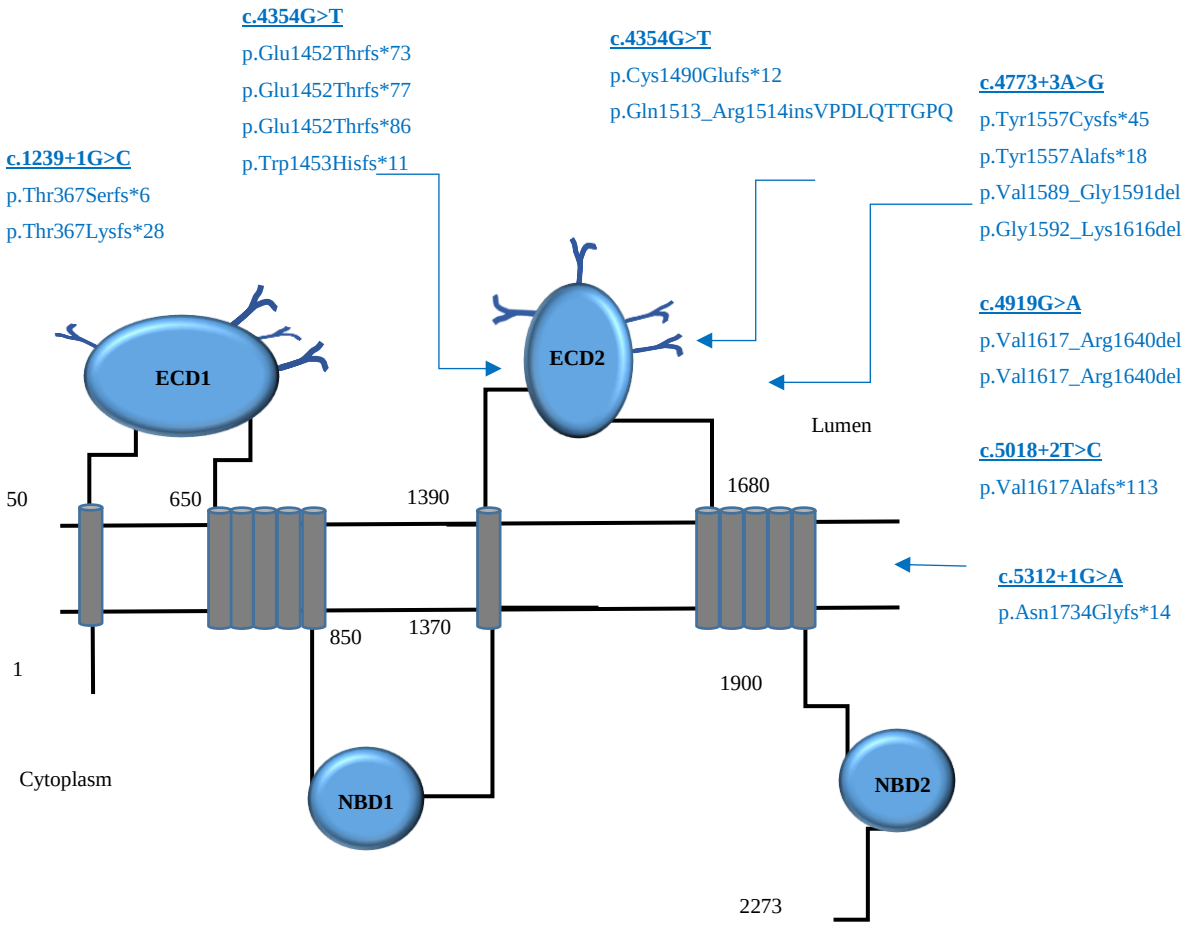

Figure 31: *Human ABCA4 topology showing the variants investigated in this study and their corresponding putative protein effect (red).

***own schematic figure based on Tsybovsky et al., 2010[22] (Fig.2 p.16) *Numbers*: position of corresponding residues in primary structure; *ECD1, ECD2*: exocytoplasmic domains 1 & 2; *NBD1, NBD2*: nucleotide binding domains 1&2**

5.3 CONSIDERATIONS FOR SPLICING AND DISEASE

Splice site variants constitute approximately 15% of registered pathogenic mutations [49,74] and some evidence suggests that 22% of mutations previously classified as missense may in fact also affect splicing. [66] Based on these findings, up to one third of all pathogenic mutations may be implicated in mRNA splicing disruption, yet despite this high occurrence rate it remains difficult to pinpoint a splicing defect as the cause of a disease. The act of mRNA splicing is highly complex, involving intricate cooperation among numerous elements. Depending on the location of the variant, a wide variety of outcomes can result, ranging from exon-skipping, activation of a cryptic splice site, or the inclusion of intronic

sequence. Ensuing consequences on the protein level are often frameshifts, or in-frame deletions/insertions, and therefore may be difficult to decipher from truncating mutations or deletions/insertions resulting from other genetic mechanisms.[71] On the other hand, incomplete protein expression, as well as tissue specificity, tend to be characteristic of splicing mutations.[75]

In considering the effects of aberrant splicing, there may be less obvious factors to consider apart from direct protein consequences. For instance, variants may have an effect on the physiological process of alternative splicing, which involves the generation of various transcripts necessary for functional diversity, and also plays an important role in regulating gene expression.[44] Intronic variants creating cryptic splice sites, or *de novo* silencer or enhancers, have been linked to the deregulation of alternative splicing, [77] thus affecting the isoforms of the mRNA and ultimately influencing phenotype manifestation. Beit-Ya'acov et al. investigated the effects of a novel *ABCA4* splicing variant on protein expression and were surprised to obtain, in addition to the normal allele transcript, three alternatively spliced transcripts in healthy retina RNA; the diseased transcript contained only the alternatively spliced isoforms.[62] These findings highlight the great difficulty researchers and clinicians face when trying to deduce a genotype-phenotype correlation in mutations affecting splicing, which may hold significance for therapy.

At present, various treatment options are being investigated in clinical trials for STGD1, including gene replacement therapy (NCT01367444; NCT01736592), subretinal transplantation of human embryonic stem cell-derived retinal pigmented epithelial cells (NCT02445612; NCT02941991) as well as the administration of C20-D3 retinylacetate (NCT02402660).[107] Specific to splicing but still in the experimental phase, one group demonstrated that *ABCA4* pre-mRNA splicing defects in photoreceptor precursor cells generated from STGD1 patient fibroblasts can be rescued by administrating antisense oligonucleotides to redirect the defect to either include or skip the (pseudo)exons.[107]

5.4 CURRENT EFFORTS FOCUSING ON ABCA4 VARIANTS AND SPLICEOGENIC EFFECTS

Of the 791 HGMD publicly-registered *ABCA4* mutations, 117 (15%) are classified as spliceogenic (http://www.hgmd.cf.ac.uk/ac/gene.php?gene=ABCA4; Appendix: **Table 33**). 68 (~58%) are canonical, 43 (~37%) are found at the splice site border, and 6 (0,5%) are deep intronic variants. This study investigated twenty-one variants predicted *in silico* to affect splicing, which could potentially add ~ 18% to the existing data. Of the nine completed variants

for this dissertation, six were located outside the highly conserved splice sites - two at the intronic splice site border and four exonic variants. Four of the six (~67%) produced spliceogenic *in vitro* results. The subsequent completion of the remaining variants by Baier (2014) showed similar findings: five of the thirteen (~38%) exonic variants produced aberrant splice products, and two additional exonic variants led to differentially spliced isoforms.[89]

In order to assess similar efforts focusing on functional analyses of *ABCA4* spliceogenic mutations, in particular those outside the highly conserved positions, a literature search of the PubMed database was conducted by combining "*ABCA4*" with the following keywords: "splicing", "exonic"; "intronic" "in vitro"; "functional assay" and "exon trapping." This yielded a meager total of seventeen studies focusing on *ABCA4* functional assays between 1997 when *ABCA4* was discovered [78] and 2018 (Appendix: **Table 35**).

Although this search cannot claim to be fully exhaustive, the scarcity of publications in the past two decades suggests that this is an area in need of increased attention. Exonic variants are more abundant and potentially pathogenic than previously assumed. [51,72,79] By activating *de novo* ectopic splice sites, exonic variants can show deleterious effects,[51] as was found by Moseley et al.[80] in their research on autosomal recessive growth hormone deficiency; or Sheikh et al.[81] in the *MECP2* gene causing Rett syndrome. Furthermore, single nucleotide changes within the coding region have also been implicated in disease by means of disrupting splicing silencer and enhancer motifs, consequently leading to aberrant splicing.[79, 82]

The growing body of research investigating putative effects of noncanonical splice site variants, the heightened demand for personalised medicine, and importance of clearly discerning the nature of variants of unknown significance, all underscore the necessity of performing functional *in vitro* splicing analyses. Only as more *in vitro* or *in vivo* data is gathered will it be possible to optimize the *in silico* prediction algorithms and generate more reliable predictions. As indicated by the marginal results found in the literature search conducted by this study, there is certainly room for improvement if medicine and science are to better serve patients suffering from retinal dystrophies. A thematic approach study in the UK involving 200 patients with inherited retinal disease explored patient understanding of/attitudes towards genetic testing. It was revealed that > 90% were in support of publicly funded diagnostic and predictive genetic testing, and also felt that genetic counselling should precede testing, yet paradoxically ~60% admitted to having a very limited understanding of what genetic testing even entailed.[90] In light of this, the suggestion brought forth by Spurdle et al. (2008) seems to be worth considering, namely that functional testing to generate *in vitro/ in vivo* data ideally take place in clinical settings. Bridging the gap between research centers and primary patient

care facilities could help heighten patient awareness and maximize counselling benefits.[40] Moreover, funding could be made dependent on agreeing to share empirical results in databases and publications.[40] This would increase the availability of data and propagate the characterization of variants, which is crucial to evaluating their clinical significance. Such a system could greatly benefit the wider retinal degeneration patient community, as well as aid clinicians and researchers in their work.

6 SUMMARY

This study conducted *in vitro* analyses to investigate the splicing effects of twenty *ABCA4* variants and one *CNGB3*, which had been predicted *in silico* to cause aberrant mRNA splicing. To circumvent the problem of tissue availability, the method of *in vitro* exon trapping was employed, based on the work of Cepko et al., [55] which capitalizes on the highly conserved sequences flanking splice sites, and implements transmissible expression vectors to generate and recover genomic inserts.[56, 57] Following replication and selection in E.*coli,* the pSPL3b vector containing the construct was transfected in transient cells, the RNA isolated, reverse transcribed, and RT-PCR amplified. Visualizing the products via gel electrophoresis allowed for an initial comparison of splicing activity between the normal allele and mutant variants. Of the twenty-one variant analyses, nine were completed within the allotted timeframe for this medical dissertation. Seven variants (three canonical, two intronic, and two exonic) demonstrated disrupted splicing behaviour *in vitro* in accordance with *in silico* predictions.

Diese Studie führte *in vitro* Analysen durch, um das Spleißverhalten von zwanzig *ABCA4*-Varianten und einer *CNGB3*-Variante zu untersuchen, bei denen *in silico* Vorhersagen darauf hindeuteten fehlerhaftes MRNA-Spleißen zu erwarten. Um das Problem der Gewebeverfügbarkeit zu umgehen, wurde die sogenannte *in-vitro*-Exon-Trapping-Methode angewandt, welche sich auf die Arbeit von Cepko et al. [55] bezieht und die hochkonservierten Sequenzen, die die Spleißstellen flankieren, zu Nutze macht. Übertragende Expressionsvektoren wurden eingesetzt, um genomische Inserts zu erzeugen bzw. wiederzugewinnen. Nach der Replikation und Selektion in E. coli wurde der pSPL3b-Vektor mit dem eingeschlossenen Konstrukt in transienten Zellen transfiziert, die RNA isoliert, revers transkribiert und RT-PCR amplifiziert. Die Visualisierung der Produkte mittels Gelelektrophorese ermöglichte einen ersten Vergleich des Spleißverhaltens zwischen den gesunden und mutierten Varianten. Von den insgesamt 21 untersuchten Varianten wurden neun innerhalb des zugewiesenen Zeitrahmens dieser Dissertation abgeschlossen. Sieben davon (drei kanonische, zwei intronische, sowie zwei exonische) zeigten in Übereinstimmung mit den *in silico*-Vorhersagen ein gestörtes Spleißverhalten *in vitro*.

7 FIGURE INDEX

8 TABLE INDEX

9 APPENDIX

Reference	Number/Nature of Spliceogenic Variants	*In vitro* Analysis of Effect
Allikmets R, Singh N, Sun H, Shroyer NF, Hutchinson A, Chidambaram A, Gerrard B, Baird L, Stauffer D, Peiffer A, Rattner A, Smallwood P, Li Y, Anderson KL, Lewis RA, Nathans J, Leppert M, Dean M, Lupski JR (1997). A photoreceptor cell-specific ATP-binding transporter gene (ABCR) is mutated in recessive Stargardt macular dystrophy. Nat Genet. 15(3), 236–246.	2 (+1, +2)	no
Allikmets R, Shroyer NF, Singh N, Seddon JM, Lewis RA, Bernstein PS, Peiffer A, Zabriskie NA, Li Y, Hutchinson A, Dean M, Lupski JR, Leppert M (1997). Mutation of the Stargardt disease gene (ABCR) in age-related macular degeneration. Science. 277(5333):1805-7.	1 (+1)	no
Gerber S, Rozet JM, van de Pol TJ, Hoyng CB, Munnich A, Blankenagel A, Kaplan J, and Cremers FP (1998). Complete exon-intron structure of the retina-specific ATP binding transporter gene (ABCR) allows the identification of novel mutations underlying Stargardt disease. Genomics 48, 139–142.	1 (-2)	no
Cremers FP, van de Pol DJ, van Driel M, den Hollander AI, van Haren FJ, Knoers NV, Tijmes N, Bergen AA, Rohrschneider K, Blankennagel A, Pinckers AJ, Deutman AF, Hoyng CB (1998). Autosomal recessive retinitis pigmentosa and cone-rod dystrophy caused by splice site mutations in the Stargardt's disease gene ABCR. Hum Mol Genet. 7(3):355-62.	2 (+1,+5)	no
Rozet JM, Gerber S, Souied E, Perrault I, Châtelin S, Ghazi I, Leowski C, Dufier JL, Munnich A, Kaplan J (1998). Spectrum of ABCR gene mutations in autosomal recessive macular dystrophies. Eur J Hum Genet. 1998 May-Jun; 6(3):291-5.	2 (+2, -2)	no
Lewis RA, Shroyer NF, Singh N, Allikmets R, Hutchinson A, Li Y, Lupski JR, Leppert M, Dean M (1999). Genotype/Phenotype analysis of a photoreceptor-specific ATP-binding cassette transporter gene, ABCR, in Stargardt disease. Am. J. Hum. Genet. 64(2):422-34.	4 (+1,+1,-1,+5)	no
Maugeri A, van Driel MA, van de Pol DJ, Klevering BJ, van Haren FJ, Tijmes N, Bergen AA, Rohrschneider K, Blankenagel A, Pinckers AJ, Dahl N, Brunner HG, Deutman AF, Hoyng CB, Cremers FP (1999). The 2588G>C mutation in the ABCR4 gene is a mild frequent founder mutation in the western European population and allows the classification of ABCR mutations in patients with Stargardt disease. Am J Hum Genet. 64(4):1024-35.	3 (+1,-1,+6)	no
Rozet JM, Gerber S, Ghazi I, Perrault I, Ducrog D, Souied E, Cabot A, Dufier JL, Munnich A, Kapla J (1999). Mutations of the retinal specific ATP binding transporter gene (ABCR) in a single family segregating both autosomal recessive retinitis pigmentosa RP19 and Stargardt disease: evidence of clinical heterogeneity at this locus. J Med Genet. 36(6):447-51.	1 (-1)	no
Papaioannou M, Ocaka L, Bessant D, Lois N, Bird A, Payne A, and Bhattacharya S (2000). An analysis of ABCR mutations in British patients with recessive retinal dystrophies. Invest. Ophthalmol. Vis. Sci. 41, 16–19.	2 (-2, +7)	no
Rivera A, White K, Stöhr H, Steiner K, Hemmrich N, Grimm T, Jurklies B, Lorenz B, Scholl, HP, Apfelstedt-Sylla E, Weber BH (2000). A comprehensive survey of sequence variation in the ABCA4 (ABCR) gene in Stargardt disease and age-related macular degeneration. Am. J. Hum. Genet. 67, 800–813.	5 (+1,+1,+2,+5,+5)	*in vitro* testing of variant effect on splicing
Yatsenko AN, Shroyer NF, Lewis RA, Lupski JR (2001). Late-onset Stargardt disease is associated with missense mutations that map outside known functional regions of ABCR (ABCA4). Hum Genet. 108(4):346-55.	1 (+1)	*in vivo* functional analysis of missense mutations in STGD1 patients
Webster AR, Héon E, Lotery AJ, Vandenburgh K, Casavant TL, Oh KT, Beck G, Fishman GA, Lam BL, Levin A, Heckenlively JR, Jacobson SG, Weleber RG, Sheffield VC, Stone EM (2001). An analysis of allelic variation in the ABCA4 gene. Invest Ophthalmol Vis Sci. 42(6):1179-89.	4 (+1,+1,-1,+5)	no
Briggs CE, Rucinski D, Rosenfeld PJ, Hirose T, Berson EL, Dryja TP (2001). Mutations in ABCR (ABCA4) in patients with Stargardt macular degeneration or cone-rod degeneration. Invest Ophthalmol Vis Sci. 42(10):2229-36.	2 (+1,+2)	no
Fumagalli A, Ferrari M, Soriani N, Gessi, A, Foglieni B, Martina E, Manitto MP, Brancato R, Dean M, Allikmets R, et al. (2001). Mutational scanning of the ABCR gene with double-gradient denaturing-gradient gel electrophoresis (DG-DGGE) in Italian Stargardt disease patients. Hum. Genet. 109, 326–338.	1 (-1)	no

Birch DG, Peters AY, Locke KL, Spencer R, Megarity CF, Travis GH (2001). Visual function in patients with cone-rod dystrophy (CRD) associated with mutations in the ABCA4 (ABCR) gene. Exp Eye Res.73 (6):877-86.	2 (+1,+2)	no
Pang CP, Lam DS (2002). Differential occurrence of mutations causative of eye diseases in the Chinese population. Hum Mutat. 19(3):189-208. Review.	2 (+1,-5)	no
Gerth C, Andrassi-Darida M, Bock M, Preising MN, Weber BH, Lorenz B (2002). Phenotypes of 16 Stargardt macular dystrophy/fundus flavimaculatus patients with known ABCA4 mutations and evaluation of genotype-phenotype correlation. Graefes Arch Clin Exp Ophthalmol. 240(8):628-38.	1 (+1)	no
Fukui T, Yamamoto S, Nakano K, Tsujikawa M, Morimura H, Nishida K, Ohguro N, Fujikado T, Irifune M, Kuniyoshi K, Okada AA, Hirakata A, Miyake Y, Tano Y (2002). ABCA4 gene mutations in japanese patients with Stargardt disease and retinitis pigmentosa. Invest Ophthalmol Vis Sci. 43(9):2819-24.	1 (+2)	no
Jaakson K, Zernant J, Külm M, Hutchinson A, Tonisson N, Glavac D, Ravnik-Glavac M, Hawlina M, Meltzer MR, Caruso RC, Testa F, Maugeri A, Hoyng CB, Gouras P, Simonelli F, Lewis RA, Lupski JR, Cremers FP, Allikmets R (2003). Genotyping microarray (gene chip) for the ABCR (ABCA4) gene. Hum Mutat. 22(5):395-403.	8 (+1,+1,+1,+1,+2, -1,-2,-2)	no
Ozgül RK, Durukan H, Turan A, Oner C, Ogüs A, Farber DB (2004). Molecular analysis of the ABCA4 gene in turkish patients with Stargardt disease and reintitis pigmentosa. Hum Mutat. 23(5):523.	2 (+4,-6)	no
Stenirri S, Fermo I, Battistella S, Galbiati S, Soriani N, Paroni R, Manitto MP, Martina E, Brancato R, Allikmets R, Ferrari M, Cremonesi L (2004). Denaturing HPLC profiling of the ABCA4 gene for reliable detection of allelic variations. Clin Chem. 50(8):1336-43.	3 (+1,-1,+3)	no
Klevering BJ, Deutman AF, Maugeri A, Cremers FP, Hoyng CB (2005). The spectrum of reintal phenotypes caused by mutations in the ABCA4 gene. Graefes Arch Clin Exp Ophthalmol. 243(2):90-100.	1 (-10)	no
Mandal MN, Heckenlively JR, Burch T, Chen L, Vasireddy V, Koenekoop RK, Sieving PA, Ayyagari R (2005). Sequencing arrays for screening multiple genes associated with early-onset human retinal degenerations on a high-throughput platform. Invest Ophthalmol Vis Sci. 46(9):3355-62.	1 (-2)	no
Riveiro-Alvarez R, Trujillo MJ, Cantalapiedra D, Vallespin E, Villaverde C, Valverde D, Ayuso C (2006). Gene symbol: ABCA4. Disease: Stargardt disease 1. Accession #Hs0512. Hum Genet. 118(6):784.	1 (-2)	no
Downs K, Zacks DN, Caruso R, Karoukis AJ, Branham K, Yashar BM, Haimann MH, Trzupek K, Meltzer M, Blain D, Richards JE, Weleber RG, Heckenlively JR, Sieving PA, Ayyagari R (2007). Molecular testing for hereditary retinal disease as part of clinical care. Arch Ophthalmol. 125(2):252-8.	1 (-3)	no
Valverde D, Riveiro-Alvarez R, Aguirre-Lamban J, Baiget M, Carballo M, Antiñolo G, Millán JM, Garcia Sandoval B, Ayuso C (2007). Spectrum of the ABCA4 gene mutations implicated in severe retinopathies in Spanish patients. Invest Ophthalmol Vis Sci. 48(3):985-90.	1 (+2)	no
Rosenberg T, Klie F, Garred P, Schwartz M (2007). N965S is a common ABCA4 variant in Stargardt-related retinopathies in the Danish population. Mol Vis. 13:1962-9.	3 (+2,+2,-2)	no
Aguirre-Lamban J, Riveiro-Alvarez R, Cantalapiedra D, Vallespin E, Avila-Fernandez A, Trujillo-Tiebas MJ, Villaverde-Montero C, Ayuso C (2008). Gene sympbol: ABCA4. Disease macular dystrophy. Hum Genet. 123(5):547.	1 (+5)	no
Kitiratschky VB, Grau T, Bernd A, Zrenner E, Jägle H, Renner AB, Kellner U, Rudolph G, Jacobson SG, Cideciyan AV, Schaich S, Kohl S, Wissinger B (2008). ABCA4 gene analysis in patients with autosomal recessive cone and cone rod dystrophies. Eur J Hum Genet. 16(7):812-9.	1 (+2)	no
Xi Q, Li L, Traboulsi EI, and Wang QK (2009). Novel ABCA4 compound heterozygous mutations cause severe progressive autosomal recessive cone-rod dystrophy presenting as Stargardt disease. Mol. Vis. 15, 638–645.	1 (+3)	no
Cideciyan AV, Swider M, Aleman TS, Tsybovsky Y, Schwartz SB, Windsor EA, Roman AJ, Sumaroka A, Steinberg JD, Jacobson SG, Stone EM, Palczewski K (2009). ABCA4 disease progression and a proposed strategy for gene therapy. Hum Mol Genet. 18(5):931-41.	1 (+2)	no
Ernest PJ, Boon CJ, Klevering BJ, Hoefsloot LH, Hoyng CB (2009). Outcome of ABCA4 microarray screening in routine clinical practice. Mol Vis. 15:2841-7.	2 (+1,+4)	no
Passerini I, Sodi A, Giambene B, Mariottini A, Menchini U, Torricelli F (2010). Novel mutations in of the ABCR gene in Italian patients with Stargardt disease (2010). Eye (Lond). 24(1):158-64.	2 (+1,-1)	no
Zernant J, Schubert C, Im KM, Burke T, Brown CM, Fishman GA, Tsang SH, Gouras P, Dean M, Allikmets R (2011). Analysis of the ABCA4 gene by next-generation sequencing. Invest Ophthalmol Vis Sci. 52(11):8479-87.	14 (+1,+1,+1,+1,-1,-1,-1,+2,-2,-2,-2,-2,,+3,-6)	no

Thiadens AA, Phan TM, Zekveld-Vroon RC, Leroy BP, van den Born LI, Hoyng CB, Klaver CC; Writing Committee for the Cone Disorders Study Group Consortium, Roosing S, Pott JW, van Schooneveld MJ, van Moll-Ramirez N, van Genderen MM, Boon CJ, den Hollander AI, Bergen AA, De Baere E, Cremers FP, Lotery AJ (2012). Clinical course, genetic etiology, and visual outcome in cone and cone-rod dystrophy. Ophthalmology. 119(4):819-26.	2 (+1,-10)	no
Fritsche LG, Fleckenstein M, Fiebig BS, Schmitz-Valckenberg S, Bindewald-Wittich A, Keilhauer CN, Renner AB, Mackensen F, Mößner A, Pauleikhoff D, Adrion C, Mansmann U, Scholl HP, Holz FG, Weber BH (2012). A subgroup of age-related macular degeneration is associated with mono-allelic sequence variants in the ABCA4 gene. Invest Ophthalmol Vis Sci. 53(4):2112-8.	3 (+1,+3,-5)	no
Westeneng-van Haaften SC, Boon CJ, Cremers FP, Hoefsloot LH, den Hollander AI, Hoyng CB (2012). Clinical and genetic characteristic of late-onset Stargardt's disease. Ophthalmology. 119(6):1199-210.	1 (+1)	no
Neveling K, Collin RW, Gilissen C, van Huet RA, Visser L, Kwint MP, Gijsen SJ, Zonneveld MN, Wieskamp N, de Ligt J, Siemiatkowska AM, Hoefsloot LH, Buckley MF, Kellner U, Branham KE, den Hollander AI, Hoischen A, Hoyng C, Klevering BJ, van den Born LI, Veltman JA, Cremers FP, Scheffer H (2012). Next-generation genetic testing for retinitis pigmentosa. Hum Mutat. 33(6):963-72.	1 (-1)	no
Testa F, Rossi S, Sodi A, Passerini I, Di Iorio V, Della Corte M, Banfi S, Surace EM, Menchini U, Auricchio A, Simonelli F (2012). Correlation between photoreceptor layer integrity and visual function in patients with Stargardt disease: implications for gene therapy. Invest Ophthalmol Vis Sci. 53(8):4409-15.	2 (+1,-2)	no
Rossi S, Testa F, Attanasio M, Orrico A, de Benedictis A, Corte MD, Simonelli F (2012). Subretinal Fibrosis in Stargardt's disease with fundus flavimaculatus and ABCA4 gene mutation. Case Rep Ophthalmol. 3(3):410-7.	1 (-2)	no
Downes SM, Packham E, Cranston T, Clouston P, Seller A, Németh AH (2012). Detection rate of pathogenic mutations in ABCA4 using direct sequencing: clinical and research implications. Arch Ophthalmol. 130(11):1486-90.	2 (-1,-3)	no
Duno M, Schwartz M, Larsen PL, Rosenberg T (2012). Phenotypic and genetic spectrum of Danish patients with ABCA4-related retinopathy. Ophthalmic Genet. 33(4):225-31.	7 (+1,+1,+1,-2,-2,+3,+5)	no
Burton DS, Ali M, McKibbin M (2013). Retinal phenotypes in patients homozygous for the G1961E mutation in the ABCA4 gene. Invest Ophthalmol Vis Sci. 54(1):520	1 (+1)	no
Chacón-Camacho OF, Granillo-Alvarez M, Ayala-Ramírez R, Zenteno JC (2013). ABCA4 mutational spectrum in Mexican patients with Stargardt disease: Identification of 12 novel mutations and evidence of a founder effect for the common p.A1773V mutation. Exp Eye Res. 109:77-82.	1 (+1)	no
Fujinami K, Sergouniotis PI, Davidson AE, Wright G, Chana RK, Tsunoda K, Tsubota K, Egan CA, Robson AG, Moore AT, Holder GE, Michaelides M, Webster AR (2013). Clinical and molecular analysis of Stargardt disease with preserved foveal structure and function. Am J Ophthalmol. 156(3):487-501	2 (+1,+2)	no
Ritter M, Zotter S, Schmidt WM, Bittner RE, Deak GG, Pircher M, Sacu S, Hitzenberger CK, Schmidt-Erfurth UM; Macula Study Group Vienna (2013). Characterization of Stargardt disease using polarization-sensitive optical coherence tomography and fundus autofluorescence imaging. Invest Ophthalmol Vis Sci. 54(9):6416-25.	1 (+3)	no
Fujinami K, Zernant J, Chana RK, Wright G, Tsunoda K, Ozawa Y, Tsubota K, Webster AR, Moore AT, Allikmets R, et al. (2013). ABCA4 gene screening by next-generation sequencing in a British cohort. Invest. Ophthalmol. Vis. Sci. 54, 6662–6674.	4 (+1,-1,-1,-9)	no
Riveiro-Alvarez R, Lopez-Martinez MA, Zernant J, Aguirre-Lamban J, Cantalapiedra D, Avila-Fernandez A, Gimenez A, Lopez-Molina MI, Garcia-Sandoval B, Blanco-Kelly F, Corton M, Tatu S, Fernandez-San Jose P, Trujillo-Tiebas MJ, Ramos C, Allikmets R, Ayuso C (2013). Outcome of ABCA4 disease-associated alleles in autosomal recessive retinal dystrophies: retrospective analysis in 420 Spanish families. Ophthalmology. 120(11):2332-7.	2 (-1,+5)	no
Braun, T. A., Mullins, R. F., Wagner, A. H., Andorf, J. L., Johnston, R. M., Bakall, B. B., Deluca, A. P., Fishman, G. A., Lam, B. L., Weleber, R. G., Cideciyan, A. V., Jacobson, S. G., Sheffield, V. C., Tucker, B. A., Stone, E. M. (2013). Non-exomic and synonymous variants in ABCA4 are an important cause of Stargardt disease. Human molecular genetics, 22(25), 5136-45.	6 (+2001, +2028, +1056, +1137,+1216,-45)	yes
Zhang, X., Ge, X., Shi, W., Huang, P., Min, Q., Li, M., Yu, X., Wu, Y., Zhao, G., Tong, Y., Jin, Z. B., Qu, J., Gu, F. (2014). Molecular diagnosis of putative Stargardt disease by capture next generation sequencing. PloS one, 9(4).	1 (+1)	no

Table 33: 50 Publications of HGMD-registered ABCA4 splice mutations,* listed by date in ascending order

***http://www.hgmd.cf.ac.uk/ac/gene.php?gene=*ABCA4*; Public Version 30.10.2018**

Canonical Variants	Splice Site Intronic Variants	Deep Intronic Variants	Total
68	43	6	117

Table 34: Summary of HGMD-registered ABCA4 splice mutations

Reference	*In vitro* Analysis of Effect
Allikments R, Wasserman WW, Hutchinson A, Smallwood P, Nathans J, Rogan PK, Schneider TD, Dean M (1998). Organization of the ABCR gene: analysis of promoter and splice junction sequences. Gene. 215(1):111	-
Schroyer NF, Lewis RA, Yatsenko AN, Lupski JR (2001*a*). Null missense ABCR (ABCA4) mutations in a family with Stargardt disease and retinitis pigmentosa. Invest Ophthalmol Vis Sci. 42(12):2757-61.	*in vitro* testing of expression
Schroyer NF, Lewis RA, Yatsenko AN, Wensel TG, Lupski JR (2001*b*).Cosegregation and functional analysis of mutant ABCR (ABCA4) alleles in families that manifest both Stargardt disease and age-related macular degeneration. Hum Mol Genet.217 (2):11-4.	*in vitro* testing of expression and ATP binding
Biswas-Fiss E.E (2003). Functional analysis of genetic mutations in nucleotide binding domain 2 of the human retina specific ABC transporter. Biochemistry. 42:10683–10696.	*in vitro* site-directed mutagenesis to investigate effect of mutated NBD2 proteins
Yatsenko AN, Shroyer NF, Lewis RA, Lupski JR (2003). An ABCA4 genomic deletion in patients with Stargardt disease. Hum Mutat. 23(5):523.	*in vitro* studies of deletion mutation on protein expression
Wiszniewski W, Zaremba CM, Yatsenko AN, Jamrich M, Wensel TG, Lewis RA, Lupski JR (2005). ABCA4 mutations causing mislocalization are found frequently in patients with severe retinal dystrophies. Hum. Mol. Genet. 14:2769–2778	*in vitro* testing of *ABCA4* missense mutations on protein processing
Beit-Ya'acov A, Mizrahi-Meissonnier L, Obolensky A, Landau C, Blumenfeld A, Rosenmann A, Banin E, and Sharon D (2007). Homozygosity for a novel ABCA4 founder splicing mutation is associated with progressive and severe Stargardt-like disease. Invest. Ophthalmol. Vis. Sci. 48, 4308–4314.	*in vitro* testing of protein expression by RT-PCR
Albert SSR, Bax N, Roosing S, van den Born L, den Engelsman-van Dijk A, Ramlal A, Stone E, Hoyng C, Cremers F (2015). Towards the identification of deep-intronic ABCA4 mutations in Stargardt patients by using induced pluripotent stem cell-derived photoreceptor progenitor cells. Association for Research in Vision and Ophthalmology 56(7):3174.	sequence analysis of *ABCA4* mRNA from iPSCs differentiated into PPCs
Bax NM., Sangermano R, Roosing S, Thiadens A A, Hoefsloot LH, den Born L., Phan M, Klevering BJ, Westeneng-van Haaften C, Braun TA, Zonneveld-Vrieling MN, Wijs I, Mutlu M, Stone EM, den Hollander AI, Klaver CC, Hoyng, CB, Cremers FP (2015). Heterozygous deep-intronic variants and deletions in *ABCA4* in persons with retinal dystrophies and one exonic *ABCA4* variant. Human Mutation, 36: 43-47.	Exonic variant
Gérard X, Perrault I, Munnich A, Kaplan J, Rozet JM (2015). Intravitreal injection of splice-switching oligonucleotides to manipulate splicing in retinal cells. Mol Ther Nucleic Acids. 2015 Sep 1;4.	Therapy option
Sangermano R, Bax NM, Bauwens M, van den Born LI, De Baere E, Garanto A, Collin RW, Goercharn-Ramlal AS, den Engelsman-van Dijk AH, Rohrschneider K, Hoyng CB, Cremers FP, Albert S (2016). Photoreceptor progenitor mRNA analysis reveals exon skipping resulting from the ABCA4 c.5461-10T→C mutation in Stargardt Disease. Ophthalmology;123(6):1375-85**.**	PPC mRNA analysis, *in vitro* mingene analysis
Aukrust I, Jansson RW, Bredrup C, Rusaas HE, Berland S, Jørgensen A, Haug MG, Rødahl E, Houge G, Knappskog PM (2017). The intronic ABCA4 c.5461-10T>C variant, frequently seen in patients with Stargardt disease, causes splice defects and reduced ABCA4 protein level. Acta Ophthalmol. 95(3):240-246.	mRNA analysis, protein analysis
Schulz HL, Grassmann F, Kellner U, Spital G, Rüther K, Jägle H, Hufendiek K, Rating P, Huchzermeyer C, Baier MJ, Weber BH, Stöhr H (2017). Mutation spectrum of the ABCA4 Gene in 335 Stargardt disease patients from a multicenter German cohort-impact of selected deep intronic variants and common SNPs. Invest Ophthalmol Vis Sci. 1;58(1):394-403.	*in vitro* splicing assay

Sangermano R, Khan M, Cornelis SS, Richelle V, Albert S, Garanto A, Elmelik D, Qamar R, Lugtenberg D, van den Born LI, Collin RWJ, Cremers FPM (2017). *ABCA4* midigenes reveal the full splice spectrum of all reported noncanonical splice site variants in Stargardt disease. Genome Res. 2018 Jan;28(1):100-110.	Midigene analysis of splicing effect
Jonsson F, Westin IM, Österman L, Sandgren O, Burstedt M, Holmberg M, Golovleva I. (2018). ATP-binding cassette subfamily A, member 4 intronic variants c.4773+3A>G and c.5461-10T>C cause Stargardt disease due to defective splicing. Acta Ophthalmol. Epub ahead of print	Minigene analysis of splicing effect
Albert S, Garanto A, Sangermano R, Khan M, Bax NM, Hoyng CB, Zernant J, Lee W, Allikmets R, Collin RWJ, Cremers FPM (2018). Identification and rescue of splice defects caused by two neighboring deep-intronic ABCA4 mutations underlying Stargardt disease. Am J Hum Genet. Apr 5;102(4):517-527.	Therapy option
Garces, F, Jiang K, Molday, LL, Stöhr, H, Weber BH, Lyons CJ, Maberley D., Molday, RS (2018). Correlating the expression and functional activity of *ABCA4* disease variants with the phenotype of patients with Stargardt disease. Invest Ophthalmol Vis Sci.2018;59:2305-2315.	

Table 35: 17 Publications gleaned from PubMed* search listed by date in ascending order.

***http://www.ncbi.nlm.nih.gov/**

Exon	Variant	Cloned construct
9	ABCA4 c.1239+1G>C	GAATTCaatcctccagcatggagttgaatgagacatgtgatgtggatacactaatgactatatt gaggttacaagcaatggggagtttctgtaaaatctgtcccttgtctcctggcagCATCCTTTT GTAATGCATTGATCCAGAGCCTGGAGTCAAATCCTTTAACCAAA ATCGCTTGGAGGGCGGCAAAGCCTTTGCTGATGGGAAAAATCG TACACTCCTGATTCACCTGCAGCACGAAGGATACTGAAGAATgta agatcccagctgggcttgccttgtgtaccctggacctcccagaagtgtgtgtgtgtgtgtgtgtg tgagagagatgtgccttcctggtagcacatctcatgtttgtttttgctaagtggactcttgcgtttcc tcccccatccacagtcatcactggaatgctttgcttcagtgGGATCC
30	ABCA4 c.4354G>T	GAATTCagaggaggaggaaagggttggcacaatttcttatgcctagggatttgtcagcaac tttgaggctgattatggaatattttcttgtcttccatgagGGAGTACCCCTGTGGCAAC TCAACACCCTGGAAGACTCCTTCTGTGTCCCCAAACATCACCCA GCTGTTCCAGAAGCAGAAATGGACACAGGTCAACCCTTCACCA TCCTGCAGGTGCAGCACCAGGGAGAAGCTCACCATGCTGCCAG AGTGCCCCGAGGGTGCCGGGGGCCTCCCGCCCCCCCAGgtacctga cctccaaacaacggggccccaggtctgcctgccacagagggactaggggagtccctggtatctc ctgagtctctcacaaactaacatttcaaactggcagttgagtaggggactaaaccaaactccctgc accGGATCC
30	ABCA4 c.4457C>T	GAATTCagaggaggaggaaagggttggcacaatttcttatgcctagggatttgtcagcaac tttgaggctgattatggaatattttcttgtcttccatgagGGAGTACCCCTGTGGCAAC TCAACACCCTGGAAGACTCCTTCTGTGTCCCCAAACATCACCCA GCTGTTCCAGAAGCAGAAATGGACACAGGTCAACCCTTCACCA TCCTGCAGGTGCAGCACCAGGGAGAAGCTCACCATGCTGCCAG AGTGCCCCGAGGGTGCCGGGGGCCTCCCGCCCCCCCAGgtacctga cctccaaacaacggggccccaggtctgcctgccacagagggactaggggagtccctggtatctc ctgagtctctcacaaactaacatttcaaactggcagttgagtaggggactaaaccaaactccctgc accGGATCC
33_34	ABCA4 c.4773+3A>G	GAATTCtttgtaaagtggagccatgttgctcgctggtccaggcaattcccccgaaagttcatgt ttccctacaaaacccgagagagctactagtaggcgtgaagttcgtggccctggtctgaggatttcc tgtttccttgtcagGTATGGAGGAATTTCCATTGGAGGAAAGCTCCCAG TCGTCCCCATCACGGGGGAAGCACTTGTTGGGTTTTTAAGCGAC CTTGGCCGGATCATGAATGTGAGCGGGgtatgtaaacagactggagatttga gtaggatttttgacttgcttaactaccatgaatgagaaactctcatgagtgataacaggaaaaaaaa attaaaaccgtcttgtttgtttgtttacatggtttttagGGCCCTATCACTAGAGAGGC CTCTAAAGAAATACCTGATTTCCTTAAACATCTAGAAACTGAAG ACAACATTAAGgtacttgacctatgtataatctgctctggatttgtaaagtggagccatgt GGATCC
35	ABCA4 c.4919G>A	GAATTCatccctcctcctgctgaaatctagcaaggaatgtcttccagctaccaaaccttcctg cttctcaaatttcctttccttcactgatttctgctttaactagctgttagtgcagcgtctcagatgtcct ctccaccctctagGTGTGGTTTAATAACAAAGGCTGGCATGCCCTGGT CAGCTTTCTCAATGTGGCCCACAACGCCATCTTACGGGCCAGCC TGCCTAAGGACAGGAGCCCCGAGGAGTATGGAATCACCGTCAT TAGCCAACCCCTGAACCTGACCAAGGAGCAGCTCTCAGAGATT ACAGTgtaagccaccacagccccagcctcaccactttcttgtcaccttctccactctttgaacat cctgagaggattctcaccaccGGATCC
35	ABCA4 c.5018+2T>C	GAATTCatccctcctcctgctgaaatctagcaaggaatgtcttccagctaccaaaccttcctg cttctcaaatttcctttccttcactgatttctgctttaactagctgttagtgcagcgtctcagatgtcct ctccaccctctagGTGTGGTTTAATAACAAAGGCTGGCATGCCCTGGT CAGCTTTCTCAATGTGGCCCACAACGCCATCTTACGGGCCAGCC TGCCTAAGGACAGGAGCCCCGAGGAGTATGGAATCACCGTCAT TAGCCAACCCCTGAACCTGACCAAGGAGCAGCTCTCAGAGATT ACAGTgtaagccaccacagccccagcctcaccactttcttgtcaccttctccactctttgaacat cctgagaggattctcaccaccGGATCC
37	ABCA4 c.5312+1G>A	GAATTCgggtggggtaggaggactagtgacagcttaacatatgtttgccaaccaagaactgt ttaaaaagcaagtcgaatcagaatcccagaccctacgagctggaggagcctggccccaccctc attttgcagagctggcagcaggtctgagaggttaagtgacttgctctcctcttctctttccgagAT

		GAATTATTCCGTGAGTGCTGGGCTGGTGGTGGGCATCTTCATCG GGTTTCAGAAGAAAGCCTACACTTCTCCAGAAAACCTTCCTGCC CTTGTGGCACTGCTCCTGCTGTATGGgtaagccgtttgggccattagctaatgc ctctgaagagaagcctggtggtgggggtgggggatcatctcctgacagaaaacctgggctgtGG ATCC
49	ABCA4 c.6732G>A	GAATTCtaccagcagggctgtatgtgaactgtggaaaatagagagcaaagtgggtaggtgg gtgtagggtgctgttttcctggaaatatctacctaatctcgctcttctcttacctctagGTGTTTTG TAAATTTTGCTAAACAGCAGACTGAAAGTCATGACCTCCCTCTG CACCCTCGAGCTGCTGGAGCCAGTCGACAAGCCCAGgtaccctgct gcttatgcagtccacagcttgaggcagttccttggctcagagcccagctggttcactgggcttgag ttgctccaaggctcagatatgccGGATCC
9	CNGB3 c.991-3T>G	ccatgctataaaatgtactgtccagaggaaaatatcactaaacaggatcttggttttttaaaaagacatatgaatgaaattattttc agtaataaaatctatttcatatagttttatttaaatatatatatttaagactaacatgcttttggatttctttgcttttctatatagTAC ACTTCATTTTTTGAATTTAATCATCACCTAGAGTCTATAATGGACAAAGCAT ATATCTACAGgtaagtataactcagtatacttgggggaaggggaaaaagcaatggtacaacattttagac ggaat ttggcagg

Table 36: Sequences of cloned constructs in this study

***purple*: Eco R1 binding site; *green:* primer; *grey highlighted*: exon; *red highlighted*: mutation site; *yellow highlighted*: SNP; *blue*: Bam H**

Variant	Size (bp)	Sequence
Exon 9 ABCA4 1239+1G>C	194	**TCTGAGTCACCTGGACAACC**TCAAAGGCACCTTTGCTAAGCTGA**GTGAACTGC** **ACTGTGACAAGC**TGCACGCTCTAGAGTCGACCCAGCAACCTGGAGATCTCCCG AGGGGACCCGACAGGCCCGAAGGAATAGAAGAAGAAGGTGGAGAGAGAGACA GAGACAGATCCATT**CGACCAATTCACTCCTCAGGTG**
	308	**TCTGAGTCACCTGGACAACC**TCAAAGGCACCTTTGCTAAGCTGA**GTGAACTGC** **ACTGTGACAAGC**TGCACGCTCTAGAGTCGACCCAGCAAGCCTGGAGTCAAATC CTTTAACCAAAATCGCTTGGAGGGCGGCAAAGCCTTTGCTGATGGGAAAAATCC TGTACACTCCTGATTCACCTGCAGCACGAAGGATACTGAAGAATACCTGGAGAT CTCCCGAGGGGACCCGACAGGCCCGAAGGAATAGAAGAAGAAGGTGGAGAGAG AGACAGAGACAGATCCATT**CGACCAATTCACTCCTCAGGTG**
	334	WT (see Table 33)
	377	**TCTGAGTCACCTGGACAACC**TCAAAGGCACCTTTGCTAAGCTGA**GTGAACTGC** **ACTGTGACAAGC**TGCACGCTCTAGAGTCGACCCAGCAcaatggggagtttctgtaaaatctgtcc cttgtctcctggcagCATCCTTTTGTAATGCATTGATCCAGAGCCTGGAGTCAAATCCTTT AACCAAAATCGCTTGGAGGGCGGCAAAGCCTTTGCTGATGGGAAAAATCCTGTA CACTCCTGATTCACCTGCAGCACGAAGGATACTGAAGAATACCTGGAGATCTCC CGAGGGGACCCGACAGGCCCGAAGGAATAGAAGAAGAAGGTGGAGAGAGAGA CAGAGACAGATCCATT**CGACCAATTCACTCCTCAGGTG**
	454	**TCTGAGTCACCTGGACAACC**TCAAAGGCACCTTTGCTAAGCTGA**GTGAACTGC** **ACTGTGACAAGC**TGCACGCTCTAGAGTCGACCCAGC**A**CATCCTTTTGTAAT GCATTGATCCAGAGCCTGGAGTCAAATCCTTTAACCAAAATCGCTTG GAGGGCGGCAAAGCCTTTGCTGATGGGAAAAATCCTGTACACTCCT GATTCACCTGCAGCACGAAGGATACTGAAGAATtcatcactggaatgctttgctt cagtgGGATCCcagatATCTGGTGATCCCGTACCTGTGTGGAAGGAAGCA ACCACCACTCTATTTTGTGCATCAGATGCTAAAGCATATGATACAGA GACCTGGAGATCTCCCGAGGGGACCCGACAGGCCCGAAGGAATAGAAGAAGAA GGTGGAGAGAGAGACAGAGACAGATCCATT**CGACCAATTCACTCCTCAGGTG**
	496	Unknown
	607	**TCTGAGTCACCTGGACAACC**TCAAAGGCACCTTTGCTAAGCTGA**GTGAACTGC** **ACTGTGACAAGC**TGCACGCTCTAGAGTCGACCCAGC**A**CATCCTTTTGTAAT GCATTGATCCAGAGCCTGGAGTCAAATCCTTTAACCAAAATCGCTTG GAGGGCGGCAAAGCCTTTGCTGATGGGAAAAATCCTGTACACTCCT GATTCACCTGCAGCACGAAGGATACTGAAGAATgtaagatcccagctgggctt gccttgtgtaccctggacctcccagaagtgtgtgtgtgtgtgtgtgtgtgagagagatgtgccttcctg gtagcacatctcatgtttgtttttgctaagtggactcttgcgtttcctcccccatccacagtcatcactgga atgctttgcttcagtgGGATCCCAGATATCTGGTGATCCCGTACCTGTGTGGAAGGAA GCAACCACCACTCTATTTTGTGCATCAGATGCTAAAGCATATGATACAGAGACCT GGAGATCTCCCGAGGGGACCCGACAGGCCCGAAGGAATAGAAGAAGAAGGTGG AGAGAGAGACAGAGACAGATCCATT**CGACCAATTCACTCCTCAGGTG**
Exon 30 ABCA4 4354G>T	194	See above
	304	**TCTGAGTCACCTGGACAACC**TCAAAGGCACCTTTGCTAAGCTGA**GTGAACTGC** **ACTGTGACAAGC**TGCACGCTCTAGAGTCGACTCAGCATACCCCTGTGGCAACTC AACACCCTGGAAGACTCCTTCTGTGTCCCCAAACATCACCCAGCTGTTCCAGAA GCAGAAATGGACACAGGTCAACCCTTCACCATCCTGCAGACCTGGAGATCTCCC GAGGGGACCCGACAGGCCCGAAGGAATAGAAGAAGAAGGTGGAGAGAGAGAC AGAGACAGATCCATT**CGACCAATTCACTCCTCAGGTG**
	308	**TCTGAGTCACCTGGACAACC**TCAAAGGCACCTTTGCTAAGCTGA**GTGAACTGC** **ACTGTGACAAGC**TGCACGCTCTAGAGTCGACTCAGCAGGAGTACCCCTGTGGC AACTCAACACCCTGGAAGACTCCTTCTGTGTCCCCAAACATCACCCAGCTGTTCC AGAAGCAGAAATGGACACAGGTCAACCCTTCACCATCCTGCAGACCTGGAGATC

		TCCCGAGGGGACCCGACAGGCCCGAAGGAATAGAAGAAGAAGGTGGAGAGAG AGACAGAGACAGATCCATT**CGACCAATTCACTCCTCAGGTG**
	377	**TCTGAGTCACCTGGACAACC**TCAAAGGCACCTTTGCTAAGCTGA**GTGAACTGC** **ACTGTGACAAGC**TGCACGCTCTAGAGTCGACCCAGCATACCCCTGTGGCAACTC AACACCCTGGAAGACTCCTTCTGTGTCCCCAAACATCACCCAGCTGTTCCAGAA GCAGAAATGGACACAGGTCAACCCTTCACCATCCTGCAGGTGCAGCACCAGGGA GAAGCTCACCATGCTGCCAGAGTGCCCCGAGGGTGCCGGGGGGCCTCCCGCCCCC CCAGACCTGGAGATCTCCCGAGGGGACCCGACAGGCCCGAAGGAATAGAAGAA GAAGGTGGAGAGAGAGACAGAGACAGATCCATT**CGACCAATTCACTCCTCAG** **GTG**
	381	WT (see Table 33)
	407	**TCTGAGTCACCTGGACAACC**TCAAAGGCACCTTTGCTAAGCTGA**GTGAACTGC** **ACTGTGACAAGC**TGCACGCTCTAGAGTCGACCCAGCATACCCCTGTGGCAACTC AACACCCTGGAAGACTCCTTCTGTGTCCCCAAACATCACCCAGCTGTTCCAGAA GCAGAAATGGACACAGGTCAACCCTTCACCATCCTGCAGGTACAGCACCAGGGA GAAGCTCACCATGCTGCCAGAGTGCCCCGAGGGTGCCGGGGGGCCTCCCGCCCCC CCAGgtacctgacctccaaacaacggggccccagACCTGGAGATCTCCCGAGGGGACCCGACAG GCCCGAAGGAATAGAAGAAGAAGGTGGAGAGAGAGACAGAGACAGATCCATT**C** **GACCAATTCACTCCTCAGGTG**
	411	**TCTGAGTCACCTGGACAACC**TCAAAGGCACCTTTGCTAAGCTGA**GTGAACTGC** **ACTGTGACAAGC**TGCACGCTCTAGAGTCGACCCAGCAGGAGTACCCCTGTGGC AACTCAACACCCTGGAAGACTCCTTCTGTGTCCCCAAACATCACCCAGCTGTTCC AGAAGCAGAAATGGACACAGGTCAACCCTTCACCATCCTGCAGGTACAGCACCA GGGAGAAGCTCACCATGCTGCCAGAGTGCCCCGAGGGTGCCGGGGGGCCTCCCGC CCCCCCAGgtacctgacctccaaacaacggggccccagACCTGGAGATCTCCCGAGGGGACCCGA CAGGCCCGAAGGAATAGAAGAAGAAGGTGGAGAGAGAGACAGAGACAGATCC ATT**CGACCAATTCACTCCTCAGGTG**
	611	**TCTGAGTCACCTGGACAACC**TCAAAGGCACCTTTGCTAAGCTGA**GTGAACTGC** **ACTGTGACAAGC**TGCACGCTCTAGAGTCGACCCAGCATACCCCTGTGGCAACTC AACACCCTGGAAGACTCCTTCTGTGTCCCCAAACATCACCCAGCTGTTCCAGAA GCAGAAATGGACACAGGTCAACCCTTCACCATCCTGCAGGTGCAGCACCAGGGA GAAGCTCACCATGCTGCCAGAGTGCCCCGAGGGTGCCGGGGGGCCTCCCGCCCCC CCAGgtacctgacctccaaacaacggggccccaggtctgcctgccacagagggactaggggagtccctggtatctcctgagtct ctcacaaactaacatttcaaactggcagttgagtaggggacTAAACCAAACTCCCTGCACCGGATCCCAG ATATCTGGTGATCCCGTACCTGTGTGGAAGGAAGCAACCACCACTCTATTTTGTG CATCAGATGCTAAAGCATATGATACAGAGACCTGGAGATCTCCCGAGGGGACCC GACAGGCCCGAAGGAATAGAAGAAGAAGGTGGAGAGAGAGACAGAGACAGAT CCATT**CGACCAATTCACTCCTCAGGTG**
	615	**TCTGAGTCACCTGGACAACC**TCAAAGGCACCTTTGCTAAGCTGA**GTGAACTGC** **ACTGTGACAAGC**TGCACGCTCTAGAGTCGACCCAGCAGGAGTACCCCTGTGGC AACTCAACACCCTGGAAGACTCCTTCTGTGTCCCCAAACATCACCCAGCTGTTCC AGAAGCAGAAATGGACACAGGTCAACCCTTCACCATCCTGCAGGTGCAGCACCA GGGAGAAGCTCACCATGCTGCCAGAGTGCCCCGAGGGTGCCGGGGGGCCTCCCGC CCCCCCAGgtacctgacctccaaacaacggggccccaggtctgcctgccacagagggactaggggagtccctggtatctcct gagtctctcacaaactaacatttcaaactggcagttgagtaggggacTAAACCAAACTCCCTGCACCGGATCC CAGATATCTGGTGATCCCGTACCTGTGTGGAAGGAAGCAACCACCACTCTATTTT GTGCATCAGATGCTAAAGCATATGATACAGAGACCTGGAGATCTCCCGAGGGGA CCCGACAGGCCCGAAGGAATAGAAGAAGAAGGTGGAGAGAGAGACAGAGACA GATCCATT**CGACCAATTCACTCCTCAGGTG**
Exon 30 ABCA4 4457C>T	194	See above
	308	**TCTGAGTCACCTGGACAACC**TCAAAGGCACCTTTGCTAAGCTGA**GTGAACTGC** **ACTGTGACAAGC**TGCACGCTCTAGAGTCGACTCAGCAGGAGTACCCCTGTGGC AACTCAACACCCTGGAAGACTCCTTCTGTGTCCCCAAACATCACCCAGCTGTTCC AGAAGCAGAAATGGACACAGGTCAACCCTTCACCATCCTGCAGACCTGGAGATC

		TCCCGAGGGGACCCGACAGGCCCGAAGGAATAGAAGAAGAAGGTGGAGAGAG AGACAGAGACAGATCCATT**CGACCAATTCACTCCTCAGGTG**
	381	WT (see Table 33)
	411	**TCTGAGTCACCTGGACAACC**TCAAAGGCACCTTTGCTAAGCTGA**GTGAACTGC ACTGTGACAAGC**TGCACGCTCTAGAGTCGACCCAGCAGGAGTACCCCTGTGGC AACTCAACACCCTGGAAGACTCCTTCTGTGTCCCCAAACATCACCCAGCTGTTCC AGAAGCAGAAATGGACACAGGTCAACCCTTCACCATCCTGCAGGTACAGCACCA GGGAGAAGCTCACCATGCTGCCAGAGTGCCCCGAGGGTGCCGGGGGCCTCCCGC CCCCCCAGgtacctgacctccaaacaacggggccccagACCTGGAGATCTCCCGAGGGGACCCGA CAGGCCCGAAGGAATAGAAGAAGAAGGTGGAGAGAGAGACAGAGACAGATCC ATT**CGACCAATTCACTCCTCAGGTG**
	615	**TCTGAGTCACCTGGACAACC**TCAAAGGCACCTTTGCTAAGCTGA**GTGAACTGC ACTGTGACAAGC**TGCACGCTCTAGAGTCGACCCAGCAGGAGTACCCCTGTGGC AACTCAACACCCTGGAAGACTCCTTCTGTGTCCCCAAACATCACCCAGCTGTTCC AGAAGCAGAAATGGACACAGGTCAACCCTTCACCATCCTGCAGGTGCAGCACCA GGGAGAAGCTCACCATGCTGCCAGAGTGCCCCGAGGGTGCCGGGGGCCTCCCGC CCCCCCAGgtacctgacctccaaacaacggggccccaggtctgcctgccacagagggactaggggagtccctggtatctcct gagtctctcacaaactaacatttcaaactggcagttgagtaggggacTAAACCAAACTCCCTGCACCGGATCC CAGATATCTGGTGATCCCGTACCTGTGTGGAAGGAAGCAACCACCACTCTATTTT GTGCATCAGATGCTAAAGCATATGATACAGAGACCTGGAGATCTCCCGAGGGGA CCCGACAGGCCCGAAGGAATAGAAGAAGAAGGTGGAGAGAGAGACAGAGACA GATCCATT**CGACCAATTCACTCCTCAGGTG**
Exon 33_34 ABCA4 4773+3A>G	194	See above
	269	**TCTGAGTCACCTGGACAACC**TCAAAGGCACCTTTGCTAAGCTGA**GTGAACTGC ACTGTGACAAGC**TGCACGCTCTAGAGTCGACCCAGC**A**GGCCCTATCACTAG AGAGGCCTCTAAAGAAATACCTGATTTCCTTAAACATCTAGAAACTG AAGACAACATTAAGACCTGGAGATCTCCCGAGGGGACCCGACAGGCCCGAA GGAATAGAAGAAGAAGGTGGAGAGAGAGACAGAGACAGATCCATT**CGACCAA TTCACTCCTCAGGTG**
	291	**TCTGAGTCACCTGGACAACC**TCAAAGGCACCTTTGCTAAGCTGA**GTGAACTGC ACTGTGACAAGC**TGCACGCTCTAGAGTCGACCCAGC**A**GTATGGAGGAATTT CCATTGGAGGAAAGCTCCCAGTCGTCCCCATCACGGGGGAAGCACT TGTTGGGTTTTTAAGCGACCTTGGCCGGATCATGAAT ACCTGGAGATCTCCCGAGGGGACCCGACAGGCCCGAAGGAATAGAAGAAGAAG GTGGAGAGAGAGACAGAGACAGATCCATT**CGACCAATTCACTCCTCAGGTG**
	300	**TCTGAGTCACCTGGACAACC**TCAAAGGCACCTTTGCTAAGCTGA**GTGAACTGC ACTGTGACAAGC**TGCACGCTCTAGAGTCGACCCAGC**A**GTATGGAGGAATTT CCATTGGAGGAAAGCTCCCAGTCGTCCCCATCACGGGGGAAGCACT TGTTGGGTTTTTAAGCGACCTTGGCCGGATCATGAATGTGAGCGGGA CCTGGAGATCTCCCGAGGGGACCCGACAGGCCCGAAGGAATAGAAGAAGAAGG TGGAGAGAGAGACAGAGACAGATCCATT**CGACCAATTCACTCCTCAGGTG**
	375	WT (see Table 33)
Exon 35 ABCA4 4919G>A	194	See above
	294	**TCTGAGTCACCTGGACAACC**TCAAAGGCACCTTTGCTAAGCTGA**GTGAACTGC ACTGTGACAAGC**TGCACGCTCTAGAGTCGACCCAGC**A** GCCAGCCTGCCTAAGGACAGGAGCCCCGAGGAGTATGGAATCACCG TCATTAGCCAACCCCTGAACCTGACCAAGGAGCAGCTCTCAGAGATT ACAGTACCTGGAGATCTCCCGAGGGGACCCGACAGGCCCGAAGGAATAGAAG

		AAGAAGGTGGAGAGAGAGACAGAGACAGATCCATT**CGACCAATTCACTCCTC AGGTG**
	364	WT (see Table 33)
	464	**TCTGAGTCACCTGGACAACC**TCAAAGGCACCTTTGCTAAGCTGA**GTGAACTGC ACTGTGACAAGC**TGCACGCTCTAGAGTCGACCCAGCActaccaaaccttcctgcttctcaaattt ccttccttcactgatttctgctttaactagctgttagtgcagcgtctcagatgtcctctccaccctctagGTGTGGTTTAATAA CAAAGGCTGGCATGCCCTGGTCAGCTTTCTCAATGTGGCCCACAACGCCATCTTA CGGGCCAGCCTGCCTAAGGACAGGAGCCCCGAGGAGTATGGAATCACCGTCATT AGCCAACCCCTGAACCTGACCAAGGAGCAGCTCTCAGAGATTACAGTACCTGGA GATCTCCCGAGGGGACCCGACAGGCCCGAAGGAATAGAAGAAGAAGGTGGAGA GAGAGACAGAGACAGATCCATT**CGACCAATTCACTCCTCAGGTG**
	538	**TCTGAGTCACCTGGACAACC**TCAAAGGCACCTTTGCTAAGCTGA**GTGAACTGC ACTGTGACAAGC**TGCACGCTCTAGAGTCGACCCAGCAGTGTGGTTTAATAACAA AGGCTGGCATGCCCTGGTCAGCTTTCTCAATGTGGCCCACAACGCCATCTTACGG GCCAGCCTGCCTAAGGACAGGAGCCCCGAGGAGTATGGAATCACCGTCATTAGC CAACCCCTGAACCTGACCAAGGAGCAGCTCTCAGAGATTACAGTgtaagccaccacagcc ccagcctcaccactttcttgtcaccttctccactctttgaacatcctgagaggattctcaccaccGGATCCCAGATATCTG GTGATCCCGTACCTGTGTGGAAGGAAGCAACCACCACTCTATTTTGTGCATCAGA TGCTAAAGCATATGATACAGAGACCTGGAGATCTCCCGAGGGGACCCGACAGGC CCGAAGGAATAGAAGAAGAAGGTGGAGAGAGAGACAGAGACAGATCCATT**CG ACCAATTCACTCCTCAGGTG**
Exon 35 ABCA4 5018+2T>C	194	See above
	364	WT (see Table 33)
	495	Unknown
	538	**TCTGAGTCACCTGGACAACC**TCAAAGGCACCTTTGCTAAGCTGA**GTGAACTGC ACTGTGACAAGC**TGCACGCTCTAGAGTCGACCCAGCAGTGTGGTTTAATAA CAAAGGCTGGCATGCCCTGGTCAGCTTTCTCAATGTGGCCCACAACG CCATCTTACGGGCCAGCCTGCCTAAGGACAGGAGCCCCGAGGAGTA TGGAATCACCGTCATTAGCCAACCCCTGAACCTGACCAAGGAGCAG CTCTCAGAGATTACAGTgtaagccaccacagccccagcctcaccactttcttgtcaccttctc cactctttgaacatcctgagaggattctcaccaccGGATCCCAGATATCTGGTGATCCCGTA CCTGTGTGGAAGGAAGCAACCACCACTCTATTTTGTGCATCAGATGCTAAAGCA TATGATACAGAGACCTGGAGATCTCCCGAGGGGACCCGACAGGCCCGAAGGAA TAGAAGAAGAAGGTGGAGAGAGAGACAGAGACAGATCCATT**CGACCAATTCA CTCCTCAGGT**
	606	unknown
Exon 49 ABCA4 6732G>A	281	WT (see Table 33)
	74	**TCTGAGTCACCTGGACAACC**TCAAAGGCACCTTTGCTAAGCTGAGTGAACTGC ACTGTGACAAGCTGCACGCTCTAGAGTCGACCCAGCAGTGTTTGTAAATTTTGCT AAACAGCAGACTGAAAGTCATGACCTCCCTCTGCACCCTCGAGCTGCTGGAGCC AGTCGACAAGCCCAGgtaccctgctgcttatgcagtccacagcttgaggcagttccttggctcagagcccagctggtt cactgggcttgagttgCTCCAAGGCTCAGATATGCCGGATCCCAGATATCTGGTGATCCCG TACCTGTGTGGAAGGAAGCAACCACCACTCTATTTTGTGCATCAGATGCTAAAG CATATGATACAGAGACCTGGAGATCTCCCGAGGGGACCCGACAGGCCCGAAGG AATAGAAGAAGAAGGTGGAGAGAGAGACAGAGACAGATCCATT**CGACCAATT CACTCCTCAGGTG**

Exon 9 CNGB 991-3T>G	259	WT (see Table 33)
	261	**TCTGAGTCACCTGGACAACC**TCAAAGGCACCTTTGCTAAGCTGA**GTGAACTGC** **ACTGTGACAAGC**TGCACGCTCTAGAGTCGACCCAGCA**Aag**TACACTTCATTTTTTG AATTTAATCATCACCTAGAGTCTATAATGGACAAAGCATATATCTACAGACCTG GAGATCTCCCGAGGGGACCCGACAGGCCCGAAGGAATAGAAGAAGAAGGTGGA GAGAGAGACAGAGACAGATCCATT**CGACCAATTCACTCCTCAGGTG**

Table 37: Sequences of all splicing transcripts in this study

Abbreviation	Meaning
’	Prime
° C	Degree Celcius
A	Acceptor
A2E	Lipofuscin fluorophore in retinal pigmented epithelial
AAP	Antarctic alkaline phosphatase
ABCA4	ATP-Binding cassette, subfamily A, member 4
AMD	Age-related macular dystrophy
Amp	Ampicillin
AS	Acceptor site
ATP	Adenosine triphosphate
Bam*H1*	Bacillus amyloliquefaciens, type II restriction endonuclease
Bp	Base pair
cDNA	Complementary DNA
cf	Confer “compare to”
cGMP	Cyclic guanosine monophosphate
cm	Centimeter
CNGA3	Cyclic nucleotide gated channel alpha 3
CNGB3	Cyclic nucleotide gated channel beta 3
CORD	Cone-rod dystrophy
CRX	Cone-rod homeobox
D	Donor
DH5α	E. coli competent cell strain - “D.H.” Doug Hanahan, Bethesda Research Laboratories, 1986
DMEM	Dulbecco`s Modified Eagle Medium
DMSO	Dimethyl sulfoxide
DNA	Deoxyribonucleic acid
dNTP	Deoxynucleotide triphosphate
DS	Donor site
ECD	Extracellular domain
E. coli	*Escherichia coli*
Eco*R1*	*Escherichia coli*, strain R, endonuclease I
Exo	Exonuclease I
EDTA	Ethylendiamintetraacetic acid
Et al.	et alii
FCS	Fetal calf serum
FF	Fundus flavimaculatus
h	Hour
HGMD	Human Gene Mutation Database
H_2O	Water
K	Potassium
kb	Kilobase
KCNV2	Potassium channel, subfamily V, member 2
kDA	Kilodalton
l	Litre
LB	Liquid broth
MAF	Minor allele frequency

$MgSO_4$	Magnesium sulfate
min	Minute
ml	Millilitre
MM	Master mix
mM	Millimolar
mRNA	Messenger ribonucleic acid
Mut	Mutant
Na	Sodium
NaCl	Sodium chloride
ng	Nanogram
Nm	Nanometer
NRPE	N-retinylidenephosphatidylethanolamine
P/S/G	Penicillin/Streptomycin/Glutamine
PB	Phosphate buffer
PBS	Phosphate buffered saline
PCR	Polymerase chain reaction
Pen/Strep	Penicillin/Streptomycin
pGEM	Cloning vector system
PROM1	Proamin 1
RNA	Ribonucleic acid
RP	Retinitis pigmentosa
RPE	Retinal pigment epithelium
RPGR	Retinitis pigmentosa GTPase regulator
rpm	Rotations per minute
RT	Room temperature
RT-PCR	Reverse Transcriptase PCR
SDS	Sodium dodecyl sulfate
sec	Second
STGD	Stardardt disease
TBE	Tris/Borate/EDTA
Tris	Tris(hydroxymethyl)aminomethane
µg	Microgram
µl	Microlitre
UV	Ultraviolet
V	Volt
V_{Total}	Total volume
VIC	Voltage-gated ion channels
WT	Wild-type

Table 38: Abbreviations used in text

Company Name	Headquarters
Abimed	Langenfeld, Germany
AppliChem	Darmstadt, Germany
Applied Biosystems	Darmstadt, Germany
B.Braun Biotech	Melsungen, Germany
BDK GmbH	Sonnenbühl, Germany
Becton, Dickson & Co.	Heidelberg, Germany
Biolabs	Ipswich, MA, USA
Biometra	Goettingen, Germany
Biomol	Hamburg, Germany
Biostep	Jahnsdorf, Germany
Biozym	Hessisch Oldendorf, Germany
Brand	Wertheim, Germany
Braun	Melsungen, Germany
Carl Roth	Karlsruhe, Germany
Corning, Inc.	Amsterdam, The Netherlands
Daewoo	Berkshire, England
eppendorf	Hamburg, Germany
Feather	Osaka, Japan
Genaxxon Bioscience	Ulm, Germany
GFL	Burgwedel, Germany
Gibco	Grand Island, NY, USA
Inst.Human Genetics UR	Regensburg, Germany
Invitrogen	Grand Island, NY, USA
KIMTECH	Neenah, WI, USA
Lauda	Lauda-Königshofen, Germany
Macherey-Nagel	Düren, Germany
Memmert	Schwabach, Germany
Merck	Darmstadt, Germany
Millipore	Darmstadt, Germany
Mirus	Madison, WI, USA
NanoDrop®	Wilmington, DE, USA
Orange Scientific	Braine-l'Alleud, Belgium
PAA	Freiburg, Germany
Promega	Madison, WI, USA
Qiagen	Venol, The Netherlands
Qualitron	Karachi, Pakistan
Sarstedt	Nümbrecht, Germany
ScientificIndustries	Bohemia, NY, USA
Scotsman	Vernon Hills, IL, USA
Serva	Heidelberg
Sigma	St. Louis, MO, USA
Systec GmbH	Wettenberg, Germany
ThermoScientific	Waltham, MA, USA
Thieme Labortechnik	Bensheim, Germany
VWR	Darmstadt, Germany

Table 39: Company name and headquarters

10 REFERENCES

1. Cideciyan AV, Swider M, Aleman TS, Tsybovsky Y, Schwartz SB, Windsor EA, Roman AJ, Sumaroka A, Steinberg JD, Jacobson SG, Stone EM, Palczewski K (2009). ABCA4 disease progression and a proposed strategy for gene therapy. Hum. Mol. Genet. 18(5):931-41.

2. Maugeri A, van Driel MA, van de Pol DJ, Klevering BJ, van Haren FJ, Tijmes N, Bergen AA, Rohrschneider K, Blankenagel A, Pinckers AJ, Dahl N, Brunner HG, Deutman AF, Hoyng CB, Cremers FP (1999). The 2588G>C mutation in the ABCR4 gene is a mild frequent founder mutation in the western European population and allows the classification of ABCR mutations in patients with Stargardt disease. Am J Hum Genet. 64(4):1024-35.

3. Burke TR, Tsang SH. Allelic and phenotypic heterogeneity in ABCA4 mutations. Ophthalmic Genet. 2011; 32:165–74.

4. Kaplan J, Gerber S, Larget-Piet D, Rozet J M, Dollfus H, Dufier JL, Odent S, Postel-Vinay A, Janin N, and Briard M L (1993). A gene for Stargardt's disease (fundus flavimaculatus) maps to the short arm of chromosome 1. Nat. Genet. 5, 308–311.

5. Edwards AO, Donoso LA, Ritter R 3rd (2001). A novel gene for autosomal dominant Stargardt-like macular dystrophy with homology to the SUR4 protein family. Invest Ophthalmol Vis Sci. 42(11):2652-63.

6. Zhang Q, Zulfiqar F, Xiao X, Riazuddin S A, Ahmad Z, Caruso R, MacDonald I, Sieving P, Riazuddin S, Hejtmancik JF (2007).Severe retinitis pigmentosa mapped to 4p15 and associated with a novel mutation in the PROM1 gene. Hum. Genet.122:293-299.

7. Sundin OH, Yang JM, Li Y, Zhu D, Hurd JN, Mitchell TN, Silva ED, Maumenee IH (2000). Genetic basis of total colour blindness among the Pingelapese islanders. Nat. Genet. 25(3):289-93.

8. Nishiguchi KM, Sandberg MA, Gorji N, Berson EL, Dryja TP (2005). Cone cGMP-gated channel mutations and clinical findings in patients with achromatopsia, macular degeneration, and other hereditary cone diseases. Hum. Mutat. 25: 248-258.

9. Kniazeva M, Chiang MF, Morgan B, Anduze AL, Zack DJ, Han M, and Zhang K. (1999). A new locus for autosomal dominant stargardt-like disease maps to chromosome 4. Am. J. Hum. Genet. 64, 1394–1399.

10. Allikments R, Wasserman WW, Hutchinson A, Smallwood P, Nathans J, Rogan PK, Schneider TD, Dean M (1998). Organization of the ABCR gene: analysis of promoter and splice junction sequences. Gene. 215(1):111-22.

11. Lewis RA, Shroyer NF, Singh N, Allikmets R, Hutchinson A, Li Y, Lupski JR, Leppert M, Dean M (1999). Genotype/Phenotype analysis of a photoreceptor-specific ATP-binding cassette transporter gene, ABCR, in Stargardt disease. Am. J. Hum. Genet. 64(2):422-34.

12. Vasiliou V, Vasiliou K, and Nebert DW (2009). Human ATP-binding cassette (ABC) transporter family. Hum. Genomics 3, 281–290.

13. Coleman JA, Quazi F, Molday RS (2013). Mammalian P4-ATPases and ABC transporters and their role in phospholipid transport. Biochim Biophys Acta. 1831(3):555-74.

14. Dean M (2002). The Human ATP-Binding Cassette (ABC) Transporter Superfamily Bethesda (MD): National Center for Biotechnology Information (US). [Internet]. http://www.ncbi.nlm.nih.gov/books/NBK31/

15. Fritsche LG, Fleckenstein M, Fiebig BS, Schmitz-Valckenberg S, Bindewald-Wittich A, Keilhauer CN, Renner AB, Mackensen F, Mossner A, Pauleikhoff D (2012). A Subgroup of Age-Related Macular Degeneration is Associated with Mono-Allelic Sequence Variants in the ABCA4 Gene. Invest. Ophthalmol. Vis. Sci. 53, 2112–2118.

16. Papermaster DS, Schneider BG, Zorn MA, Kraehenbuhl JP (1978). Immunocytochemical localization of a large intrinsic membrane protein to the incisures and margins of frog rod outer segment disks. J. Cell. Biol. 78(2):415-25.

17. Molday LL, Rabin AR, Molday RS (2000). ABCR expression in foveal cone photoreceptors and its role in Stargardt macular dystrophy. Nat. Genet.25:257–8.

18. Meitinger T (1997). Widening the view. Nat. Genet. 15(3):224-5.

19. Tsybovsky Y, Orban T, Molday RS, Taylor D, Palczewski K (2013). Molecular organization and ATP-induced conformational changes of ABCA4, the photoreceptor-specific ABC transporter. Structure. 21(5):854-60.

20. Bungert S, Molday LL, Molday RS (2001). Membrane topology of the ATP binding cassette transporter ABCR and its relationship to ABC1 and related ABCA transporters: identification of N-linked glycosylation sites. J Biol Chem. 276(26):23539-46.

21. Tsybovsky Y, Wang B, Quazi F, Molday RS, Palczewski K (2011). Posttranslational modifications of the photoreceptor-specific ABC transporter ABCA4. Biochemistry. 50(32):6855-66.

22. Tsybovsky Y, Molday RS, Palczewski K (2010). The ATP-binding cassette transporter ABCA4: structural and functional properties and role in retinal disease. Adv Exp Med Biol. 703:105-25.

23. Quazi F, Molday RS (2013). Differential Phospholipid Substrates and Directional Transport by ATP Binding Cassettte Proteins ABCA1, ABCA7, and ABCA4 and Disease-causing Mutants. J. Biol. Chem. [Epub ahead of print] PMID: 24097981.

24. Moiseyev G, Nikolaeva O, Chen Y, Farjo K, Takahashi Y, Ma JX (2010). Inhibition of the visual cycle by A2E through direct interaction with RPE65 and implications in Stargardt disease. PNAS. 107(41):17551-17556.

25. Shroyer NF, Lewis RA, Allikmets R, Singh N, Dean M, Leppert M, Lupski JR (1999). The rod photoreceptor ATP-binding cassette transporter gene ABCR, and retinal disease: from monogenic to multifactorial. Vision Res. 39(15):2537-44.

26. Wiszniewski W, Zaremba CM, Yatsenko AN, Jamrich M, Wensel TG, Lewis RA, Lupski JR (2005). ABCA4 mutations causing mislocalization are found frequently in patients with severe retinal dystrophies. Hum Mol Gen 14(19):2769-2778.

27. Schindler EI, Nylen EL, Ko AC, Affatigato LM, Heggen AC, Wang K, Sheffield VC, and Stone EM (2010). Deducing the pathogenic contribution of recessive ABCA4 alleles in an outbred population. Hum. Mol. Genet. 19, 3693–3701.

28. Zhong H, Molday LL, Molday RS, Yau KW (2002). The heteromeric cyclic nucleotide-gated channel adopts a 3A:1B stoichiometry. Nature. 420(6912):193-8.

29. Ding XQ, Harry CS, Umino Y, Matveev AV, Fliesler SJ, Barlow RB (2009). Impaired cone function and cone degeneration resulting from CNGB3 deficiency: down-regulation of CNGA3 biosynthesis as a potential mechanism. Hum. Mol. Genet. 18(24):4770-80.

30. Johnson S, Michaelides M, Aligianis IA, Ainsworth JR, Mollon JD, Maher ER, Moore AT, and Hunt DM (2004). Achromatopsia caused by novel mutations in both CNGA3 and CNGB3. J. Med. Genet. 41(2):e20.

31. Kohl S, Baumann B, Broghammer M, Jägle H, Sieving P, Kellner U, Spegal R, Anastasi M, Zrenner E, Sharpe LT, Wissinger B (2000). Mutations in the CNGB3 gene encoding the beta-subunit of the cone photoreceptor cGMP-gated channel are responsible for achromatopsia (ACHM3) linked to chromosome 8q21. Hum. Mol. Genet. 9(14):2107-16.

32. Liu C, Sherpa T, Varnum MD (2013). Disease-associated mutations in CNGB3 promote cytotoxicity in photoreceptor-derived cells. Mol. Vis. 19:1268–81.

33. Hamel CP (2007). Cone rod dystrophies. Orphanet J Rare Dis. (2):7.

34. Thiadens, AA, Phan TM, Zekveld-Vroon RC, Leroy BP, van den Born LI, Hoyng CB, Klaver CC; Writing Committee for the Cone Disorders Study Group Consortium: Roosing S, Pott JW, van Schooneveld MJ, van Moll-Ramirez N, van Genderen MM, Boon CJ, den Hollander AI, Bergen AA, De Baere E, Cremers FP, Lotery AJ (2012). Clinical course, genetic etiology, and visual outcome in cone and cone-rod dystrophy. Ophthalmology. 119(4):819-26.

35. Brunak S, Engelbrecht J, Knudsen S (1990). Neural network detects errors in the assignment of mRNA splice sites. Nucl. Acids Res. 18:4797-4801.

36. Mount SM (1982). A catalogue of splice junction sequences. Nucl. Acids Res. 10:459-472.

37. Padgett RA, Grabowski PJ, Konarska MM, Seiler S, Sharp PA (1986). Splicing of messenger RNA precursors. Annu. Rev. Biochem. 55:1119-50.

38. Senapathy P, Shapiro MB, Harris NL (1990): Splice junctions, branch point sites, and exons: sequence statistics, identification, and applications to genome project. Meth. Enzym. 183:252-278.

39. Roca X, Krainer AR, and Eperon IC (2013). Pick one, but be quick: 5’ splice sites and the problems of too many choices. Genes Dev. 27, 129–144.

40. Spurdle AB, Couch FJ, Hogervorst FBL, Radice P, and Sinilnikova OM (2008). Prediction and assessment of splicing alterations: implications for clinical testing. Hum. Mutat. 29, 1304–1313.

41. Pettigrew CA, and Brown MA (2008). Pre-mRNA splicing aberrations and cancer. Front. Biosci. 13, 1090–1105.

42. Rassow J, Hauser K, Netzker R, Deutzmann R. (2006). Biochemie. Duale Reihe. Thieme: Stuttgart.

43. Wang Z and Burge CB (2008). Splicing regulation: from a parts list of regulatory elements to an integrated splicing code. RNA 14, 802–813.

44. Singh RK and Cooper TA (2012). Pre-mRNA splicing in disease and therapeutics. Trends Mol. Med. 18, 472–482.

45. Maquat LE (1996). Defects in RNA splicing and the consequence of shortened translational reading frames. Am.J.Hum.Genet. 59:279-286.

46. Webster AR, Héon E, Lotery AJ, Vandenburgh K, Casavant TL, Oh KT, Beck G, Fishman GA, Lam BL, Levin A, et al. (2001). An analysis of allelic variation in the ABCA4 gene. Invest. Ophthalmol. Vis. Sci. 42, 1179–1189.

47. Braun TA, Mullins RF, Wagner AH, Andorf JL, Johnston RM, Bakall BB, Deluca AP, Fishman GA, Lam BL, Weleber RG, Cideciyan AV, Jacobson SG, Sheffield VC, Tucker BA, Stone EM (2013). Non-exomic and synonymous variants in ABCA4 are an important cause of Stargardt disease. Hum. Mol. Genet. [Epub ahead of print] PMID: 2391866.

48. Schindler EI, Nylen EL, Ko AC, Affatigato LM, Heggen AC, Wang K, Sheffield VC, and Stone EM (2010). Deducing the pathogenic contribution of recessive ABCA4 alleles in an outbred population. Hum. Mol. Genet. 19, 3693–3701.

49. Krawczak M, Reiss J, Cooper DN (1992). The mutational spectrum of single base-pair substitutions in mRNA splice junctions of human genes: causes and consequences. Hum. Genet. 90(1-2):41-54.

50. Liu HX, Cartegni L, Zhang MQ, Krainer AR (2001). A mechanism for exon skipping caused by nonsense or missense mutations in BRCA1 and other genes. Nat Genet. 27:55-58.

51. Woolfe A, Mullikin JC, and Elnitski L (2010). Genomic features defining exonic variants that modulate splicing. Genome Biol. 11, R20.

52. Théry JC, Krieger S, Gaildrat P, Révillion F, Buisine MP, Killian A, Duponchel C, Rousselin A, Vaur D, Peyrat JP, et al. (2011). Contribution of bioinformatics predictions and functional splicing assays to the interpretation of unclassified variants of the BRCA genes. Eur. J. Hum. Genet. 19, 1052–1058.

53. Vreeswijk MPG, Kraan JN, van der Klift HM, Vink GR, Cornelisse CJ, Wijnen JT, Bakker E, van Asperen CJ, and Devilee P (2009). Intronic variants in BRCA1 and BRCA2 that affect RNA splicing can be reliably selected by splice-site prediction programs. Hum. Mutat. 30, 107–114.

54. Houdayer C, Dehainault C, Mattler C, Michaux D, Caux-Moncoutier V, Pagès-Berhouet S, d'Enghien CD, Laugé A, Castera L, Gauthier-Villars M. (2008). Evaluation of i*n silico* splice tools for decision-making in molecular diagnosis. Hum. Mutat. 29, 975–982.

55. Cepko CL, Roberts BE, Mulligan RC (1984).Construction and applications of a highly transmissible murine retrovirus shuttle vector. Cell. 37(3):1053-62.

56. Duyk GM, Kim SW, Myers RM, Cox DR (1990). Exon trapping: a genetic screen to identify candidate transcribed sequences in cloned mammalian genomic DNA. Proc Natl Acad Sci USA. 87(22):8995-9.

57. Wenderfer SE and Monaco JJ (2004). Exon trapping for positional cloning and fingerprinting.Methods Mol. Biol. 256:7-20.

58. Buckler AJ, Chang DD, Graw SL, Brook JD, Haber DA, Sharp PA, Housman DE (1991). Exon amplification: a strategy to isolate mammalian genes based on RNA splicing. Proc Natl Acad Sci USA. 88(9):4005-9.

59. Hamaguchi M, Sakamoto H, Tsuruta H, Sasaki H, Muto T, Sugimura T, Terada M. (1992). Establishment of a highly sensitive and specific exon-trapping system. Proc. Natl. Acad. Sci. U. S. A. 89, 9779–9783.

60. Eriksson M, Brown WT, Gordon LB, Glynn MW, Singer J, Scott L, Erdos MR, Robbins CM, Moses TY, Berglund P, Dutra A, Pak E, Durkin S, Csoka AB, Boehnke M, Glover TW, Collins FS (2003). Recurrent de novo point mutations in lamin A cause Hutchinson-Gilford progeria syndrome. Nature, 423:293-298.

61. Moseley CT, Mullis PE, Prince MA, Phillips JA (2002). An exon splice enhancer mutation causes autosomal dominant GH deficiency. J Clin Endocrinol Metab. 87:847-852.

62. Beit-Ya'acov A, Mizrahi-Meissonnier L, Obolensky A, Landau C, Blumenfeld A, Rosenmann A, Banin E, and Sharon D (2007). Homozygosity for a novel ABCA4 founder splicing mutation is associated with progressive and severe Stargardt-like disease. Invest. Ophthalmol. Vis. Sci. 48, 4308–4314.

63. Houdayer C, Caux-Moncoutier V, Krieger S, Barrois M, Bonnet F, Bourdon V, Bronner M, Buisson M, Coulet F, Gaildrat P, et al. (2012). Guidelines for splicing analysis in molecular diagnosis derived from a set of 327 combined in silico/in vitro studies on BRCA1 and BRCA2 variants. Hum. Mutat. 33, 1228–1238.

64. Petersen SM, Dandanell M, Rasmussen LJ, Gerdes AM, Krogh LN, Bernstein I, Okkels H, Wikman F, Nielsen FC, and Hansen TVO (2013). Functional examination of MLH1, MSH2, and MSH6 intronic mutations identified in Danish colorectal cancer patients. BMC Med. Genet. 14: 103.

65. Sterne-Weiler T, Howard J, Mort M, Cooper DN, Sanford JR (2011). Loss of exon identity is a common mechanism of human inherited disease. Genome Res. 10:1563-71

66. Lim KH, Ferraris L, Filloux ME, Raphael BJ, and Fairbrother WG (2011). Using positional distribution to identify splicing elements and predict pre-mRNA processing defects in human genes. Proc. Natl. Acad. Sci. U. S. A. 108, 11093–11098.

67. Cartegni L, Wang J, Zhu Z, Zhang MQ, Krainer AR. (2003). ESEfinder: A web resource to identify exonic splicing enhancers. Nucleic Acids Res. 31, 3568–3571.

68. Fairbrother WG, Yeh RF, Sharp PA, Burge, CB. (2002). Predictive identification of exonic splicing enhancers in human genes. Science 297, 1007–1013.

69. Sahashi K, Masuda A, Matsuura T, Shinmi J, Zhang Z, Takeshima Y, Matsuo M, Sobue G, and Ohno K. (2007). In vitro and in silico analysis reveals an efficient algorithm to predict the splicing consequences of mutations at the 5' splice sites. Nucleic Acids Res. 35, 5995–6003.

70. Buratti E, Chivers M, Královicová J, Romano M, Baralle M, Krainer AR, Vorechovsky I. (2007). Aberrant 5' splice sites in human disease genes: mutation pattern, nucleotide structure and comparison of computational tools that predict their utilization. Nucleic Acids Res. 35, 4250–4263.

71. Tosi M, Stamm S, and Baralle D. (2010). RNA splicing meets genetic testing: detection and interpretation of splicing defects in genetic diseases. Eur J Genet.18 (6):737-738.

72. Wappenschmidt B, Becker AA, Hauke J, Weber U, Engert S, Köhler J, Kast K, Arnold N, Rhiem K, Hahnen E, et al. (2012). Analysis of 30 putative BRCA1 splicing mutations in hereditary breast and ovarian cancer families identifies exonic splice site mutations that escape in silico prediction. PLoS One *7*, e50800.

73. Colombo M, de Vecchi G, Caleca L, Foglia C, Ripamonti CB, Ficarazzi F, Barile M, Varesco L, Peissel B, Manoukian S, (2013). Comparative In Vitro and In Silico Analyses of Variants in Splicing Regions of BRCA1 and BRCA2 Genes and Characterization of Novel Pathogenic Mutations. PLoS One 8.

74. Krawczak M, Thomas NST, Hundrieser B, Mort M, Wittig M, Hampe J, and Cooper DN (2007). Single base-pair substitutions in exon-intron junctions of human genes: nature, distribution, and consequences for mRNA splicing. Hum. Mutat. 28, 150–158.

75. Baralle D, Lucassen A, Buratti E (2009). Missed threads. The impact of pre-mRNA splicing defects on clinical practice. EMBO Rep.10:810-816

76. Fackenthal JD and Godley LA (2008). Aberrant RNA splicing and its functional consequences in cancer cells. Dis Model Mech. 1(1):37-42.

77. Havens MA, Duelli DM, Hastings ML (2013). Targeting RNA splicing for disease therapy. WIREs RNA. 4(3): 247-266.

78. Allikmets R, Singh N, Sun H, Shroyer NF, Hutchinson A, Chidambaram A, Gerrard B, Baird L, Stauffer D, Peiffer A, Rattner A, Smallwood P, Li Y, Anderson KL, Lewis RA, Nathans J, Leppert M, Dean M, Lupski JR (1997). A photoreceptor cell-specific ATP-binding transporter gene (ABCR) is mutated in recessive Stargardt macular dystrophy. Nat Genet. 15(3), 236–246.

79. Cartegni L, Krainer AR (2002). Disruption of an SF2/ASF-dependent exonic splicing enhancer in SMN2 causes spinal muscular atrophy in the absence of SMN1. Nat Genet. 30:377-384.

80. Moseley CT, Mullis PE, Prince MA, Phillips JA (2002). An exon splice enhancer mutation causes autosomal dominant GH deficiency. J Clin Endocrinol Metab. 87:847-852.

81. Sheikh TI, Mittal K, Willis MJ, Vincent JB (2013). A synonymous change, p.Gly16Gly in MECP2 Exon 1, causes a cryptic splice event in a Rett syndrome patient.Orphanet J Rare Dis.18:108.

82. Boichard A, Venet L, Naas T, Boutron A, Chevret L, de Baulny HO, De Lonlay P, Legrand A, Nordman P, Brivet M (2008). Two silent substitutions in the PDHA1 gene cause exon 5 skipping by disruption of a putative exonic splicing enhancer. Mol Genet Metab. 93:323-330.

83. Maquat LE (2005). Nonsense-mediated mRNA decay in mammals. J. Cell. Sci. 118:1773-1776.

84. Steffensen AY, Dandanell M, Jonson L, Ejlertsen B, Gerdes AM, Nielsen FC, Hansen TvO (2014). Functional characterization of BRCA1 gene variants by mini-gene splicing assay. Eur J Hum Genet. [Epub ahead of print] PMID:24667779

85. Biswas –Fiss EE, Kurpad DS, Joshi K, Biswas SB (2010). Interaction of extracellular domain 2 of the human retina-specific ATP-binding cassette transporter (ABCA4) with all-trans-retinal. J Biol Chem, 285:19372-19383.

86. Fitzgerald ML, Morris AL, Rhee JS, Andersson LP, Mendez AJ, Freeman MW (2002). Naturally occurring mutations in the largest extracellular loops of ABCA1 can disrupt its direct interaction with apolipoprotein A-I. J Biol Chem. 277:33178-33187.

87. Riolfi Julia (2014). Vergleich transkriptioneller und epigenetischer Profile von retinalen Zellen und Geweben bei Mensch und Maus. Masters Thesis, Universität Regensburg.

88. Farkas MH, Grant GR, White JA, Sousa ME, Consugar MB, Pierce EA (2013). Transcriptome analyses of the human retina identify unprecedented transcript diversity and 3.5 Mb of novel transcribed sequence via significant alternative splicing and novel genes. BMC Genomics, 14:486.

89. Baier, Maria (2014). Funktionelle Charakterisierung genetischer Varianten des ABCA4-Gens. Bachelor Thesis, Universität Regensburg.

90. Willis TA, Potrata B, Ahmed M, Hewison J, Gale R, Downey L, Mckibbin M (2013). Understanding of and attitudes to genetic testing for inherited retinal disease: a patient perspective. Br J Ophthalmol. 97(9):1148-1154.

91. Roca X, Sachidanandam R, and Krainer AR (2003). Intrinsic differences between authentic and cryptic 5’ splice sites. Nucleic Acids Res. 31, 6321–6333.

92. Lewandowska MA (2013). The missing puzzle piece: splicing mutations. Int J Clin Exp Pathol. 6(12): 2675-2682.

93. Zhang C, Hastings ML, Krainer AR, Zhang MQ (2007). Dual-specificity splice sites function alternatively as 5’ and 3’ splice sites. Proc Natl Acad Sci USA 104(38): 15028-33.

94. Reed R (1989). The organization of 3’ splice-site sequences in mammalian introns. Genes Dev. 3:2113-2123.

95. Shepard PJ, Choi EA, Busch A, Hertel KJ (2011). Efficient internal exon recognition depends on near equal contributions from the 3' and 5' splice sites. Nucleic Acids Res. 39(20) 8928-8937.

96. Srebrow A, Kornblihtt AR (2006). The connection between splicing and cancer. J Cell Sci. 119(13): 2635-41.

97. Hoskins AA & Moore MJ (2012). The spliceosome: a flexible, reversible macromolecule machine. Trends Biochem Sci. 37(5):179-188.

98. Cooper TA, Wan L, Dreyfuss G (2009). RNA and Disease. Cell. 136(4):777-793.

99. Weber, BH. Head of Institute for Human Genetics, University of Regensburg. Personal conversation, September 2014.

100. Piton A, Jouan L, Rochefort D, Dobrzeniecka S, Lachapelle K, Dion P, Gauthier J, Rouleau A (2013). Analysis of the effects of rare variants on splicing identifies alterations in $GABA_A$ receptor genes in autism spectrum disorder individuals. Eur J Hum Genet.21 (7):749-56.

101. Claverie-Martin F, Gonzalez-Paredes FJ, Ramos-Trujillo E (2015). Splicing defects caused by exonic mutations in PKD1 as a new mechanism of pathogenesis in autosomal dominant polycystic kidney disease. RNA Biol.12 (4):369-74.

102. Soukarieh O, Gaildrat P, Hamieh M, Drouet A, Baert-Desurmont, S, Frébourg T, Martins A. (2016). Exonic Splicing Mutations Are More Prevalent than Currently Estimated and Can Be Predicted by Using *In Silico* Tools. PLoS Genetics, 12(1).

103. Leman R, Gaildrat P, Gac GL, et al. Novel diagnostic tool for prediction of variant spliceogenicity derived from a set of 395 combined *in silico/in vitro* studies: an international collaborative effort. Nucleic Acids Research. 2018; 46(15).

104. Anna A, Monika G. Splicing mutations in human genetic disorders: examples, detection, and confirmation. Journal of Applied Genetics. 2018; 59(3):253-268.

105. Sangermano R, Khan M, Cornelis SS, Richelle V, Albert S, Garanto A, Elmelik D, Qamar R, Lugtenberg D, van den Born LI, Collin RWJ, Cremers FPM (2017). *ABCA4* midigenes reveal the full splice spectrum of all reported noncanonical splice site variants in Stargardt disease. Genome Res. 2018 Jan; 28(1):100-110.

106. Murphy D, Cieply B, Carstens R, Ramamerthy V, Stoilov P (2016). The Musashi 1 controls the splicing of photoreceptor-specific exons in the vertebrate retina. PloS Genet 12.

107. Albert S, Garanto A, Sangerman R, Khan M, Bax NM, Hoyng CB, Zernant J, Lee W, Allikmets R, Collin R, Cremers F (2018). Identification and Rescue of Splice Defects Caused by Two Neighboring Deep-Intronic ABCA4 Mutations Underlying Stargardt Disease. American journal of human genetics, 102(4), 517-527.

11 OTHER REFERENCES

Allikmets R, Shroyer NF, Singh N, Seddon JM, Lewis RA, Bernstein PS, Peiffer A, Zabriskie NA, Li Y, Hutchinson A, Dean M, Lupski JR, Leppert M (1997). Mutation of the Stargardt disease gene (ABCR) in age-related macular degeneration. Science. 277(5333):1805-7.

Clancy S. (2008). RNA splicing: introns, exons and spliceosome. Nature Education. *1(1)*

Krawczak M, Cooper DN (1991). Gene deletions causing human genetic disease: mechanisms of mutagenesis and the role of the local DNA sequence environment. Hum Genet. 86(5):425-41.

Molday RS, Zhang K (2010). Defective lipid transport and biosynthesis in recessive and dominant Stargardt macular degeneration. Prog. Lipid Res. 49(4):476-92.

NanoDrop 1000 Spectrophotometer V3.7 User's Manual (2008). Thermo Fisher Scientific: Waltam, MA, USA.

PCR clean-up gel extraction user manual (2012). Macherey-Nagel: Düren, Germany.

Peter K, Rogan PK, Faux BM., Schneider TD. (1998). Information analysis of human splice site mutations. Human Mutation 12: 153-171.

pGEM®-T and pGEM®-T Easy vector systems technical manual (2010). Promega: Madison, WI, USA.

Plasmid DNA purification user manual (2010). Macherey-Nagel: Düren, Germany.

Rivera A, White K, Stöhr H, Steiner K, Hemmrich N, Grimm T, Jurklies B, Lorenz B, Scholl, HP, Apfelstedt-Sylla E, Weber BH (2000). A comprehensive survey of sequence variation in the ABCA4 (ABCR) gene in Stargardt disease and age-related macular degeneration. Am. J. Hum. Genet. 67, 800–813.